

Aus dem Lehrstuhl für Neurophysiologie
am Mannheimer Centrum für Translationale Neurowissenschaft
der Medizinischen Fakultät Mannheim
(Direktor: Prof. Dr. med. Rolf-Detlef Treede)

**Timing matters: the impact of repeated restraint stress
on NGF induced sensitization of spinal dorsal horn neurons
in an animal model of myofascial low back pain.**

Inauguraldissertation
zur Erlangung des Doctor scientiarum humanarum (Dr. sc. hum.)
der
Medizinischen Fakultät Mannheim
der Ruprecht-Karls-Universität
zu
Heidelberg

vorgelegt von
Sathish Kumar Singaravelu

aus
Salem, India
2021

Dekan: Prof. Dr. med. Sergij Goerd
Referent: Prof. Dr. med. Rolf-Detlef Treede

in memory of my dad

TABLE OF CONTENTS

	Page
ABBREVIATIONS	1
1 INTRODUCTION	3
1.1 Adverse childhood experiences.....	3
1.1.1 Stress	5
1.2 Relationship between pain and stress	6
1.3 Chronic stress and low back pain	7
1.4 Non-specific low back pain	8
1.4.1 Overview of non-specific low back pain.....	8
1.4.2 Source of non-specific low back pain	9
1.5 Animal model with NGF-induced non-specific low back pain	10
1.5.1 Role of NGF in muscle disorders.....	11
1.5.2 NGF-induced sensitization.....	12
1.6 The role of glial cells in pain processing.....	14
1.6.1 Role of microglia in pain	15
1.6.2 Role of astrocytes in pain	19
1.7 Research focus of this thesis.....	19
1.7.1 Electrophysiological recordings of dorsal horn neurons	20
1.7.2 Immunohistochemical staining of glial cells in the dorsal horn	20
1.7.3 Hypothesis and aims	21
2 MATERIALS AND METHODS.....	23
2.1 In vivo electrophysiology study (study 1).....	23
2.1.1 Animals and treatment groups.....	23
2.1.2 Repeated restraint stress	24
2.1.3 Intramuscular injection of nerve growth factor	25
2.1.4 Pressure pain threshold of the low back.....	26
2.1.5 Electrophysiological recordings of the spinal dorsal horn neurons	27
2.1.6 Data analysis	34

2.2 Quantitative immunohistochemistry (study 2)	35
2.2.1 Animals and treatment groups.....	35
2.2.2 Repeated restraint stress	37
2.2.3 Injection of nerve growth factor and saline	37
2.2.4 Behavioral tests	38
2.2.5 Perfusion and tissue processing.....	39
2.2.6 Immunofluorescence labeling.....	40
2.2.7 Image processing and quantification	41
2.2.8 Reactive microgliosis and classification of microglia states	46
2.2.9 Data analysis	47
2.3 Swimming training (study 3)	48
2.3.1 Animals and treatment groups.....	48
2.3.2 Behavioral test and exercise protocol.....	48
2.3.3 Experimental design	48
2.3.4 Data analysis	49
 3 RESULTS.....	 50
3.1 Study 1: Electrophysiology	50
3.1.1 Body weight and pressure pain threshold of the low back.....	50
3.1.2 General features of recorded dorsal horn neurons.....	52
3.1.3 Responsiveness of dorsal horn neurons to mechanical stimulation	55
3.1.4 Resting activity of the dorsal horn neurons.....	56
3.2 Study 2: Behavioral and immunohistological findings.....	59
3.2.1 Body weight	59
3.2.2 Pressure pain threshold measured in the left low back after stress.....	59
3.2.3 Paw withdrawal threshold of the left hind paw after stress	59
3.2.4 Pressure pain threshold measured in the left low back after saline/NGF injections.....	61
3.2.5 Paw withdrawal threshold of the hind paws after saline/NGF injections	62
3.2.6 Iba-1 and GFAP staining intensities	63
3.2.7 Iba-1 stained number of microglial cells.....	65
3.2.8 Structural plasticity of Iba-1 stained microglial cells.....	67
3.2.9 Proportion and distribution of microglial cells in the dorsal horn.....	70
3.2.10 Analysis of morphological changes in microglial cells	74
3.3 Study 3: Swimming training attenuates chronic muscle pain.....	78

4 DISCUSSION	80
4.1 Repeated restraint stress alters pain sensitivity	81
4.2 Manifestation of altered pain sensitivity due to stress.....	83
4.3 Persistent effects of stress in combination with NGF	85
4.4 Potential mechanisms for the stress and NGF-induced sensitization.....	90
4.5 Limitations	92
4.6 Conclusions.....	94
 5 SUMMARY	 95
 6 REFERENCES.....	 98
 7 APPENDIX	 117
 8 CURRICULUM VITAE	 141
 9 ACKNOWLEDGEMENTS.....	 145

ABBREVIATIONS

ACE	adverse childhood experience
AMPA	α -amino-3-hydroxy-5-methyl-4-isoxazolepropionic acid
ANOVA	analysis of variance
CNS	central nervous system
CO ₂	carbon dioxide
con.	contralateral
DHN	dorsal horn neuron
DRG	dorsal root ganglion
GFAP	glial fibrillary acidic protein
GS	gastrocnemius-soleus
i.p.	intraperitoneal
i.m.	intramuscular
i.v.	intravenously
Iba-1	ionized calcium-binding adapter molecule 1
IL	interleukin
ip.	ipsilateral
LB	low back
LBP	low back pain
LTP	long-term potentiation
Mac-1	macrophage antigen complex-1
MAPK	mitogen-activated protein kinase
MCP 1	monocyte chemoattractant protein-1
MF	multifidus
NGF	nerve growth factor
NMDA	N-methyl-D-aspartate
NO	nitric oxide
O ₂	Oxygen
PBS	phosphate-buffered saline
PFA	paraformaldehyde
PGE ₂	prostaglandin E ₂
PKC ϵ	protein kinase C ϵ
PNS	peripheral nervous system
PPT	pressure pain threshold
PWT	paw withdrawal threshold
RF	receptive field
ROI	region of interest
SD	standard deviation

SEM	standard error of the mean
SNL	spinal nerve ligation
SNS	sympathetic nervous system
SRIF	somatotropin release-inhibiting factor
TCA	tricarboxylic acid cycle
TLF	thoracolumbar fascia
TLR	toll-like receptor
TNF- α	tumor necrosis factor-alpha
Trk	tyrosine receptor kinase
TRPV	transient receptor potential vanilloid
V _c	subnucleus caudalis

INTRODUCTION

The studies in this thesis work are based on the hypothesis that the sensitization of dorsal horn neurons (DHN) plays a key role in the development of non-specific chronic low back pain. Adverse childhood experiences (ACEs) are known predictors for the chronicity of low back pain (Tesarz et al., 2016) and repeated restraint stress or a single intramuscular nerve growth factor (NGF) injection in adulthood are known to induce low back pain by priming the DHNs (Hoheisel et al., 2013; Hoheisel et al., 2015). It is anticipated that the timing of the stressor and an additional nociceptive input after stress play a key role in determining whether this sensitization process is latent or manifest. This sensitization could be mediated by the activation of glial cells (Zhang, 2016).

1.1 Adverse childhood experiences

Globally, more than 450 million people fulfil the criteria of a mental disorder, accounting for 13% of the Disability Adjusted Life Years of all diseases (Vigo et al., 2016). Adverse childhood experiences (ACEs), such as abuse and neglect (Ganzel et al., 2010; Herzog and Schmahl, 2018), are a major risk factors for the development of both mental (Gilbert et al., 2009) and physical disorders such as low back pain (LBP) (Tesarz et al., 2016) a major global health burden (Rice et al., 2016). ACEs can have long-lasting adverse effects on the central nervous system (CNS) and other somatic systems, specifically through epigenetic mechanisms and is shown to have influences on brain development (Heim and Binder, 2012; Raabe and Spengler, 2013). A prior experience of an ACE can end in multifaceted clinical profiles with co-occurring mental and somatic disorders in adulthood (Herzog and Schmahl, 2018; Mielke et al., 2020). Somatic symptom disorder, including abnormal pain perception with and without corresponding somatic pathology e.g., chronic pain vs. pain during childbirth has shown to be enhanced after ACE (Cloitre et al., 2009; Leeners et al., 2016; Tesarz et al., 2016).

Even though a wide-ranging stress effect in the development of the disorders is known, the role of ACE type and ACE timing is not well understood. But this is of particular interest in terms of prevention and treatment of ACE-related psychiatric and somatic conditions (Herzog and Schmahl, 2018; Mielke et al., 2020). Both in humans

and animals, throughout development, there are critical windows of enhanced neuroplasticity during which adverse events may have long-term effects on physical and mental well-being (Rice and Barone, 2000), this is also expected to be the case with ACE-related disorders (Baker et al., 2013; Heim and Binder, 2012; Herzog and Schmahl, 2018; Kaplow and Widom, 2007; Mielke et al., 2020; Teicher and Samson, 2013). Studies have also pointed out certain neurobiological alterations such as volumetric changes in the amygdala and hippocampus and were associated with sensitive periods during development (Andersen et al., 2008; Pechtel et al., 2014; Riem et al., 2015). Furthermore, evidence suggests that depending on the types of ACE, individuals are prone to different disorders, e.g., the experience of physical violence may induce aggression-related conditions (Fanning et al., 2014), while the experience of neglect may be related to the development of emotional difficulties or metabolic syndromes (Colvert et al., 2008). Especially adversities in earlier life such as emotional abuse are associated with enhanced temporal summation of pain, and sexual abuse with enhanced touch sensitivity (Tesarz et al., 2016). Another influential factor to be considered is the duration of ACE (i.e., if ACE took place over the course of several developmental windows) on the severity of neurocognitive alterations demonstrated (Cowell et al., 2015; Jaffee and Maikovich-Fong, 2011).

A broad-spectrum of studies on animals suggest that adversities across adolescence inducing robust and long-lasting effects on pain summation (Burke et al., 2013; Deng et al., 2017; Genty et al., 2018; Le Coz et al., 2017; Vilela et al., 2017). Throughout this long developmental window (male rats: ~ PD 21 – ~ PD 80; female rats: ~ PD 15 - ~ PD 60) (Schneider, 2013), the type and timing of the stressor also have significant effects on the chronic pain development. For instance, maternal separation stress is one of the most common types of early life stressors (pre-weaning) and has shown to have bidirectional effects on sensitivity to pain in adulthood (Burke et al., 2013; Genty et al., 2018; Vilela et al., 2017). These observed effects might be led on by differential microglia activation and are known to be a potential mechanism of action for modulating sensitivity to pain and stress (Tsuda et al., 2004; Tynan et al., 2010) which will be further introduced in section 1.4.

1.1.1 Stress

The term stress in psychology is defined as a particular relationship between the person and the environment that is appraised by the person as taxing or exceeding his or her resources and endangering his or her well-being (Folkman, 2013). The human body responds to stress in several ways and to study this, Hans Selye developed a model known as general adaptation syndrome, which consists of three states: the alarm reaction, the stage of resistance and the stage of exhaustion (Selye, 1946). The alarm stage occurs when a stressor is first presented and corresponds to the well-known phrase 'fight or flight' response. At this stage, the autonomic nervous system is known to be involved and changes in body functions occur (e.g. increased energy-levels and muscle tension, reduced sensitivity to pain, increase in blood pressure) (Gottlieb, B.H., 1997) (1997; Coon, 2013). In the second stage the body builds up resistance trying to cope and overcome the stress or reacts improperly leading to onset of psychosomatic disorders (Coon, 2013). The exhaustion is the final stage when the body can no longer sustain and meet any energy demands leading to anxiety and irritability, and continuing stress could be harmful and even fatal (Selye, 1946). Different animals tend to react differently even when a similar stress is applied and the anticipation of stress itself could cause a physiological response (Mason, 1971). Stressors can be divided into different types which include either a physical component like physiological stressors (heat and toxins), or a mental component psychological stressors (e.g. exposure to a novel environment and fear), or both physiological stressors with psychological component (e.g. immobilization).

Stress is not necessarily a bad thing. On the one hand, it could be beneficial depending on the type and its duration during which the organism can adapt to a new steady state and respond to an environmental challenge also called as eustress (McEwen, 1998; Selye, 1975). However, increased frequency and intensity of exposure to stressors could lead to mal-adaptation of the response system causing a permanent damage, not only in peripheral tissues but also in the CNS (McEwen, 1999; Selye, 1975) and is called distress. When a challenging stimulus is presented to the internal or external environment, a stress response is induced triggering physiological and behavioral responses to ensure the organisms survival and

disrupting the homeostasis. This abnormal response leads to an activation of two major systems, the sympathetic nervous system (SNS) by releasing endorphins and secreting adrenalin and noradrenalin; and the hypothalamic-pituitary-adrenal (HPA) axis leading to secretion of glucocorticoids and activating the immunological response (Herbert and Cohen, 1993). Thus, when a stressor is presented, the SNS reacts within seconds by releasing catecholamines from the medulla of the adrenal glands into the bloodstream followed by the activation of the HPA axis which in turn release glucocorticoids from the adrenal cortex (1997; Coon, 2013). Therefore, in humans, psychological or physical traumatic events in early life are risk factors for several neuronal and physical disorders and may account for the differential susceptibility to chronic pain in later life (Burke et al., 2016).

1.2 Relationship between pain and stress

According to the International Association for the Study of Pain (IASP), pain is defined as ‘an unpleasant sensory and emotional experience associated with, or resembling that associated with, actual or potential tissue damage’ (Raja et al., 2020). Pain is a subjective experience and is characterized by a combination of changes in sensory-motor information, central processing, pain-related behaviors, emotions and beliefs (Gatchel et al., 2007). Pain is broadly classified into two types: acute and chronic. Acute pain is usually short-lasting and the onset is immediately after an injury or trauma, while chronic pain is long-lasting and persists beyond the expected time for tissue healing (van der Windt et al., 2000). In the acute phase, pain is usually transitory, acting as a physiological response lasting only until the noxious stimuli are removed or the underlying pathology is healed. On the other hand, chronic or persistent pain loses its transitory role and may continue in the absence of a potential or actual tissue damage e.g. non-specific LBP. This state reflects the complex interactions between the nervous and the immune system by releasing inflammatory mediators and activation of glial cells that can result in peripheral and central sensitization which are some of the essential components to the development of chronic pain (Mifflin and Kerr, 2014).

Several studies have noted that people suffering from chronic pain disorders also suffer from high psychological stress (Diepenmaat et al., 2006; Uveges et al., 1990;

Van Uum et al., 2008). Both in humans and animals, studies have shown that early life stressors (ELS) could have an impact on neuronal circuits and the immune system development leading to an enhanced vulnerability to physio-and pathophysiological states in adulthood (Heim et al., 2010; Schmidt, 2010). In humans, ACEs and stress are risk factors for the chronicity of subacute LBP (Mendelek et al., 2013) and the development of chronic widespread pain (Tesarz et al., 2015). Nonetheless, the relationship between stress and pain acts bidirectional, with interdependent mechanisms (Chapman et al., 2008).

As a fight or flight response to an acute stress, elevated cortisol levels lead to releasing glucose into the blood stream and breaking down muscle proteins to provide energy. In situations of persistent stress, this continuous and abnormal secretion of cortisol leads to toxic effects on the nervous system and may form a background for the development of chronic pain disorders (Hannibal and Bishop, 2014). Prolonged stress is linked with cortisol hypersecretion and might provoke resistance of glucocorticoid receptors leading to increase in release of pro-inflammatory neurotransmitters (e.g. norepinephrine). This release could evoke peripheral muscle nociceptor-sensitization and local muscle tension reactions that stabilize and do not return to a relaxed state (Wippert and Wiebking, 2018). Alternatively, prolonged stress could induce hypo-functioning of the HPA axis leading to low cortisol levels influencing the descending anti-nociceptive serotonergic and noradrenergic pathways (Wippert and Wiebking, 2018). It has also been suggested that during chronic stress, a previous muscle strain or injury may become a trigger area and become vulnerable to subsequent minor injuries or pain flare-ups in cases of musculoskeletal pain disorders (Hannibal and Bishop, 2014).

1.3 Chronic stress and low back pain

Chronic musculoskeletal pain disorder is defined as persistent or recurrent pain that arises as a part of a disease process directly affecting muscles, bones, joints, tendons, ligaments or related tissues (Nicholas et al., 2019; Perrot et al., 2019; Treede et al., 2015), and is the leading cause of disability, affecting 1.3 billion people worldwide (Disease et al., 2016). Amidst musculoskeletal pain disorders, low back pain (LBP) is the leading cause of disability with a lifetime prevalence of 84% and has

become a major public health problem affecting performance at work and general well-being (Rice et al., 2016) with a chronic prevalence of approximately 23% (Balague et al., 2012; Hoy et al., 2014). Due to its multifaceted nature, persistent LBP has substantial negative influences on sufferers resulting in fear-avoidance behaviors, kinesiophobia, pain catastrophizing thoughts and mood disorders, such as depression and anxiety (Demyttenaere et al., 2007; Knezevic et al., 2021; Picavet et al., 2002; Waddell et al., 1993).

In majority of the cases, acute LBP resolves in the first few weeks from onset (da et al., 2012) and conventional medical treatments (e.g., using non-steroidal anti-inflammatory drugs or physical therapy) are available (Bernstein et al., 2017). However, when LBP pain persists and becomes chronic, the underlying mechanisms are poorly understood and almost 90% of cases have no identifiable cause and are identified as non-specific LBP (Hua and Van der Does, 1994; Maher et al., 2017). According to the IASP classification of chronic pain for the international classification of diseases (ICD-11), in conditions such as non-specific LBP, the persistent state may be conceived as a disease on its own with no known cause (Treede et al., 2019).

1.4 Non-specific low back pain

1.4.1 Overview of non-specific low back pain

Globally, low back pain (LBP), is the most common condition and is the leading cause of years lived with disability and burden of all health conditions (Balague et al., 2012; Hoy et al., 2014; Knezevic et al., 2021; Vos et al., 2012). According to the course of pain, LBP can be divided into sub-classes such as: acute, sub-acute, and chronic (Qaseem et al., 2017), becomes a continuous burden of relentless suffering (Debono et al., 2013). Non-specific LBP is diagnosed when organic causes are ruled out and the condition is rarely curable, thus a leading contributor to disability and major burden to global health (Hoy et al., 2012). The onset is complicated and in some cases the causes are known, such as the instability of vertebrae (Ferrari et al., 2015), irritation of nerve roots by the herniated nucleus material from the intervertebral disc (radiculopathy) (Indahl, 2004), mechanical damage to the lumbar

intervertebral disc (pseudoradicular) (Park et al., 2020), facet joint or sacroiliac joint (musculoskeletal) (Hancock et al., 2007). There are also several physical and psychological risk factors including mechanical factors like sedentary lifestyle (Chen et al., 2009), and psychological trauma (Tesarz et al., 2015) involved.

Non-specific LBP is defined as low back pain with no underlying pathology (Balague et al., 2012; Mendelek et al., 2013) (i.e. infection, tumor, fracture, inflammatory disorder etc.), and 80% - 90% of low back pain is classified as non-specific low back pain (Bardin et al., 2017; Deyo and Phillips, 1996; Frank, 1993; Hua and Van der Does, 1994; Maher et al., 2017). Patients suffering from non-specific LBP show signs of both peripheral and central sensitization. While peripheral sensitization is characterized by an increase in pain sensitivity of nociceptors located in deep tissues (Graven-Nielsen and Arendt-Nielsen, 2010), central sensitization (including the brain and the spinal cord) is indicated by an increased excitability and synaptic efficacy of neurons in central nociceptive pathways which is initiated by intense peripheral noxious stimuli, tissue injury or nerve damage (Ji et al., 2003; Woolf, 2011). In general, the body adapts when a noxious stimulus is presented, but the duration, frequency and type of the nociceptive stimuli presented play an important role in inducing persistent central sensitization, which might trigger the mechanism of chronic pain. This abnormal central sensitization plays a role in the transition from acute to chronic state (Arendt-Nielsen and Graven-Nielsen, 2003) even in the absence and/or with only very little peripheral nociceptive inputs (Staud, 2011). The excitability of spinal neurons is modulated both by descending facilitatory and inhibitory pain pathways. In particular, descending pain facilitatory pathways are critical in initiating and maintaining this central hyper-excitability and any irregularity in these pathways could lead to spinal neuron excitability contributing to persisting pain (Staud, 2011; Suzuki and Dickenson, 2005; Suzuki et al., 2002).

1.4.2 Source of non-specific low back pain

As mentioned in the last section (1.2), chronic primary musculoskeletal pain may be conceived as a disease on its own from an unknown cause (Treede et al., 2019). Nevertheless, several factors have been postulated as the cause of LBP or related with its development and progression (Balague et al., 2012). Conflicting findings from

a human study reported that dysregulation of cortisol release plays a role in LBP versus temporomandibular pain (Garofalo et al., 2007). The results indicate a positive association between high cortisol levels at baseline and pain severity at follow-up in individuals with temporomandibular disorders, whereas the later shows a negative relationship between low cortisol levels and high pain severity in individuals with LBP (Garofalo et al., 2007). According to another 6 months prospective case-control study, there were significantly higher proportions of tumor necrosis factor-alpha (TNF- α) positive participants in the LBP patients groups than in the control groups (Wang et al., 2008). In addition to TNF- α , substances released from nucleus pulposus tissue within the intervertebral discs might contribute to spinal nerve roots sensitization and induce pain (Murata et al., 2005). NGF extracted from these degenerated tissues might also play a role in this pain transmission, by promoting axonal growth and substance P production (Balague et al., 2012).

Recently, both in human and animal experiments, studies have shown the importance of fascia as an origin of non-specific LBP. In humans, experiments with hypertonic saline injection into thoracolumbar fascia (TLF), and in animals, NGF injections into the multifidus (MF) have shown the involvement of TLF as a potential source of non-specific LBP muscle (Hoheisel et al., 2013; Hua and Van der Does, 1994; Malanga and Cruz Colon, 2010; Schilder et al., 2014; Stecco et al., 2011). In another animal model of chronic mechanical LBP using intervertebral disc puncture, increased expression of somatostatin (SRIF) was observed in the lumbar dorsal root ganglia (DRGs) suggesting a potential role of SRIF in modulating chronic LBP (Park et al., 2020). Nevertheless, the neuronal mechanisms underlying the development of non-specific LBP is still poorly understood.

1.5 Animal model with NGF-induced non-specific low back pain

Considering the low back muscle as a potential origin of non-specific LBP, an animal model of myofascial LBP induced by NGF injections into the MF muscle has been established to study the hyper-excitability of dorsal horn neurons (DHNs) along with the hyperalgesic behavior in a LBP state (Hoheisel et al., 2013; La Porta and Tappe-Theodor, 2020; Reed et al., 2021; Reed et al., 2020; Zhang et al., 2017). Here, two NGF injections were administered into the MF muscle at the vertebral level L5 with an interval of five days. The resulting manifest sensitization was characterized by

mechanical hyperalgesia. Spinal dorsal horn neurons show a significant increase in resting activity, and the appearance of new receptive fields in the deep tissues of the distal hind limb (Hoheisel et al., 2013; Zhang et al., 2017). In a similar study in humans by (Deising et al., 2012), single NGF injection into the fascia of the erector spinae muscle induced a long lasting hypersensitivity of the muscle fascia to both mechanical and chemical stimulations but no ongoing pain was observed.

1.5.1 Role of NGF in muscle disorders

NGF is a neurotrophic factor regulating neuronal development, proliferation, growth and maintenance of neurons, and is involved in the regulation of the immune system. The association of NGF in many painful muscle disorders or non-painful but functionally overloaded muscles has been observed in several studies (Hayashi et al., 2011; Murase et al., 2010). Hayashi and colleagues (2011) found an increased expression of NGF in regenerating muscle cells after eccentric contraction, mimicking the condition of myofascial pain syndrome and exhibiting signs of long-term mechanical hyperalgesia. This sensitizing effect of NGF expressed in regenerating muscle cells might be critical in persistent mechanical muscle hyperalgesia. Another study showed that NGF injection into the gastrocnemius muscle induced mechanical hyperalgesia and upregulated NGF mRNA and protein over a comparable time course after lengthening and contraction of muscles (Murase et al., 2010). In humans, intramuscular administration of NGF evokes a long-lasting mechanical hyperalgesia, in both shoulder muscle (lasting 1 day) (Nie et al., 2009) and masseter muscle (lasting at 7 least days) (Svensson et al., 2003), and induces a long-lasting mechanical and chemical hyperalgesia when injected in muscle fascia (Deising et al., 2012). On the other hand, inhibiting NGF alleviated chronic LBP in patients (Markman et al., 2020).

In animals, repeated NGF injections into the MF muscle induce sensitization and are likely to play an important role in altering the pain threshold of the lower back and the hyper-excitability of dorsal horn neurons (Hoheisel et al., 2013; Zhang et al., 2017). Nerve growth factor plays a role in maintaining the sensitivity of the primary afferent fibers in the peripheral tissues (Mann et al., 2006), resulting in an increased sensitivity at the ending of those fibers. Murase and colleagues (2010) showed NGF-

induced mechanical hypersensitivity in the periphery 2 h after the NGF injection, when they recorded the activity of single muscle afferents (majority C-fibers) in vitro. In humans, Mann and colleagues (2006) found that NGF decreased the mechanical threshold of a small population of masseter muscle afferent fibers. In rats, Hoheisel and colleagues (Hoheisel et al., 2005) found that NGF excited exclusively the nociceptive muscle afferents which evoked mainly subthreshold potentials in the DHNs (Hoheisel et al., 2007).

Since in DHNs the appearance of new receptive fields (RFs) was observed far from the repeated NGF injection site in the LBP pain model, the sensitization of DHNs could be associated with central sensitization (Hoheisel et al., 2013). The strength of the synaptic contacts vary at the synaptic level. While some synapses are ineffective, and cannot produce any postsynaptic response (silent or sleeping synapse), some are highly effective and can evoke action potentials with lesser transmitter release (potentiated state) (Kuner, 2010). Therefore, based on the findings from Hoheisel and colleagues (2013), it is possible that the silent synapses were opened by repeated NGF-induced afferent input and were mainly connected with deep tissues both in and outside the low back.

Moreover, glial cells are known to be involved in the sensitization of dorsal horn neurons induced by 2 NGF injections and there is increasing evidence that spinal glial cells play an important role in the development of chronic pain states (Clark et al., 2015; Clark and Malcangio, 2012; La Porta and Tappe-Theodor, 2020; Sessler et al., 2021; Sideris-Lampretsas and Malcangio, 2021; Zhang et al., 2017).

1.5.2 NGF-induced sensitization

A single intramuscular NGF injection into the low back muscle resulted in a transient mechanical hyperalgesia, for about 2 days, but hyperalgesia was absent at day 5 after the injection. The electrophysiological findings showed that the NGF injection just before the recording period of 4 h or 5 days after the NGF injection, did not induce an acute sensitization, while the proportion of neurons responding to the mechanical stimulation of deep tissues or neurons with convergent input did not differ compared to saline injections (Hoheisel et al., 2013). But when intramuscular NGF

injections were repeated at an interval of 5 days, the mechanical hyperalgesia lasted longer up to day 14 and the spinal neurons were now sensitized within the 4 h recording period after the second NGF injection, exhibiting the increased proportions of neurons with input from deep tissues of the low back, outside the low back, and increased convergent input (Hoheisel et al., 2013). These findings tell us that after the first NGF injection, there is a phase of 'latent sensitization' or priming, that intensifies the sensitivity of the neurons to a following NGF injection (Hoheisel et al., 2013). This demonstrates that two NGF injections, but not a single NGF injection caused a significant hyper-excitability (hypersensitivity) of DHNs, indicating stronger and longer-lasting 'manifest sensitization' (Hoheisel et al., 2013). This central latent sensitization or priming resembles the hyperalgesic priming of peripheral nociceptors in muscle, mediating the transition from acute to chronic pain (Ferrari et al., 2010; Reichling and Levine, 2009).

A recent publication by Zhang and colleagues (2017) showed that activation of glial cells plays an important role in central sensitization. Especially, microglia are known to be involved in this process of latent sensitization, while blocking the microglia activation by minocycline prevented this sensitization. Sessler and colleagues (2021) found that blocking fractalkine signaling in a dose-dependent manner also prevented NGF-induced sensitization suggesting the critical role of neuron-to-microglia signaling via the CX3CL1-CX3CR-1 pathway. Another possible explanation for this sensitization might be associated with the increased release of excitatory amino acids. Skyba and colleagues observed increased concentrations of glutamate and aspartate after two injections of acidic saline into the gastrocnemius muscle and induced secondary mechanical hyperalgesia that continued for up to 4 weeks. Activation of the spinal N-methyl-D-aspartate (NMDA) and α -amino-3-hydroxy-5-methyl-4-isoxazolepropionic acid (AMPA) /kainite receptors were involved in this hyperalgesia process (Skyba et al., 2005). Studies have also shown that activation of protein kinase C ϵ in the peripheral terminals are involved in hyperalgesic priming (Ferrari et al., 2010; Reichling and Levine, 2009) and could also be associated with the latent sensitization observed after NGF injection.

In the NGF-induced myofascial LBP model, fifty microliters of 0.8 μ M NGF solution were injected into the multifidus muscle twice, with an interval of 5 days (Hoheisel et

al., 2013). The NGF concentration used is known to be not painful but to induce hyperalgesia when intramuscularly injected both in human and animal studies (Deising et al., 2012; Hoheisel et al., 2013; Hoheisel et al., 2007; Svensson et al., 2003). Apart from the non-specific LBP model, a single NGF injection into the gastrocnemius-soleus (GS) muscle induced an excitatory action on subpopulations of group IV muscle afferent units (Hoheisel et al., 2005). In another study by Hoheisel et al (2007), repeated NGF injections into the GS muscle induced hyper-excitability of dorsal horn neurons in the lumbar segment L4. Murase and colleagues (2010) found NGF-induced mechanical hyperalgesia of muscle afferents 3 h after the NGF injection into the gastrocnemius muscle and this sensitization lasted up to 48 hours after the injection. All the above-mentioned studies show that a concentration of 0.8 μ M NGF when injected into the muscle of animals was sufficient for increasing the sensitivity of afferents or neurons. In humans, intradermal NGF injection was used for the study of axonal sensitization (Obreja et al., 2011; Rukwied et al., 2014), and NGF injection into the muscle fascia or muscle was applied to induce a long-lasting sensitization of the muscle fascia or muscle to mechanical and/or chemical stimuli (Deising et al., 2012; Nie et al., 2009; Svensson et al., 2003; Weinkauff et al., 2015).

In the non-specific LBP model, histological observations showed no visible sign of muscle inflammation 5 or 12 days after the NGF injection (Hoheisel et al., 2013). No signs of evoked pain-related behavior was observed after one NGF injection into the GS muscle (Ulrich Hoheisel and Siegfried Mense, unpublished data). In humans, intramuscular NGF injections did not induce acute or spontaneous pain (Svensson et al., 2003), likewise when NGF was injected into the fascia (Deising et al., 2012).

1.6 The role of glial cells in pain processing

Glial cells or neuroglia, are non-neuronal cells in the CNS (brain and spinal cord) and the peripheral nervous system that do not produce electrical impulses (Fields et al., 2014). In the CNS, glial cells include microglia, astrocytes and oligodendrocytes, and in the peripheral nervous system (PNS), there are mainly schwann cells, satellite cells and macrophages. Glial cells perform a wide-range of functions such as maintaining homeostasis, forming myelin to modulate the rate of nerve signal propagation, providing nutrients and oxygen to neurons, regulating synapse formation and controlling synaptic strength, and play a pivotal role in the recovery

process or potentiating damage following neural injury. Upon tissue or neuronal damage, glial cells modify the signaling between neurons and contribute to central sensitization resulting in allodynia and/or hyperalgesia (Chacur et al., 2009; Fields and Stevens-Graham, 2002; Gerhold et al., 2015; Tsuda et al., 2013). Studies have shown that glial cells and neurons are closely associated (i.e. neuron-glia communication) and perhaps neural activity can be measured by monitoring the activity of glia (Fields and Stevens-Graham, 2002).

Increasing evidence suggest that glial cells in the spinal cord and in the brainstem play a crucial role in pain sensitization, especially when pain becomes persistent. Glial cells such as microglia and astrocytes are involved in nociceptive process, an important step in generation of pain perception (Chacur et al., 2009; Ledeboer et al., 2005; Raghavendra et al., 2004; Tsuda et al., 2013). In the non-specific LBP animal model, involvement of activated spinal glial cells has been observed (La Porta and Tappe-Theodor, 2020; Sessler et al., 2021; Zhang et al., 2017).

1.6.1 Role of microglia in pain

Function of microglia

Microglia are macrophage-like cells in the CNS. On the one hand, they act as the main form of active immune cells and on the other hand, they regulate neuronal functions and help in maintaining homeostasis (Cserep et al., 2020). Microglia regulate and survey their surrounding tissues for pathogen apoptotic debris and trigger neuroinflammation (Fields and Stevens-Graham, 2002; Tremblay et al., 2011; Xanthos and Sandkuhler, 2014). They sense the cellular environment with their ramified processes, and undergo rapid changes and are activated by various environmental changes or diseases, such as brain local injury (Nimmerjahn et al., 2005), Alzheimer' disease (Baron et al., 2014; Puli et al., 2012), and chronic stress (Hinwood et al., 2012). Several pre-clinical studies on chronic pain have shown activation of microglia in the spinal cord, i.e. after spinal nerve injury (Sweitzer et al., 2001), peripheral inflammation (Bao et al., 2001), peripheral nerve inflammation (Milligan et al., 2003), chronic opioid treatment (Raghavendra et al., 2002), non-specific LBP (Sessler et al., 2021; Zhang et al., 2017), and restraint stress (La Porta

and Tappe-Theodor, 2020). Activation of microglia has been observed under various pathophysiological situations, such as CNS injury, microbial invasion and other pain states (Marchand et al., 2005; Raghavendra et al., 2003). Pre-clinical studies have also shown that repeated NGF injections lead to microglia activation (Zhang et al., 2017) and result in an increase in the production of various pro-inflammatory cytokines such as interleukin (IL) -1 β , IL-6, TNF- α , chemokines (i.e. fractalkine (FKN), and other potentially pain-producing substances (i.e. prostaglandin E2 (PGE2), nitric oxide (NO)) (Durrenberger et al., 2004; Holguin et al., 2004; Kawasaki et al., 2008; Marchand et al., 2005). This release facilitates the excitatory synaptic transmission, leading to pain hypersensitivity (Clark et al., 2015; Kawasaki et al., 2008; Raghavendra et al., 2003; Sessler et al., 2021; Sideris-Lampretsas and Malcangio, 2021; Zhong et al., 2010).

Microglial activation

Gliosis is a nonspecific reactive change of glial cells in response to injuries and insults and often involves the proliferation or hypertrophy of glial cells (Chen et al., 2018). Activated microglial cells express ionized calcium – binding adapter molecule 1 (Iba-1), as the microglial specific marker increases and the morphology of microglial cells alters from ramified to amoeboid shapes with enlarged cell bodies and shortened processes (Chen et al., 2018; Hinwood et al., 2012; Romero-Sandoval et al., 2008; Streit et al., 1999). A number of studies have focused on the morphological changes of microglia in different circumstances, such as in the animal models of Alzheimer's disease, injured cerebral cortex and chronic stress (Baron et al., 2014; Hinwood et al., 2012). Preclinical studies on chronic stress (i.e., restraint stress) in pain have shown involvement of brain microglia and the changes to their morphology with an arrested hyper-ramified state (Hinwood et al., 2012; Hinwood et al., 2013; Kopp et al., 2013; Park et al., 2011; Tynan et al., 2010). In the mature CNS, surveilling microglial cells provide neurotrophic support, maintain homeostasis, modulate the release of neurotransmitters and hormones, regulate pain, respond to psychological stress, prevent neurons from damage and respond to changes in the microenvironment (Karperien et al., 2013). Activated microglial cells are unramified and play a pivotal role in the immune-inflammatory process, in which they migrate to

injury site to recruit or activate other cells, proliferate, clear debris by phagocytosis, and result in recovery and cortical reorganization (Karperien et al., 2013).

Studies have shown that early life stress disrupts the normal development of the CNS and this in turn primes microglia to a reactive state in later life leading to increased pain (see Fig. 1) (Burke et al., 2016). Chronic lifestyle stress also sensitizes microglia toward a primed phenotype and induces neuroinflammation in the adult brain (Ramirez et al., 2016; Wohleb et al., 2014). Acute stress increases the number of microglia (Lehmann et al., 2016), while chronic stress decreases it (Tong et al., 2017). Studies were made on the morphological changes of microglial cells in animal model of chronic stress (Hinwood et al., 2012). Several morphological parameters including basic parameters (i.e., size, boundary of microglia) and advanced parameters (the length of the processes, the number of the endpoints of processes of microglia) were measured, reflecting the structure of microglial cells in details. Eriksson and colleagues, showed microgliosis in the pain-modulating spinal cord and brain stem regions after nerve injury using immunostaining of OX-42 (Eriksson et al., 1993). In inflammatory or neuropathic pain models the activation of microglial cells was only evaluated according to the immunostaining intensity of a molecular marker (Iba-1 or OX-42) or basic morphological parameters (Chacur et al., 2009; Ledeboer et al., 2005; Romero-Sandoval et al., 2008; Tsuda et al., 2004). Minocycline, a non-specific microglial inhibitor, has shown to be effective in inhibiting mechanical hyperalgesia and allodynia and prevented spinal neuron sensitization (Raghavendra et al., 2003; Zhang et al., 2017).

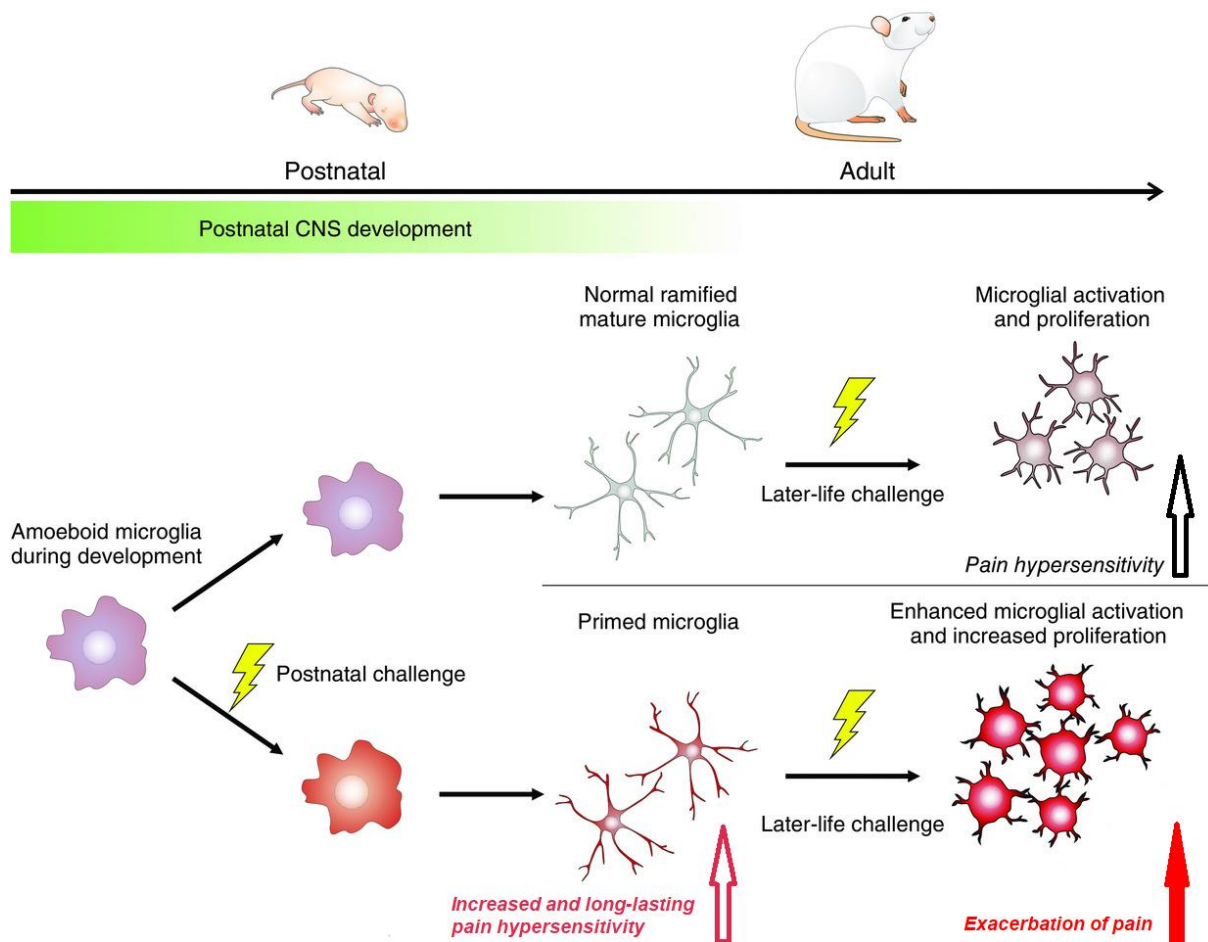


Figure 1: Early life stress and disruption of microglia.

Amoeboid microglia during postnatal development. (Upper part): microglia normally mature into ramified (surveilling) state. A challenge in adulthood (later-life) leads to pain hypersensitivity and microglia also responds to the challenge by taking a reactive amoeboid shape by thickening and retracting branches. (Lower part): challenges during adolescent (postnatal) periods lead to increased and long-lasting pain hypersensitivity and prime microglia. A challenge in adulthood (later-life) leads to exacerbation of pain and microglia proliferates taking an amoeboid shape.

Image modified from (Burke et al., 2016).

1.6.2 Role of astrocytes in pain

Function of astrocytes

Astrocytes are star-shaped most abundant glial cells in the CNS, constituting 40% to 50% of all glial cells forming networks with themselves and linked with neurons and blood vessels. Astrocytes regulate the external chemical environment of neurons during synaptic transmissions, by maintaining extracellular ion balance, removing positively charged potassium ions from the extracellular space, metabolizing glucose and neurotransmitters (Moraga-Amaro et al., 2014). Upon injury, they respond by clearing cellular debris, releasing trophic factors and form scars (Fields and Stevens-Graham, 2002; Gao and Ji, 2010). Astrocytes become activated to many CNS pathologies, resulting in an inflammatory response, change of external chemical environment of cells and the strength of synaptic transmission (Pekny and Nilsson, 2005). Zhang and colleagues (2017) showed that blocking the astrocyte activation (Flurocitrate) significantly reduced the proportion of neurons responding to deep tissue inputs. Unlike microglia, much less is known about the role and functional plasticity of astrocytes in modulating pain. Therefore this thesis focuses on microglia.

1.7 Research focus of this thesis

A number of psychosocial stress models are available in pre-clinical research to study the altered stress response which is implicated in various psychological disorders (Hannibal and Bishop, 2014; Hinwood et al., 2012; Hinwood et al., 2013; Kopp et al., 2013; Lehmann et al., 2016; Tynan et al., 2010) and here we focus on the altered pain-related responses after stress. Amongst other stress models such as social isolation etc., the repeated restraint stress also known as immobilization stress is a robust model that includes both physical and psychological component to study acute and chronic stress and its pathological changes (Hinwood et al., 2012; Hinwood et al., 2013; Kopp et al., 2013; La Porta and Tappe-Theodor, 2020; Park et al., 2011; Tynan et al., 2010). Only few animal studies are available that focused on restraint stress as a risk factor to induce or enhance low back pain (Hoheisel and Mense, 2015; La Porta and Tappe-Theodor, 2020). Hoheisel and colleagues (2015) showed that repeated immobilization stress was sufficient to alter the responsiveness

of spinal dorsal neurons processing input from the low back deep tissues. A number of studies based on nociceptive NGF injections have shown central sensitization to inputs from low back muscles or the thoracolumbar fascia (Hoheisel et al., 2013; Hoheisel et al., 2007; Reed et al., 2020; Sessler et al., 2021; Taguchi et al., 2008; Zhang et al., 2017). Therefore, the present study mainly focused on the impact and timing of repeated restraint stress in combination with NGF on the sensitization of spinalcord to input from low back muscles.

1.7.1 Electrophysiological recordings of dorsal horn neurons

Pre-clinical studies have shown the involvement of altered neuronal reponses and activation of glial cells in pain states including inflammatory, neuropathic, and non-specific low back pain, but evidence of their contribution in non-specific LBP after stress is understudied. A wide-range of studies use behavioral, immunohistochemical staining, electrophysiological techniques to explore the involvement of glial cells in pain, but studies on spinal neuronal activity and spinal sensitization after induction of stress are few (Hoheisel and Mense, 2015; La Porta and Tappe-Theodor, 2020). Since priming or latent sensitization is known to mediate the transition from an acute to a chronic state of low back pain, neuronal mechanism in this process needs to be studied. Electrophysiology can assess the neuronal responses to peripheral stimuli, receptive field modulation and ongoing activity.

1.7.2 Immunohistochemical staining of glial cells in the dorsal horn

Spinal glial cells are known to be involved and activated in the animal model of non-specific LBP. There is no morphological evidence on the functional plasticity of spinal microglial cells in the NGF-induced spinal sensitization of dorsal horn neurons preceded by restraint stress. As a response to an insult or injury, microglia are known to proliferate and transform their shape from surveilling to phagocytic state (Streit et al., 1999). Therefore, immunohistological staining was used to find out the morphological changes of microglia in the dorsal horn on the lumbar segment L2.

1.7.3 Hypothesis and aims

Hypothesis: A single injection of nerve growth factor (NGF) into a low back muscle of animals that have experienced repeated restraint stress is sufficient for a manifest sensitization of spinal dorsal horn neurons.

Aim of the project: The aim of this project was to investigate the differences in the sensitization process of the dorsal horn neurons based on the timing of the stressor.

Study 1:

Specific aim: To investigate whether repeated restraint stress in adulthood followed by NGF injection leads to manifest sensitization of the lumbar dorsal horn neurons.

In this study, animals in adulthood were subjected to restraint stress followed by single NGF injection into the multifidus muscle. Behavioral test was performed to test for mechanical hyperalgesia and the sensitivity of the DHNs were measured using *in-vivo* electrophysiology technique.

Questions addressed in this study are:

- (1) Whether animals that experience repeated restraint stress alone leads to drop in low back pain threshold?
- (2) Whether a subsequent NGF injection leads to manifest sensitization of the spinal neurons?

This study got recently published (Singaravelu et al., 2021b).

Study 2:

Specific aim: To investigate whether repeated restraint stress in early adolescence primes for long-lasting hyperalgesia followed by NGF injection in adulthood leading to enhanced sensitization.

In this study, animals in early adolescence were subjected to restraint stress followed by single NGF injection into the multifidus muscle in adulthood. Behavioral experiments were performed to assess mechanical hyperalgesia and the morphological changes of glial cells of the lumbar section L2 were analyzed using immunohistochemical staining technique.

Questions addressed in this study are:

- (1) Whether animals that experience repeated restraint stress alone across adolescence exhibit drop in low back pain threshold, and whether such hypersensitivity spreads to remote region?
- (2) Whether these animals experience long-lasting hyperalgesia in adulthood?
- (3) Whether a subsequent NGF injection in adulthood leads to enhanced pain-like behavior and show signs of activation of glial cells in the spinal lumbar segment L2.

2 MATERIALS UND METHODS

2.1 *In vivo* electrophysiology (study 1)

2.1.1 Animals and treatment groups

Animals

The electrophysiological experiments were performed on Sprague-Dawley rats. 11 rats (body weight: 380 – 450 g) were used for data acquisition. Eight weeks old male rats arrived from (Janvier labs) and were housed in groups of two in standard macrolon cages (length, width, height: 55x35x20 cm) and habituated for a week in the animal keeping room. The animals had free access to food and water *ad libitum* and were kept in 12h light/dark cycle. All the experimental procedures were approved by the committee on animal care and use (Regierungspräsidium Karlsruhe, Germany) and were carried out in accordance with German law on the protection of animals and ethical proposals of the International Association for the Study of Pain (IASP).

Treatment groups with a single NGF injection

In the electrophysiological study two treatment groups were tested and all animals received a single injection of nerve growth factor (NGF) into the left multifidus (MF) muscle directly before the recordings of the dorsal horn neurons (DHNs) started (see section: 2.1.3; Fig. 2).

Group 1

Repeated restraint stress + NGF: Repeated restraint (stress) was induced in five animals on 12 consecutive days for 1 hour every day in a narrow plastic restrainer (see section 2.1.2).

Group 2

Control + NGF: Six animals served as a control. The animals were handled on 12 consecutive days (transported to the laboratory, picked up by hand) like the stress animals but did not experience stress.

(This section in parts has been taken from Singaravelu et al., 2021b)

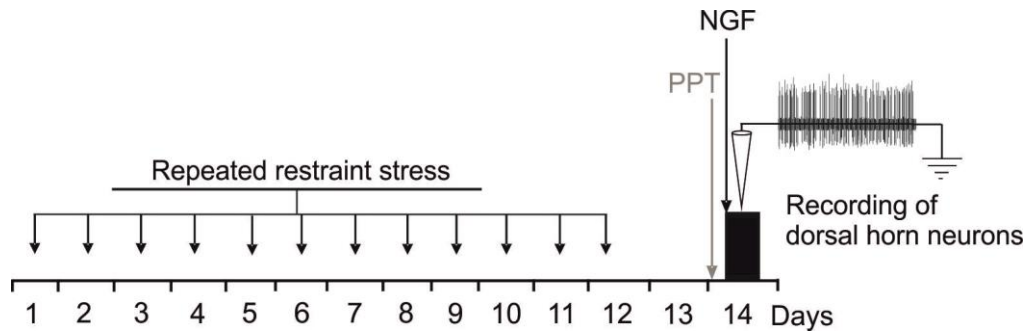


Figure 2: Experimental procedure.

Animals of the stress group were repeatedly stressed in a narrow plastic restrainer on 12 consecutive days for 1 hour every day. The pressure pain threshold (PPT) of the left multifidus muscle at vertebral level L5 was measured on day 14. On the same day, recordings of single spinal dorsal horn neurons were made (black bar). All animals received a single injection of NGF into the multifidus muscle directly before the electrophysiological recordings but after the PPT measurement.

Image modified from (Singaravelu et al., 2021b).

2.1.2 Repeated restraint stress

After one-week habituation to laboratory conditions, stress was induced in five animals similar to previous studies (Grundt et al., 2009; Hoheisel et al., 2015). The animals were placed for 1 hour every day on 12 consecutive days in a narrow plastic restrainer (inner length 17.5; inner height 5.5 in cms, Fig. 3). During the stress paradigm, signs of distress such as defecation, struggling during restraint (escape movements), and vocalization were observed.

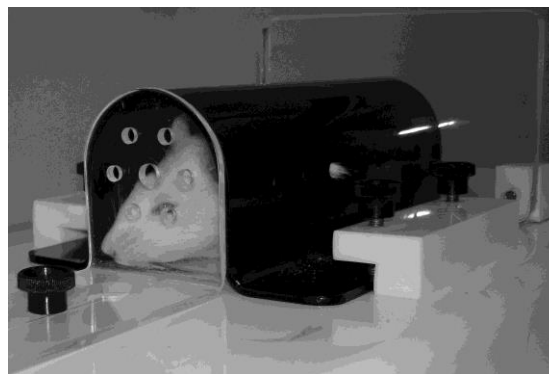


Figure 3: Repeated restraint stress.

Image of a rat placed inside the restrainer device used for the stress paradigm.

Image modified from (Singaravelu et al., 2021b).

2.1.3 Intramuscular injection of nerve growth factor

All the animals used in this study received a single injection of NGF. Directly before the recordings started intramuscular injections of 50 μ L nerve growth factor (NGF, human recombinant, Calbiochem®, Merck, Germany) at a concentration of 0.8 μ M (1.04 μ g NGF in 50 μ L PBS; pH of the solution: 7.2 – 7.3) was injected into the left multifidus (MF) muscle at the vertebral level L5 (Hoheisel et al., 2013; Hoheisel et al., 2007; Zhang et al., 2017). The NGF injections were made under final anesthesia (see 2.1.5) 3 mm lateral to the spinous process of L5 (Fig. 4) with a 27-gauge needle. The final concentration of NGF in the muscles after the injection was not determined in the experiments but the NGF concentration used is known to cause hyperalgesia when injected into the fascia of human erector spinae muscle (Deising et al., 2012), the GS muscle of rats (Hoheisel et al., 2007) and human masseter muscle (Svensson et al., 2003). The NGF injection was made by fixing the animal with hand (see fig. PPT) and pushing the needle (3 mm lateral) through the fascia and the MF muscle until it contacted the transverse process of the vertebra. The needle was then withdrawn 1 mm (see Fig. 4) and NGF was injected close to the transverse process into the muscle.

(This section in parts has been taken from Singaravelu et al., 2021b)

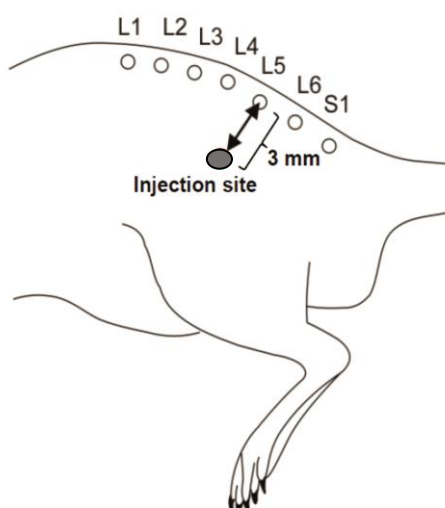


Figure 4: NGF injection site in low back multifidus muscle.

The site of NGF injection (grey dot) shown in the outline of rat body and the injection was made 3 mm lateral to the spinous process L5.

Image modified from dissertation (Zhang, 2016).

2.1.4 Pressure pain threshold of the low back

To test for mechanical hyper- or hypoalgesia caused by stress, we measured the pressure pain threshold (PPT) of the low back MF muscle. Right before the animal was anesthetized, the PPT was determined right before the animal was anesthetized with an electronic Von Frey anaesthesiometer (Life Science Instruments, Woodland Hills, CA, USA) on day 14 (see Fig. 2). Once the animal was fixed, a blunt tip with an area of 3.46 mm^2 was pressed with an increasing intensity to the MF muscle through intact skin at the vertebral level L5 (see Fig. 5). It is known that with the blunt tip, mainly nociceptors in deep tissue are excited but not or marginally in the skin (Takahashi et al., 2005). The PPT was defined as the minimum pressure intensity that is required to elicit a pain-related reaction (withdrawal and escape movements, vocalization).

(This section in parts has been taken from Singaravelu et al., 2021b)

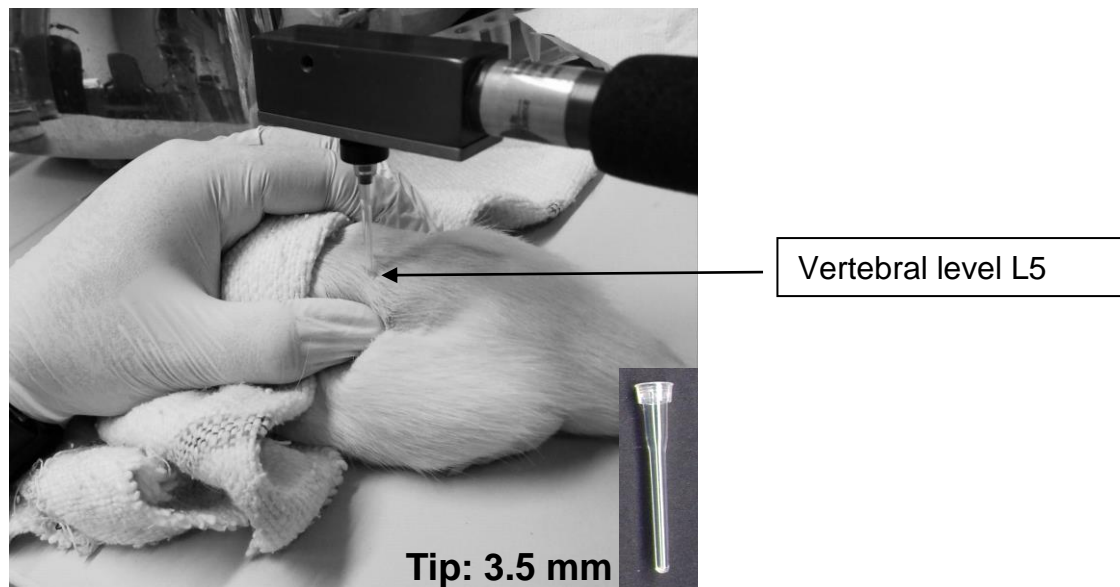


Figure 5: Pressure pain threshold of the low back multifidus muscle.

The PPT measurement at the vertebral level L5 with von Frey anaesthesiometer. The inset in the image shows the blunt tip used.

Image modified from master thesis (Goitom, 2021).

2.1.5 Electrophysiological recordings of the spinal dorsal horn neurons

Anesthesia

To induce deep anesthesia, the animals were intraperitoneally (i.p.) injected with thiopental sodium (Trapanal ®, Inresa GmbH, Germany), with an initial dosage of 100 mg/kg followed by 10 – 20 mg/kg x h of the same anesthetic intravenously (i.v.) with the help of an infusion pump (AL-1000, World Precision Instruments, Inc., USA) in order to maintain deep and constant level of anesthesia. To judge the depth of anesthesia before and during the surgery, the flexor-reflex was tested by pinching the hind paws or tail. Absence of the flexor-reflex was defined as a sign of deep anesthesia. In order to achieve muscle relaxation, an initial dosage of 0.5 ml i.v. of pancuronium bromide (pancuronium®, Inresa GmbH, Germany) was injected followed by 0.3 ml every hour. Pancuronium acts as a typical non-depolarizing curare-mimetic muscle relaxant by blocking the neuromuscular endplates. Because pancuronium relaxes the muscles and abolishes flexor-reflexes, during the experiment, marked blood pressure (BP) reaction to noxious stimulation was used to check the level of anesthesia. The anesthesia was considered deep when the increase in BP did not exceed 10 mmHg while presenting noxious stimuli i.e., pinch. When the BP reactions increased above 10 mmHg, the infusion of thiopental sodium was increased to reach a deeper level of anesthesia.

Surgical preparation

- Catheter implantation

A medical incision was made from the chest to chin with the help of a surgical blade (number 10, Swann-Morton, England). The salivary glands and muscles were separated using blunt forceps to expose the trachea, the right common carotid artery, and the right jugular vein. For catheterization purposes, polythene tube (Smiths Medical International Ltd., Great Britain) was used with an inner diameter of 1 mm and outer diameter 2 mm. The tubes were manually pulled out to the required diameter for the insertion into the right carotid artery for online BP registration and the right jugular vein for drug administration. The catheter of the right common carotid artery and the attached syringe were filled with Liquemin (Liquemin 5000, active ingredient: Heparin-Sodium, Ratiopharma GmbH, Germany) in tyrode to prevent blood clotting (0.5 ml Liquemin in 50 ml Tyrode). Tyrode was used as an artificial

interstitial fluid, containing salts and glucose, whose osmotic pressure and ion concentration are similar to interstitial fluids and which is often used in physiological and tissue culture experiments. The artery catheter was connected to a digital BP monitoring device (Blood Pressure display unit, Stoelting, USA) to measure the mean arterial BP. The continuous administration of the anesthetic was infused into the vein catheter with the help of an infusion pump. The mean arterial BP was always maintained above the physiological level 80 mmHg and when the BP dropped below this level for more than 10 min, the experiment was terminated for that particular animal.

- *Artificial ventilation*

The animals were connected to a respiratory pump via a trachea canula for artificial ventilation. The ventilation pump (Rodent Ventilator Model 683, Harvard Apparatus, Inc., USA) was set to a breath frequency of 90 – 100 breaths per minute and the breath volume to 2.0 ml/breath. It has been shown in literature that the breath volume of a rat is around 1.3 - 2.0 ml/breath at 60 – 114 breaths per minute (Waynforth and Flecknell, 1995). For ventilation, a gas mixture of 47.5% O₂, 2.5% CO₂, and 50% N₂ was used. This mixture causes a pO₂ of above 100 mmHg, pCO₂ between 30 and 40 mmHg and pH close to 7.4 in blood (Lambertz et al., 2008).

- *Body temperature*

The core body temperature of the animals was measured using a digital thermometer. Under anesthesia, the animals cannot regulate their body temperature. For this purpose, a thermometer was inserted 3 – 4 cm into the rectum and was monitored continuously. To maintain an optimum body temperature (37 – 38 °C) under anesthesia the animals were placed under warm lamps throughout the experiment.

- *Laminectomy*

To expose the spinal cord the animals were mounted on a spinal frame (David Kopf Instruments, USA) and an incision was made by cutting the skin parallel to the vertebrae thoracal 9 to lumbar 6. The vertebrae were prepared and the spinal column was supported both towards the cranial and caudal side using clamps. The spinal segments Th11 – L5 were exposed by removing the dorsal vertebrae extensions.

The spinal cord segments L2 – L6 are located at the vertebrae Th12 – L1. The dorsal roots of the spinal cord segments L4 – L6 appear in a V-shape. The dura mater was incised longitudinally exposing the dorsal roots. The vertebral column was fixed using metal clamps and the dorsal roots L3 – L5 were isolated using a parafilm and exposed for applying the electrical search stimulus (see Fig. 6). A unilateral pneumothorax was performed to avoid any breathing related movement of the spinal cord by inserting a small tube (inner diameter 3 mm, outer diameter 4.5 mm) in the 8th intercostal space. A tyrode-moistened cotton ball was used to cover the exposed spinal cord and corresponding dorsal roots and covered with skin warm agar solution (0.5 g agar to 20 ml Tyrode) in order to stabilize the spinal cord. Once the agar-gel hardened, the moistened cotton call was cut out and the exposed spinal cord was covered with silicon oil (M100Roth, Carl Roth GmbH, Germany) for electrical isolation. The caudal back muscles and the overlying fascia at the vertebral level L5 were not affected by the laminectomy because the spinal segments are located 3 – 5 cm cranially from these muscles (Taguchi et al., 2008).

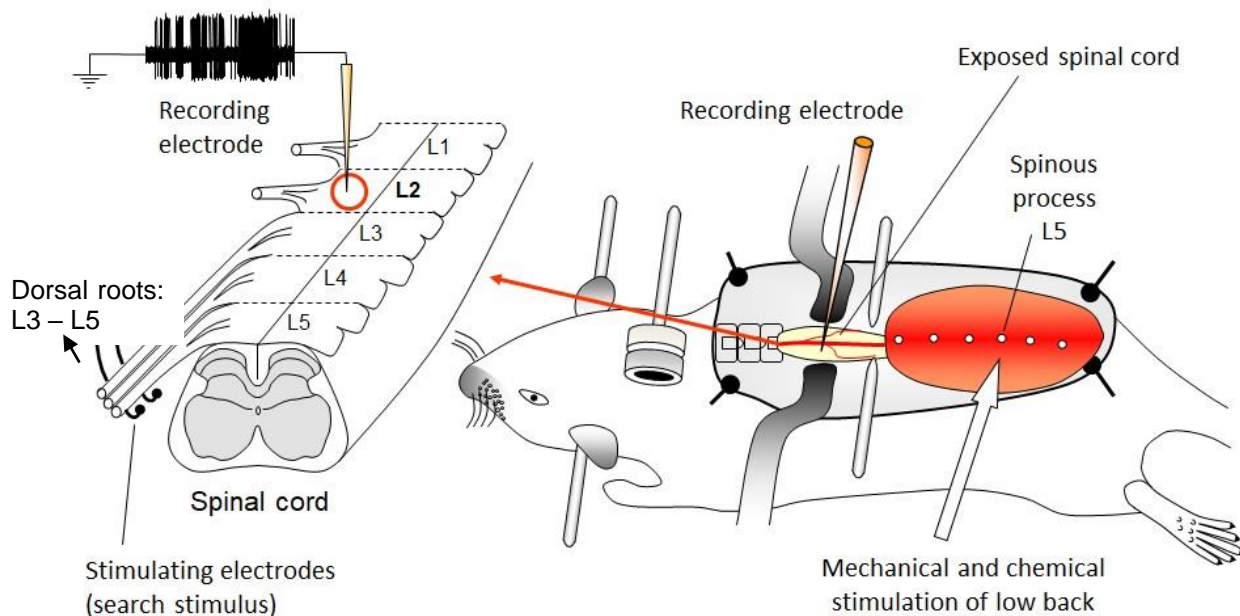


Figure 6: Setup and extracellular recording of dorsal horn neurons with input from low back.

Schematic picture of the setup. The animal was mounted on the spinal frame using clamps. As a search stimulus, the dorsal roots L3 – L5 were electrically stimulated using a bipolar electrode. The recording electrode was made with glass/microelectrode filled with 5% NaCl and the recording were made in the segment L2 where the inputs from low back muscles are mainly processed. NGF was injected 3 mm lateral to the spinous process L5. Mechanical and chemical stimulation of the low back and outside were presented close to the spinous process L5.

Image modified from (Taguchi et al., 2008).

- *In-vivo recording of single dorsal horn neurons*

In-vivo extracellular recordings of the single DHNs were made in the spinal segment L2 ipsilateral to the site of the NGF injection (Fig. 6). This segment is known to receive strong afferent input from the deep tissues in the low back located at the vertebral level L5 (Taguchi et al., 2008). For recording purpose, glass microelectrodes were prepared from borosilicate glass capillaries (outer diameter 1.5 mm and inner diameter 0.86 mm, GB150F-10, Science Products, GmbH, Germany) with the help of a horizontal pipette puller (Brown-Flaming Micropipette Puller, Model P-80, Sutter Instrument Co., USA). The glass microelectrodes were filled with 5% sodium chloride (NaCl) to record extracellular action potentials (APs) of single DHNs. Penetrations were made up to a depth of 1000 μ m from the dorsal surface of the spinal cord. The recorded APs were amplified 10 times with the help of a preamplifier (EXT-10C, npi electronic GmbH, Germany) and again 10 times by an AC-DC amplifier (neurology 106, DigitimerNeurolog System, Digitimer Ltd., Great Britain). The APs were filtered (low frequency: 5-500 Hz, high frequency: 50 kHz; Neurolog 125, Digitimer Neurology System, Digitimer Ltd., Great Britain) and all the recordings were monitored with the help of an oscilloscope (Classic 6000 DSO, Gould Instrument Systems, USA). The analog signals were digitized using an analog to digital convertor (CED-1410 interface; Cambridge Electronic Design Limited, Great Britain) at a sampling rate of 20 kHz. The data were recorded and stored in a computer using Spike 2 software (Cambridge Electronic Design Limited, Great Britain) and the APs were counted using a template criterion.

- *Electrical search stimulation*

In order to have an unbiased sampling of the DHNs, an electrical search stimulus was delivered with the help of a single bipolar, hooked ball platinum electrode to the dorsal roots L3, L4 during the microelectrode tracking (intensity 5 V, width 0.3 ms, and frequency 0.33 Hz, see Fig. 6). All the DHNs exhibiting a stable response to this search stimulus were used for the study. The stimulus intensity and frequency used is known to not induce long-term potentiation (Hoheisel et al., 2007). The DHNs were differentiated from the primary afferent axons when the neuronal APs demonstrated a clear jitter (the variability in latencies) and did not follow a high-frequency stimulation at 333 Hz (Hoheisel and Mense, 2015; Taguchi et al., 2008). During recording, the general parameters such as the threshold and latency of an AP and the depth of

recording of the neuron were noted down. This was followed by measuring the neuronal resting (ongoing) activity for one minute before further testing with mechanical or chemical stimuli. The neurons that showed ≥ 1 impulse/min were considered to have resting activity (Hoheisel et al., 2013). Once a neuronal connection was established, the electrical stimulus was turned off followed by a mechanical or chemical stimulus presented on the low back and hind limb (see Fig. 7) and the also the neuron type was determined. The recordings of DHNs lasted for maximum 4 hours after the NGF injection. The number of DHNs recorded within that time is given in Table 1. At the end of the recordings the animals were euthanized with an overdose of anesthetic under deep anesthesia.

- *Mechanical and Chemical Stimulation*

After the electrical search stimulus and recording of resting activity, mechanical and chemical stimuli were applied to identify receptive fields (RFs) and the response of that neuron. The types of mechanical stimulation that were used are: as an innocuous stimulus, a touch with an artist's brush was used on the skin and thoracolumbar fascia (TLF); a moderate pressure was applied using a blunt probe (back side of the artist's brush) on the skin, muscles and TLF, and for noxious stimuli, pinching with a sharp watchmaker's forceps (skin and TLF) or as a noxious pressure with a blunt probe (muscles and TLF) was used. Five percent hypertonic saline (50 μ l) was injected to a muscle as noxious chemical stimuli to identify RFs underlying the skin or fascia.

- *Receptive field identification and neuronal classification*

A receptive field is defined as the region of the body in which presenting a stimulus leads to firing of action potentials in a neuron. The search for RFs of each neuron was performed using a standardized protocol (see Fig. 7) and were identified with ranked mechanical stimuli (innocuous to noxious), applied to the low back structures, left hind limb, hip, lateral abdominal wall, and the tail. The responsiveness to mechanical stimulation was tested only to the ipsilateral side of the injection because former studies did not show evidence for contralateral RF expansions (Hoheisel et al., 2013; Hoheisel et al., 2015).

(This section in parts has been taken from Singaravelu et al., 2021b and the dissertation of Zhang, 2016).

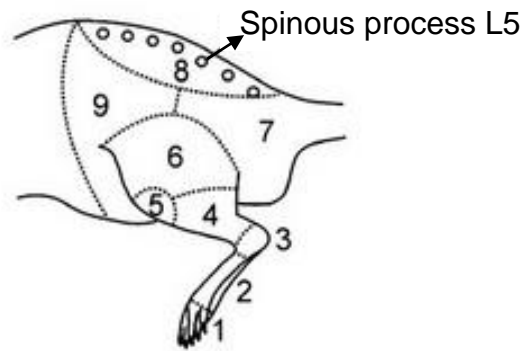


Figure 7: Standardized protocol for receptive field search.

Schematic picture of the standard outline of the rat low back and hind limb used to searching for receptive fields: 1) toes, 2) metatarsus, 3) heel, 4) lower leg, 5) knee, 6) thigh, 7) base of tail, 8) low back, and 9) lateral abdomen.

Image modified from (Hoheisel et al., 2015).

When a neuron responded to touching or pinching of the skin, it was considered as a neuron with cutaneous input (see Fig. 8 A). Neurons were considered having a deep input when they responded to pressure applied to a muscle or any other deep tissues with a blunt probe but did not respond to the touching or pinching of the overlaying skin (see Fig. 8 B). Neurons that received both cutaneous and deep input (i.e., skin plus muscle or fascia) were considered as convergent input (see Fig. 8 C). Intramuscular injections of 5% hypertonic saline was applied to check for RFs in a muscle underneath a mechanosensitive RF in the TLF or skin. When a neuron responded to the electrical search stimulus but could not be excited by the mechanical stimuli then the neuron was considered without an RF. The location and the size of the receptive fields (RFs) were also determined and marked on a standard outline of the rat low back and the hind limb (see Fig. 8). The proportion of neurons with skin input, deep input, convergent input and unknown inputs were calculated and compared.

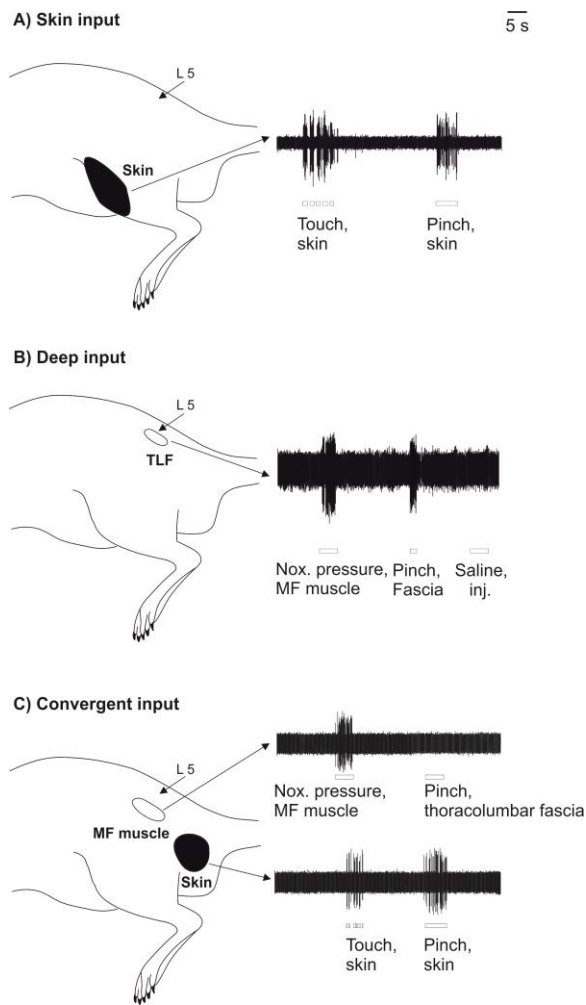


Figure 8: Responses of a single dorsal horn neuron.

A) Example of a DHN having skin input from the knee and thigh regions (stress + NGF group). The neuron responded to the touching and pinching of skin. **B)** Example of a DHN having deep input the TLF (stress + NGF group). The neuron responded to noxious pressure applied to the muscle, and to pinching of the overlying thoracolumbar fascia (TLF) but not to the injection of isotonic saline. **C)** Example of a convergent neuron having input from the lumbar MF muscle and input from the skin close to the tail base (stress + NGF group). (TOP) the neuron responded to noxious pressure applied to the muscle but not to pinching of TLF, indicating a receptive field (RF) in the muscle under the fascia. (Bottom) the same neuron responded to touching and pinching the skin. The schemes show the location and size of the RFs from which the neuron could be activated. Open outline: RF in the MF muscles; black area: RF in the skin. Open bars indicate the time and duration of stimulation. L5: spinous process L5. NGF: nerve growth factor.

2.1.6 Data analysis

The pressure pain threshold and resting activity data for study 1 are shown as individual values with their respective median. For the latency, discharge frequency, conduction velocity and recording depth (Table 1), data are shown as an interquartile range: median (quartile 3 - quartile 1) showing a measure of statistical dispersion. The proportion of neurons was compared using the Fisher exact probability test. The values of the PPT and resting activity were compared using the Mann-Whitney U (Wilcoxon) test. A probability level of less than 5% ($p < 0.05$, 2-tailed; statistical software: GraphPad Prism 6) was regarded as significant. The effect sizes were determined using Cohen's d (difference in means divided by pooled SD) (Cohen, 1969). An effect size > 0.2 was considered as 'small effect', > 0.5 as 'moderate', and > 0.8 as 'large'.

The experimenters were not blinded for study 1. To minimize investigator bias, an electrical search stimulus was used for unbiased sampling of DHNs and the search for RFs strictly followed a standard protocol (refer section 2.1.5, receptive field identification).

(This section in parts has been taken from Singaravelu et al., 2021b)

2.2 Quantitative immunohistochemistry (study 2)

2.2.1 Animals and treatment groups

Animals

In this immunohistochemical study, the experiments were performed on Wistar rats. Three weeks old (postnatal day (PD) 21) male rats arrived from (ENVIGO, Netherlands) and were housed in groups of four in standard macrolon cages (length, width, height: 55x35x20 cm). In contrast to SD rats, Wistar rats are known to be more sensitive to stressors (Lopez-Rubalcava and Lucki, 2000) and are more suitable to investigate long-term effects of adolescent stress on pain modulation. 23 rats were used for data acquisition in immunohistochemistry. All the animals had free access to food and water *ad libitum* and were kept in a normal 12h light/dark cycle. All the experimental procedures were approved by the committee on animal care and use (Regierungspräsidium Karlsruhe, Germany) and were carried out in accordance with German law on the protection of animals and ethical proposals of the International Association for the Study of Pain (IASP). One animal died and the results were excluded from further analysis.

Treatment groups with injections of NGF or saline or both

On arrival, animals were briefly (2 hours) habituated to their new home cage in the animal keeping room followed by 1 hour to the experimental procedure room. The repeated restraint stress (R) paradigm (refer to section 2.2.2) was induced similar to study 1 but in the early adolescence phase (PD 21). The aim of study 2 is the impact of stress in adolescence (study 1: adulthood) and for this reason the animals were habituated to the animal facility briefly on arrival and before stress was induced. The injections of saline or NGF or both into the left multifidus (MF) muscle was injected in adulthood (Schneider, 2013) and all the animals received two injections at an interval of five days (see section 2.2.3). In this study, animals were randomly assigned to four treatment groups. Two treatment groups refer to the 'latent sensitization', (i) handling animals (control, C) in adolescence and injection of saline (S) followed by NGF (N) (see Sec: *Group 1*), and (ii) where repeated restraint stress (R) in adolescence alone followed by two saline (SS) injections in adulthood (see *Group 2*), and in adulthood primes microglia in DHNs. The other two groups refer to 'manifest sensitization', (iii) handling animals (control, C) in adolescence followed by two NGF injections (NN)

(see Sec: *Group 3*), and (iv) where repeated restraint stress (R) in adolescence and injection of saline (S) followed by NGF (N) in adulthood (see *Group 4*), and in adulthood activates microglia in DHNs. The experiments were performed in the inactive phase of the animals. The perfusion (refer to section 2.2.5) and tissue collection (refer to section 2.2.5) were performed within 5 hours from the start of the inactive cycle. All the animals were transcardially perfused one day after the second injection of either saline or NGF and the spinal cord of lumbar segments L1 – L5 were harvested for immunohistological analyses (see Fig. 9).

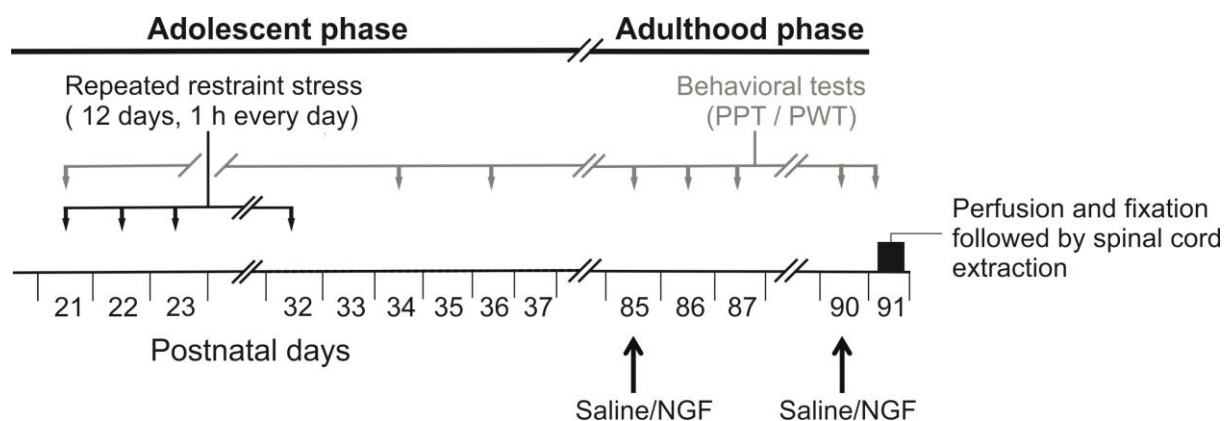


Figure 9: Experimental design.

Animals of the stress group were repeatedly stressed (R) in a narrow plastic restrainer for 12 consecutive days for 1 h every day on postnatal days (PD21 - 32; early adolescent phase). The pressure pain threshold (PPT) of the multifidus muscle at vertebral level L5 and paw withdrawal threshold (PWT) of the hind paws were measured at different time points (grey line) (refer to section 2.2.4). All animals received injections of saline/NGF on PD85 and PD90 (adulthood phase) respective to the group they belonged to (refer to section 2.1.1). On PD91 (black bar) all animals were perfused and fixed. The spinal cord tissues were extracted and stored at -80°C .

Image modified from (Singaravelu et al., 2021a).

Group 1

Control + Saline + NGF (CSN): The animals ($n = 6$) in this group were handled on 12 consecutive days (transported to the laboratory and manipulated by hand) similar to the stress animals but without repeated restraint stress. These animals received saline (vehicle) as their 1st injection followed by NGF at an interval of 5 days.

Group 2

Repeated restraint stress + Saline + Saline (RSS): In this group, R ($n = 6$) was induced on 12 consecutive days for 1 hour every day in a narrow plastic restrainer (refer section 2.2.2). These animals received 2 saline injections 5 days apart.

Group 3

Control + NGF + NGF (CNN): The positive control animals (n=6) were handled similarly to stress animals but without repeated restraint stress. These animals received 2 NGF injections at a 5-day interval in adulthood.

Group 4

Repeated restraint stress + Saline + NGF (RSN): In this group, R (n = 5) was induced on 12 consecutive days for 1 hour every day in a narrow plastic restrainer (refer section 2.2.2). These animals received 2 saline injections 5 days apart.

(This section in parts has been taken from a preprint server Singaravelu et al., 2021a and master thesis of Goitom, 2021)

2.2.2 Repeated restraint stress (R)

The R was induced as previously described in section 2.1.2., by placing the animals in a narrow plastic restrainer (refer to Fig. 3). The size of the restrainer used in this study was adapted according to the young age of the animals (inner length 15 cm; inner height 4 cm). The body weight was measured on 12 consecutive days before the start of the stress paradigm and on days before the behavioral experiments (see section 2.2.4; Fig. 9). We also observed signs of distress such as vocalization, struggling during restraint (escape movements), urination, and/or defecation during the R paradigm.

(This section in parts has been taken from a preprint server Singaravelu et al., 2021a)

2.2.3 Injection of nerve growth factor and saline

In this study, as a second intervention all the animals received injections of saline and NGF or both at two different time points (PD 85 and PD 90) with an interval of five days (see Fig. 9). Intramuscular injections of NGF and saline were performed as described in section 2.1.3 and both the injections were administrated at the same site (see Fig. 4). Injections of isotonic saline (50 µl, 0.9 %) served as control. In a former study no visible signs of muscle inflammation were observed after the injections of either saline or NGF (Hoheisel et al., 2013).

(This section has been taken from a preprint server Singaravelu et al., 2021a)

2.2.4 Behavioral tests

- *Pressure pain threshold*

To assess for mechanical hyperalgesia both local and outside at the site of injection, behavioral tests such as pressure pain threshold (PPT; local) and paw withdrawal threshold (PWT; away) was tested. The PPT of the low back MF muscle was performed as mentioned in the section 2.1.4. The PWT, by testing the plantar skin of the paw was tested to evaluate spreading of hyperalgesia into other body regions after stress and NGF/saline injections. The tests were performed before and after stress and in conjunction with the intramuscular injections (see greyline in Fig. 9).

- *Paw withdrawal threshold*

To test the paw withdrawal sensitivity to noxious mechanical stimuli, an electronic von Frey esthesiometer equipped with a rigid cylindrical tip of 0.8 sq.mm (Electronic von Frey esthesiometer, IITC Inc. Life Science, USA) was used. Following the PPT measurement of the low back, the animals were placed into a plexiglass box (length: 20 cms, width: 10 cms; height: 14 cms) with a metal grid as a base for a further 30 mins of acclimatization (see Fig. 10). Before the first measurement on PD 36, all the animals were habituated to the metal grid table on two consecutive days (PD 34 and PD 35) for 45 minutes. With the electronic esthesiometer, pressure was applied to the plantar surface of both the hind paws (ipsilateral to the injection site followed by the contralateral side) until the animal withdrew it. The PWT measures nociception by provoking the nocifensive hind-paw flexion reflex with mechanical stimulation and was calculated as the mean of five independent recordings (Caspani et al., 2014). This reflex corresponds to the human lower limb flexor reflex but does not equal the complexity of feeling pain. Nevertheless, the reflex intensity correlates well with pain perception in humans (Sandrini et al., 2005) and is valuable to monitor the changes at peripheral and spinal levels of the somatosensory system (Reitz et al., 2016).

(This section in parts has been taken from a preprint server Singaravelu et al., 2021a and master thesis of Goitom, 2021)

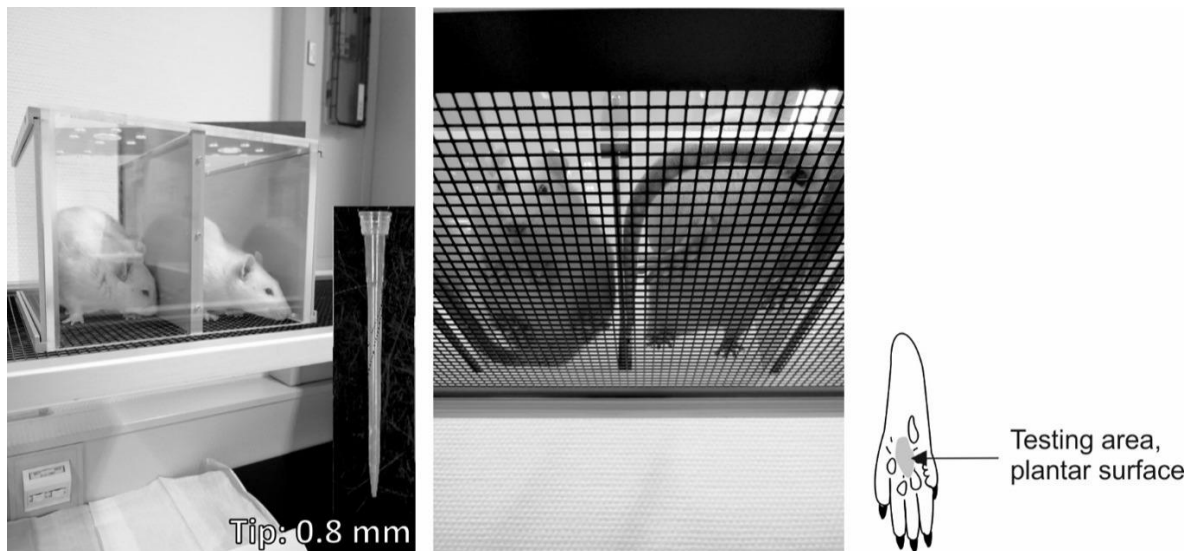


Figure 10: Paw withdrawal threshold of the hind paws.

The images show rats placed in plexiglass box on a metal grid habituating for the PWT measurement and the test site was plantar surface of the hind paws. The inset in the image shows the rigid cylindrical tip used to test PWT.

2.2.5 Perfusion and tissue processing

- *Transcardial perfusion*

On PD 91, one day after the second injection (see Fig. 9; black bar), the animals were euthanized with an overdose of intraperitoneal injection of thiopental sodium (Trapanal®, Inresa GmbH, Germany) and transcardially perfused. With the help of blunt scissors, a 5 – 6 cms horizontal incision was made through the skin and the abdominal wall beneath the thoracic cavity, and the liver was separated from the diaphragm. The thoracic cavity was opened by carefully making an incision in the diaphragm. The ribs were cut bilaterally along the sternum exposing the thoracic cavity. The mediastinum and other tissues connecting or surrounding the heart were separated carefully to expose the whole heart. The apex (posterior end of the left ventricle) was cut with scissors and a blunt perfusion needle was inserted through the left ventricle into the ascending aorta. The needle tip was visible through the aorta wall and it was made sure it did not reach the aortic arch where the brachial and carotid arteries diverge. The needle was secured using a hemostat to prevent any leakage during perfusion and a second incision was made to the right atrium with iris scissors. The perfusion started with 0.1 M phosphate buffered saline (PBS) for 1 – 2 minutes followed by 4 % paraformaldehyde (PFA) in 0.1 M PBS. The clearing of the liver blood was used as an indicator for good perfusion. Once the liver was clear

(pale coloration after blood removed from the system), 4 % PFA was perfused for 20 – 30 minutes which was followed by 20 – 30 minutes of PBS perfusion.

- *Tissue processing*

Once the perfusion was complete, a laminectomy was performed and the spinal segments L1 – L5 were removed. Individual segments L1 – L5 were separated and a thin needle was carefully inserted on the ventral horn to the contralateral side of saline/NGF injections to mark and differentiate the contralateral from ipsilateral side for analysis (see red circle Fig. 11 A). The segments were then stored in a falcon tube filled with 10% sucrose solution in 0.1 M PBS at 4 °C for 24 hours. Later, the spinal segments were transferred to another falcon containing 30% sucrose solution in 0.1 M PBS at 4 °C also for 24 hours. On the following day, tissues were rapidly frozen on dry ice and the 30% sucrose solution served as a cryoprotectant, dehydrated the tissue, and prevented formation of ice crystal artifacts. 20 µm thick cross sections of the spinal L2 segments were made on a cryostat (Cryostat NX70, Thermo Fisher Scientific Inc., USA) and mounted on glass slides. The segment L2 was chosen as it is known to receive strong input from deep tissues in the low back located at the vertebral level L5 (site of NGF/saline injections) (Taguchi et al., 2008). For immunofluorescence, staining five animals per group were chosen which were controlled for good perfusion and tissue quality. Three cross-sections of the intact spinal segment L2 were selected from each animal at random.

(This section in parts has been taken from a preprint server Singaravelu et al., 2021a and dissertation of Zhang, 2016)

2.2.6 Immunofluorescence labeling

- *Double immunofluorescence labeling*

A mixture of both the primary and both the secondary antibodies were used to perform immunohistochemistry.

Iba-1 labeling for microglia

To visualize the structural changes of microglial cells, L2 spinal cord sections were immunohistochemically stained for ionized calcium-binding adapter molecule 1 (Iba-1), a protein explicitly expressed in microglia and is upregulated during microglia activation (Hinwood et al., 2012; Hinwood et al., 2013; La Porta and Tappe-Theodor,

2020; Romero-Sandoval et al., 2008). The spinal cord sections were first incubated in 10% Roti®-block (Carl Roth, Germany) at room temperature for 1 hour. The tissues were then incubated in rabbit anti-Iba-1 polyclonal antibody (1:1000; Abcam, United Kingdom) also at room temperature for 16 hours. Followed by incubation in secondary antibodies, Cy3™ – conjugated goat-anti-rabbit IgG antibody (1:500; Jackson ImmunoResearch, USA) at room temperature in dark for 4 hours. The tissues were washed three times in PBS for five minutes each and mounted with Roti® mounting medium (Carl Roth, Germany).

GFAP labeling for astrocytes

To visualize the structural changes of astrocytes, L2 spinal cord sections were stained for glial fibrillary acidic protein (GFAP), an intermediate filament protein explicitly expressed astrocytes (Okada-Ogawa et al., 2009; Reeves et al., 2011). The staining was carried out in the same sections along with Iba-1 staining. The tissues were incubated in mouse anti-GFAP monoclonal antibody (1:500; Sigma-Aldrich, USA) at room temperature for 16 hours. Followed by incubation in secondary antibodies, DyLight TM488-conjugated donkey anti-mouse IgG antibody (1:250; Jackson ImmunoResearch, USA) at room temperature in dark for 4 hours. The tissues were washed three times in PBS for five minutes each and mounted with Roti® mounting medium (Carl Roth, Germany). Negative control experiments were performed by omission of two primary antibodies to test for unspecific staining.

(This section in parts has been taken from a preprint server Singaravelu et al., 2021a and master thesis of Goitom, 2021)

2.2.7 Image processing and quantification

We obtained digitized images of the immunolabelled spinal cord tissues with the help of a confocal laser-scanning microscope (Leica TCS SP8 ABOS, Wetzlar, Germany) using 10x and 40x oil immersion objective lens with a computer-based imaging software LAS-AF (Leica, Germany) (see Fig. 11 B). Immunofluorescence was acquired using a scanning sequential mode to avoid crosstalk among simultaneously scanned channels with two laser lines. The Cy3™-conjugated secondary antibody was detected by a DPSS-laser at 561 nm and the DyLight TM488-conjugated secondary antibody was detected using Argon-laser at 488 nm (Leica Microsystems,

Germany). Three-dimensional images were acquired at 40x magnification over 20 μm z-axis with a step size of 1 μm and all the images were prepared with a maximum intensity in Z-stack projection.

Eight regions of interest (ROIs) at 40x magnification were selected from the dorsal horn neuron of every section for quantitative analysis on the ipsilateral (Ip.) and contralateral (Con.) side to the injection of saline/NGF. Four ROIs of 256 μm x 256 μm were defined both on the Ip. and Con. side, two of which were located in the superficial DH (medial and lateral; laminae I – II), and two at various depths in the deep DH (dorsally and ventrally deep; laminae IV – V; see Fig. 11 A). All the images used in this study were made using identical parameters.

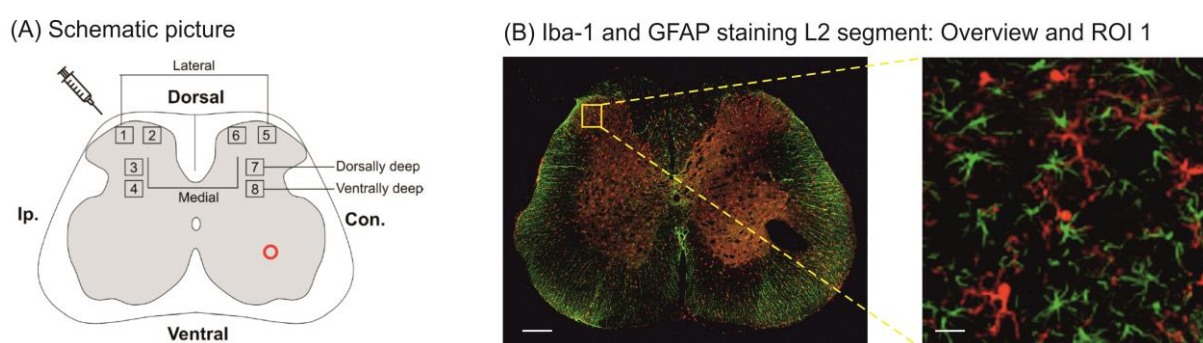


Figure 11: Spinal L2 segment with region of interests

A) A schematic illustration of the region of interests on a spinal lumbar 2 (L2) section (refer to section 2.2.7). The red circle on the ventral horn of the contralateral side denotes the manually made pinhole to identify the contralateral side. **B)** An example overview image (10x) of an Iba-1 (red) and GFAP (green) stained L2 section (scale bar: 300 μm) and magnified image (40x) of ROI 1 (scale bar: 100 μm). The hole on the ventral horn of the contralateral side denotes the manually made hole with a pin for the identification of contralateral side. Ip., ipsilateral; Con., contralateral; Iba-1, ionized calcium binding adapter molecule 1; GFAP, glial fibrillary acidic protein; ROI, region of interest.

Image modified from (A) dissertation of (Zhang, 2016) and (B) (Singaravelu et al., 2021a).

In total 480 images with 40x magnification were captured and analyzed (8 ROIs per section x 3 sections per animal x 5 animals per group x 4 groups). All the obtained images were quantitatively evaluated with an image analysis software (Fiji Image J; NIH, USA). The immunostaining intensity for both Iba-1 and GFAP i.e. the threshold level for immunostaining against background was defined with the default threshold given by the software. This is calculated by the software using the formula: $\text{threshold} = (\text{average background} + \text{average objects})/2$.

- *Description of general parameters for single microglial cell evaluation*

The below evaluations were performed based on the findings from the dissertation of Zhang J.J., 2016 and can be chosen in the Fiji Image J software under the tab analyze -> set measurements. The following measurements were made:

(i) Intensity of a given ROI: is the brightness of immunostaining represented in mean grayscale value within the immunoreactive area. A grayscale value '0' refers to black and '255' refers to white and a higher intensity of immunostaining refers to higher gray value (Chacur et al., 2009).

(ii) Immunoreactive area of a single cell: This selection was made to calculate the Iba-1 stained individual cell area in a given ROI and is the area of selection in square pixels. Area is in calibrated units such as micrometers (μm). The immunoreactive area (see Fig. 12 A; yellow area) is expected to increase with the hypertrophism of cells (Chacur et al., 2009).

(iii) Perimeter of a single cell: is calculated based on the outline length (boundary length) of the immunoreactive area and is expressed in μm . Microglial cells that are activated tend to show a lower boundary length because the cells are less ramified (Zanier et al., 2015). In short, the length of the outside boundary of a selected cell (see Fig. 12 B; length of the yellow border).

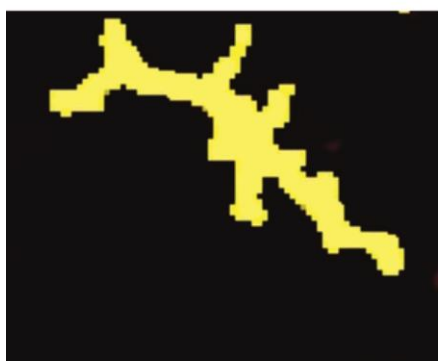
(iv) Feret's diameter of a single cell: is the longest distance between two parallel lines in perpendicular to that distance (the longest distance) and drawn at boundary of the immunoreactive area. Microglial cells that are activated tend to have a smaller Feret's diameter because the cells are less ramified (Zanier et al., 2015). In short, the longest distance between any two points along the cell boundary (see Fig. 12 C; arrowed line measuring length between two longest points).

(v) Circularity of a single cell: is calculated using the formula $4\pi \times (\text{area}/\text{perimeter}^2)$ and varies from '0' (linear polygon) to 1 (perfect circular object). The cells become more circular in activated and phagocytic state because of fewer or no ramification

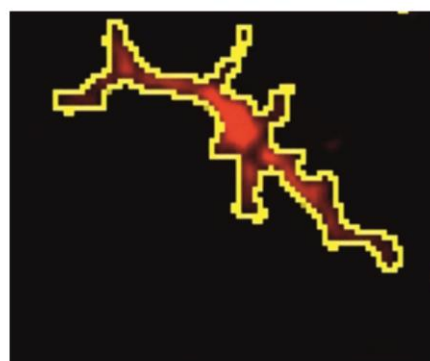
(Zanier et al., 2015). In short, a value of '1' indicates a perfect circle and as the value approaches '0', it indicates an increasingly elongated shape (see Fig. 12 D).

(This section in parts has been taken from a preprint server Singaravelu et al., 2021a and dissertation of Zhang, 2016)

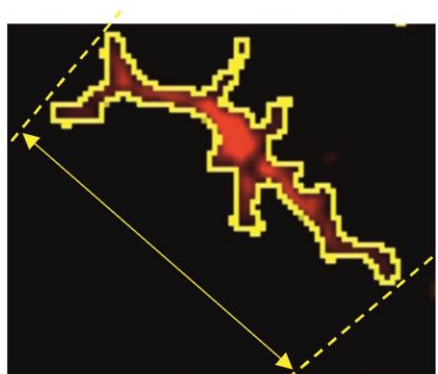
(A) Immunoreactive area



(B) Perimeter



(C) Feret's diameter



(D) Circularity



Figure 12: Parameters for single microglial cell evaluation

A) Immunoreactive area: area of selection (yellow area) in square pixels. Area is calibrated in units μm^2 . **B)** Perimeter: the length of the outside boundary (yellow line) of the selected cell expressed in μm . **C)** Feret's diameter: the longest distance between any two points (yellow line with arrow heads) along the cell boundary in μm . **D)** Circularity: is calculated using the formula $4\pi \cdot \text{area} / \text{perimeter}^2$. A value of 1.0 indicates a perfect circle and as the value approaches 0.0, it indicates an increasingly elongated shape. (TOP) example of a phagocytic state microglia cell showing strong circularity. (Bottom) example of a phagocytic state microglia cell showing weak circularity.

- Pixel classification

The pixel classification is one of the most popular workflow in ilastik. This workflow assigns labels to pixels based on pixel features and user annotations (Berg et al., 2019). The technique was only applied for microglial cells to identify their soma and its neighboring processes, which belonged to the cell but not connected to the soma, and to remove the processes that did not show any neighboring soma (see Fig. 13). Out of the 480 images, ten images were randomly selected and two semantic classes were defined such as 'microglia' and 'background' (see Fig. 13 B). For each class, examples were provided by painting brushstrokes of two different colors directly on the input data. For each pixel of the image, ilastik then estimates the probability that the pixel belongs to each of the above-mentioned semantic classes (see Fig. 13 C). When the training was sufficient enough to distinguish microglia and background, all the 480 images were loaded for pixel classification. The generated probability maps (see Fig. 13 D), were stored and directly used for evaluating the quantitative changes in the functional plasticity with Image J (NIH, USA). For each ROI, the intensity of stained microglial cells was measured and the background was measured (Fig. 13 D; red dashed lines) and subtracted. The number of Iba-1 stained microglial cells were counted manually in each ROI and their states were classified as explained in the following sub section and all the images were analyzed with identical parameters.

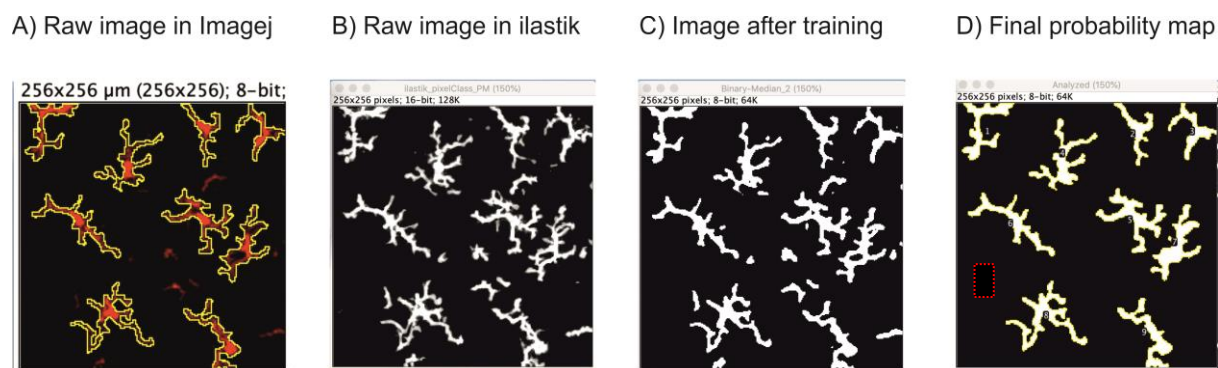


Figure 13: Pixel classification using ilastik.

A) Example ROI image opened with imageJ highlighting individual microglial cells. **B)** Example ROI image opened with ilastik showing individual microglial cells. **C)** Example ROI image with ilastik showing individual microglial cells after pixel classification training. **D)** Generated probability map as a final image used for microglial cell evaluation for parameters such as immunoreactive area, perimeter, Feret's diameter and circularity. Red dashed lines was the unstained area for the measurement of the background.

2.2.8 Reactive microgliosis and classification of microglia states

The term gliosis means a nonspecific reactive change that occur in glial cells as a response to injury or insult leading to proliferation or hypertrophy (Chen et al., 2018). The functional plasticity and classification of different states of microglia (see Fig. 14) were adapted from (Streit et al., 1999) and differentiated from resting to phagocytic state. Resting microglia are also referred to surveilling microglia and are characterized by small cell bodies, long, thin and highly motile processes (Kettenmann et al., 2011; Stratoulis et al., 2019; Tay et al., 2019; Wolf et al., 2017). Hyper-ramified (intermediate) state is characterized by long and thick process. The reactive microglia (also referred to as activated state are) characterized by an enlarged and darkened soma, with thick and less ramified processes (Ayoub and Salm, 2003; Swanson et al., 2020). The activated microglia sometimes are also rod shaped and are characterized by long and polarized processes, fewer branches and quite long planar angles (Nissl, 1899). The phagocytic state microglia are characterized by an amoeboid shape with enlarged and densely stained soma with few (upto 4 processes in this study) or no processes (Davis et al., 1994) (e.g. see Fig. 12 D). This state represents a maximally reactive microglial state in response to an injury and contributes to neuropathological outcomes by removing cellular debris and dead cells (Brockhaus et al., 1996; Petersen and Dailey, 2004) and or by secreting inflammatory mediators such as TNF- α and IL-1 β leading to neurotoxicity (Deng et al., 2008).

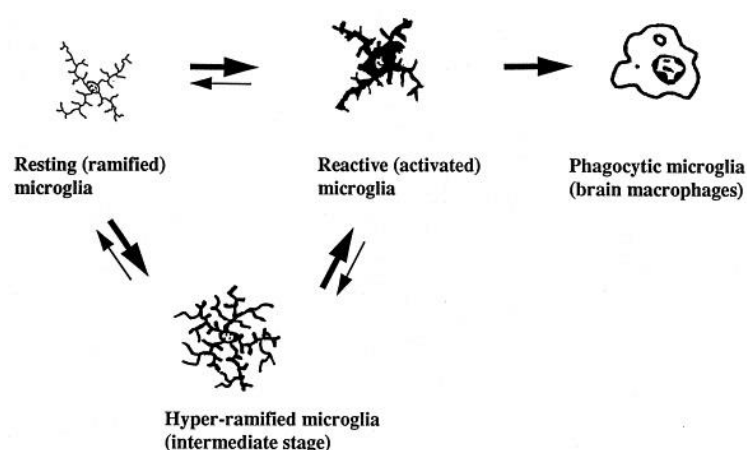


Figure 14: Classification of microglial states.

A graphical illustration of different stages of microglia from resting to phagocytic state.

Image modified from (Streit et al., 1999).

(This section in parts has been taken from a preprint server Singaravelu et al., 2021a)

2.2.9 Data analysis

Before calculation, the data of pressure pain threshold (PPT) and paw withdrawal threshold (PWT) were transformed into decadic logarithms in order to achieve a secondary normal distribution (Bartlett, 1947), since previous data obtained in larger cohorts provided solid evidence for the log-normal distribution of PPT and other psychophysical data (Rolke et al., 2005). The log values were then normalized to the control group ($\text{mean.R.stress}/\text{mean control} \times 100$), for further analysis (equivalent to calculating percentage changes in both PPT and PWT).

The statistics were performed with GraphPad (version 6) by using analysis of variance (ANOVA) followed by Tukey *post hoc* analysis. Normal distribution of the data was tested with Kolmogorov-Smirnov test and when data did not fit the rules of parametric analysis, comparisons were made with the Mann-Whitney *U* test. A probability level of less than 5% ($p < 0.05$, two tailed) was considered as significant. The PPT data after saline/NGF injections are shown as individual paired values and effect sizes were calculated using Cohen's *d* (see Section: 2.1.6).

The experimenter doing the behavioral experiments and immunohistochemical analysis was blinded to the treatments the animals received.

(This section in parts has been taken from a preprint server Singaravelu et al., 2021a)

2.3 Swimming training (study 3)

This study is outside my thesis work and was a part of my summer internship at the University of Campinas, Brazil. The purpose of this internship was to learn immunohistochemistry on lumbar sections and to perform swimming training on rodents. A brief introduction and aim of this study is stated in appendix 20.

2.3.1 Animals and treatment groups

Animals: Swiss male mice from CEMIB/UNICAMP.

Drugs: Carrageenan (Cg, 100 µg; 20 µl) was injected into gastrocnemius (GS) muscle to induce acute muscle hyperalgesia and, 10 days later, an injection of Prostaglandin E2 (PGE₂, 1µg; 20 µl) was used, in the same site, to reveal the chronic state. Lambda Carrageenan and Prostaglandin E2 (PGE₂, (5Z,11α,13E,15S)-11,15-Dihydroxy-9-oxoprostano-5,13-dienoic acid, Dinoprostone) from Sigma Aldrich.

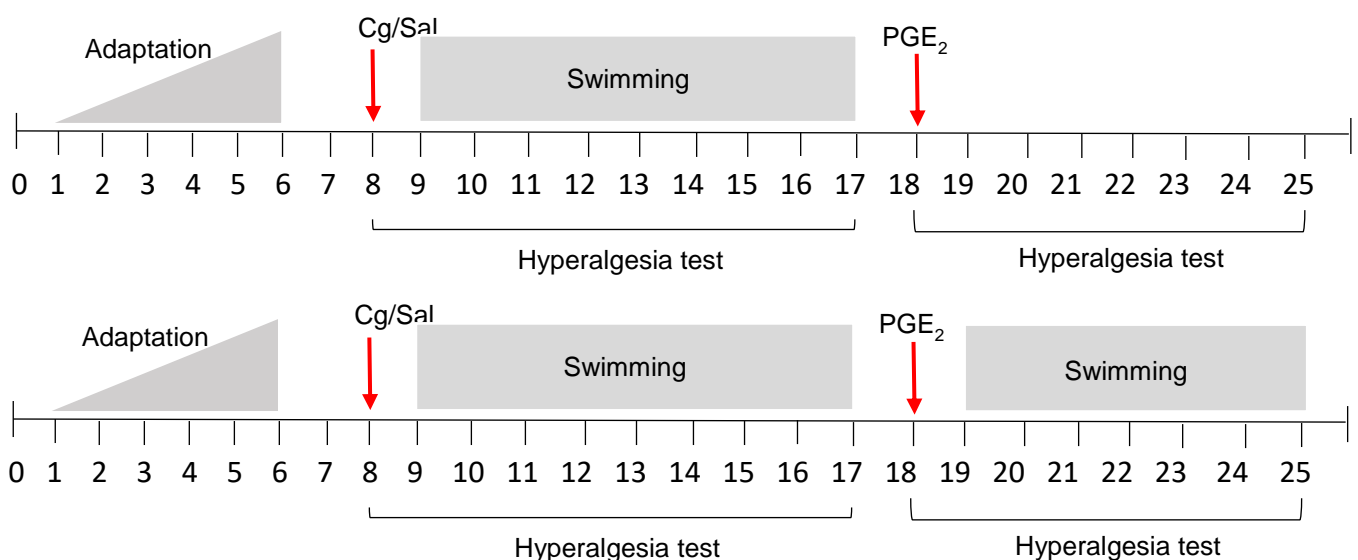
2.3.2 Behavioral test and exercise protocol

Test: Randall-Selitto test was used to quantify the muscle hyperalgesia in both periods of acute (from day 9 to day 17) and chronic (from day 18 to day 25) muscle hyperalgesia.

Protocols of short-term swimming training:

Starting 24h after Cg, 30 min/day for 9 consecutive days, without load or with loads of 1.5%, 3% and 4% of body weight (bw). For load of 1.5%, training was also performed after PGE₂ for 7 consecutive days.

2.3.3 Experimental design



2.3.4 Data analysis

Area Under the Curve was used to evaluate the chronic period of muscle hyperalgesia and the statistical analysis was performed by One Way ANOVA with Tukey post hoc test. *P* value set at 0.05.

3 RESULTS

The data of the electrophysiological experiment (study 1) has been published recently (Singaravelu et al., 2021b). The figures in study 1 were modified from the publication but additional unpublished figures are also presented in the results section. Preliminary findings of the study 2 (behavioral and immunohistochemistry experiment) have been uploaded in a preprint server (Singaravelu et al., 2021a). The behavioral findings of study 2 are also a part of master thesis by (Goitom, 2021) titled 'Early life psychophysical stress primes rat dorsal horn neurons for long-term sensitization by a short-lasting nociceptive low back input involving activation of microglia'. Some figures in the results of study 2 were used in modified form for this thesis and are marked. The data of study 2 are being prepared for submission (Singaravelu SK., Goitom AD., Surakka AP., Moerz H., Schilder A., Hoheisel U., Spanagel R., Treede R-D; Microglia contributes to long-term sensitization of rat spinal neurons induced by a mild-nociceptive lumbar input when preceded by adolescent restraint stress).

The data of study 3 is not published.

3.1 Study 1: Electrophysiology

3.1.1 Body weight and pressure pain threshold of the low back

The body weight for all the animals was measured on day 14 before measuring the PPT and anesthetizing the animal (see Fig. 2). We found a non-significant difference lower body weight in stressed animals (control + NGF: 437 ± 29 g, stress + NGF: 407 ± 21 g; $p = 0.052$; see Fig. 15). The result show that the well-being of the animals was not impaired.

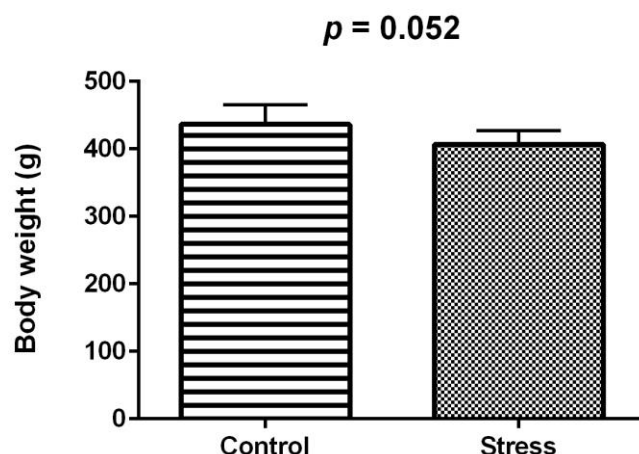


Figure 15: Body weight.

Body weight shown in grams and the data is plotted with the (mean ± SEM) values. P value: Mann-Whitney U test.

Two days after the stress paradigm (see Fig. 2), the PPT of the multifidus muscle was determined before the intramuscular NGF injection. There was no significant difference in PPT, suggesting that the stress paradigm induced a latent rather than manifest sensitization. However, animals of the stress group showed a tendency to a lowered PPT ($p = 0.415$; Cohen's $d = 0.83$, large effect size; Fig. 16). This section in parts has been taken from (Singaravelu et al., 2021b).

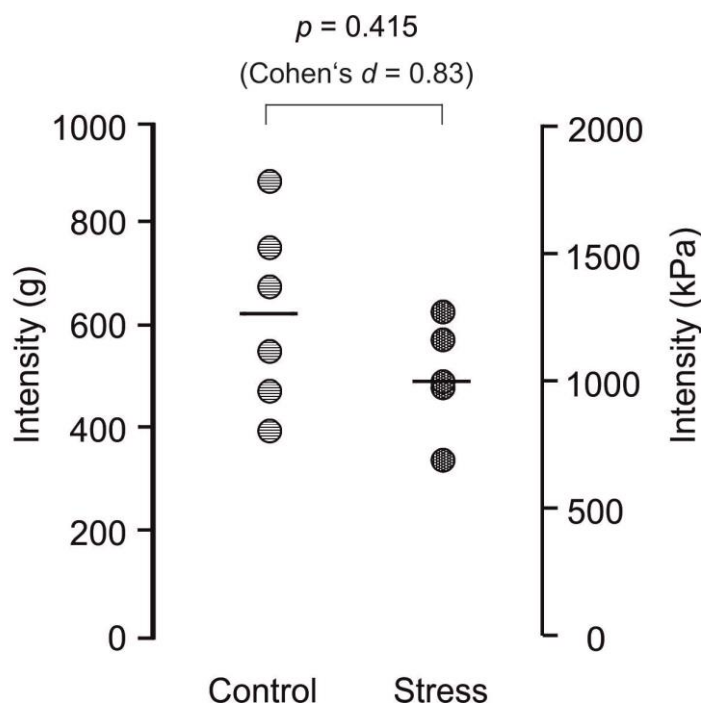


Figure 16: Pressure pain threshold of the low back before NGF injection.

The force (in 'g' on the left y-axis) required to elicit a pain-related reaction (withdrawal behavior, escape movements, vocalization) using a blunt probe with an area of 3.46 sq.mm when applied to the multifidus muscle of the low back. For comparison with human data, the right y-axis shows the pressure force in 'kPa'. Note that thresholds were measured before the NGF injection. P value: Mann-Whitney U test.

Image modified from (Singaravelu et al., 2021b).

3.1.2 General features of recorded dorsal horn neurons

- *Recording depth*

In total, 60 neurons responding to the electrical search stimulus at A-fiber strength were recorded. The recording depth in the dorsal horn ranged from 160 to 960 μm . Their interquartile range was 650 (745 – 460) μm in control + NGF and 510 (720 – 380) μm in the stress + NGF groups (see Fig. 17). We observed no significant differences between both groups. The majority of the neurons (47 of 60; 78%) were recorded at depths between 400 and 800 μm corresponding to deep dorsal horn laminae IV, V, and VI (refer Table 1, recording depth). The result indicates that all the recorded neurons were equally distributed within the dorsal horn in both the groups.

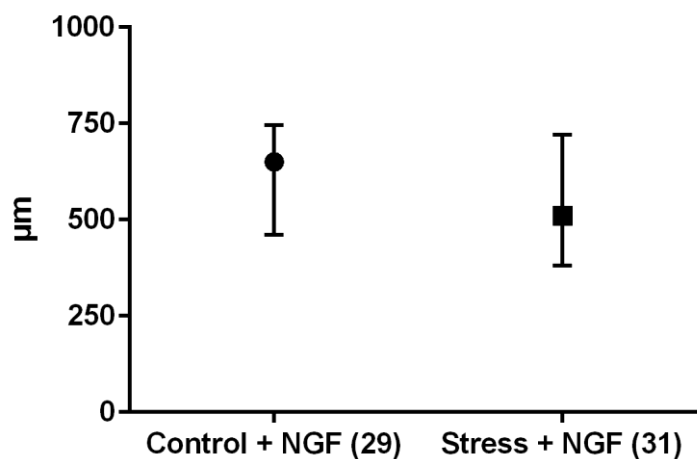


Figure 17: Recording depth of dorsal horn neurons.

The numbers in brackets represent the number of neurons that were recorded in the respective group. The full black circle shows the median recording depth for the control + NGF group and their interquartile range. The full black square shows the median recording depth for the stress + NGF group and their interquartile range.

- *Latency and conduction velocity*

The latencies of the electrically evoked action potentials (APs) ranged from 0.8 to 3.4 ms. Their interquartile ranged from 1.8 (2.1 – 1.6) ms in control + NGF and 1.8 (2.1 – 1.8) ms in the stress + NGF group (see Fig. 18) (refer Table 1, latency). We did not observe any significant differences between the treatment groups. The distance between the recording and the stimulating electrodes (~35 mm) showed that all neurons tested reacted to A-fiber stimulation.

All the neurons had myelinated afferent inputs, and the estimated conduction velocities were consistent with ranges in both A-fiber nociceptors and non-nociceptors (Djouhri and Lawson, 2004). The conduction velocity was calculated

using the formula: conduction velocity = distance (μm) \div latency (ms). Their interquartile range was 19 (22 – 17) μm in control + NGF and 19 (19 – 17) m/s in the stress + NGF groups (see Fig. 19) (refer to Table 1, conduction velocity). No significant differences were observed between the groups. Additional C-fiber input was likely activated by the mechanical stimuli that we used in this study (Hoheisel et al., 2019), but this could not be verified by electrical search stimulus because such stimuli may induce long-term potentiation (Zhang et al., 2016).

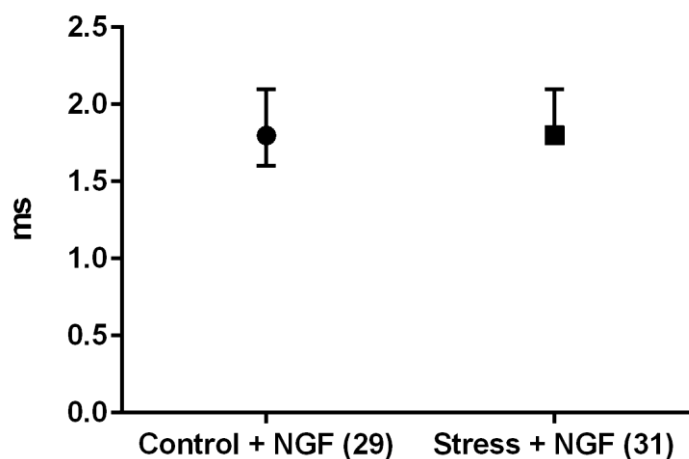


Figure 18: Latency of the recorded dorsal horn neurons.

The numbers in brackets represent the number of neurons that were recorded in the respective group. The full black circle shows the median latency for the control + NGF group and their interquartile range. The full black square shows the median latency for the stress + NGF group and their interquartile range.

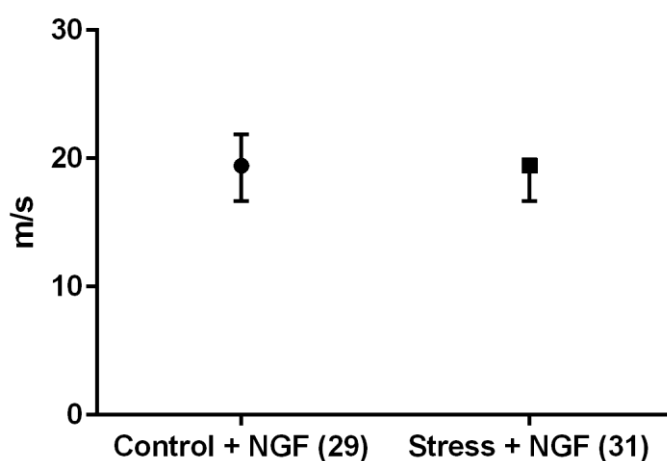


Figure 19: Conduction velocity of the recorded dorsal horn neurons.

The numbers in brackets represent the number of neurons that were recorded in the respective group. The full black circle shows the median conduction velocity for the control + NGF group and their interquartile range. The full black square shows the median conduction velocity for the stress + NGF group and their interquartile range.

Additional information on the characteristics of the recorded neurons is presented as a table in the Appendix 1 A: stress + NGF; Appendix 1 B: control + NGF.

Table 1: Input sources of dorsal horn neurons recorded in this study.

Groups	Control + NGF	Stress + NGF	<i>p</i> Value
Total number of neurons	29	31	
Recording depth	650 (745 – 460)	510 (720 – 380)	
Latency	1.8 (2.1 – 1.6)	1.8 (2.1 – 1.8)	
Conduction velocity	19 (22 – 17)	19 (19 – 17)	
Neurons with deep input	4/29 (14%)	12/31 (39%)	<i>p</i> = 0.041
Recording depth	750 (798 – 568)	620 (803 – 403)	
low back	2/29 (7%)	4/31 (13%)	<i>p</i> = 0.671
outside low back	2/29 (7%)	8/31 (26%)	<i>p</i> = 0.081
Neurons with skin input	19/29 (65%)	19/31 (61%)	<i>p</i> = 0.793
Recording depth	660 (710 – 420)	590 (770 – 380)	
Neurons with convergent input	2/29 (7%)	7/31 (23%)	<i>p</i> = 0.147
Recording depth	755 (800 – 710)	640 (830 – 470)	
Neurons without receptive fields (RFs)	8/29 (28%)	7/31 (23%)	<i>p</i> = 0.768
Recording depth	620 (850 – 453)	470 (510 – 305)	
Neurons with resting activity	8/29 (28%)	17/31 (55%)	<i>p</i> = 0.039
Recording depth	685 (725 – 520)	510 (685 – 345)	
resting activity, with deep input	0/29 (0%)	8/31 (26%)	<i>p</i> = 0.004
resting activity, with skin input	8/29 (28%)	12/31 (39%)	<i>p</i> = 0.419
resting activity, with convergent input	0/29 (0%)	5/31 (16%)	<i>p</i> = 0.052
resting activity, without receptive fields	0/29 (0%)	2/31 (6%)	<i>p</i> = 0.492

The table gives the number of neurons recorded for each group studied. Control+NGF: animals that were handled but not stressed and received single NGF-injections into the multifidus muscle. Stress+NGF: animals that were stressed by repeated restraint and subsequently received single NGF-injections. Recording depth, latency and conduction velocity are shown for total neurons recorded and recording depth for each input type. Deep tissues: neurons with input from deep tissues (e.g. muscle, fascia); skin: neurons with input from the skin; Convergent: neurons with input from deep tissues and skin. Without receptive fields: neurons that responded to the electrical search stimulus but could not be excited with the mechanical stimuli used. Resting activity: neurons that show spontaneous activity without presenting any mechanical or chemical stimuli.

Recording depth, latency and conduction velocity are expressed as the interquartile range: median (quartile 3 – quartile 1).

The proportion of neurons are expressed as the number of neurons recorded to a specific input type / total number of neurons recorded for a group (percentage of the response). *P* values are calculated using Fisher's exact probability test and a *p*-value of < 0.05 was considered significant.

Table modified from (Singaravelu et al., 2021b).

3.1.3 Responsiveness of dorsal horn neurons to mechanical stimulation

Of all the 60 neurons recorded in this study, 45 (75%) responded to at least one of the mechanical test stimuli used (control + NGF: $n = 21$, stress + NGF: $n = 24$); 15 neurons (25%) responded to the electrical search stimulus but could not be activated by the test stimuli applied to the low back and the hind limb (see Fig. 7; see Table 1, without receptive fields). Out of the 45 responding neurons, 36% (16 of 45) received input from deep tissues, 84% (38 of 45) input from the skin, and 20% (9 of 45) had convergent input. Most of the neurons having input from deep somatic tissues (13 of 16; 81%) were located in deep laminae. An example of a neuron having convergent input from the multifidus muscle and the skin is shown in the Fig. 8. C.

Animals of the NGF group and preceded by stress showed a significant increase in the proportion of neurons having input from deep tissues including fascia compared to the NGF alone group (control + NGF: 4 of 29, 14%; stress + NGF: 12 of 31, 39%; $p = 0.041$; Fig. 20 A). The proportion of neurons having skin input did not differ between both the groups (control + NGF: 19 of 29, 65%; stress + NGF: 19 of 31, 61%; $p = 0.793$; Fig. 20 B). The proportion of neurons having convergent input also increased but the difference was not significant (control + NGF: 2 of 29, 7%; stress + NGF: 7 of 31, 23%; $p = 0.147$; Fig. 20 C). A table with the summary of p values calculated using Fisher's exact test could be found in Appendix 2.

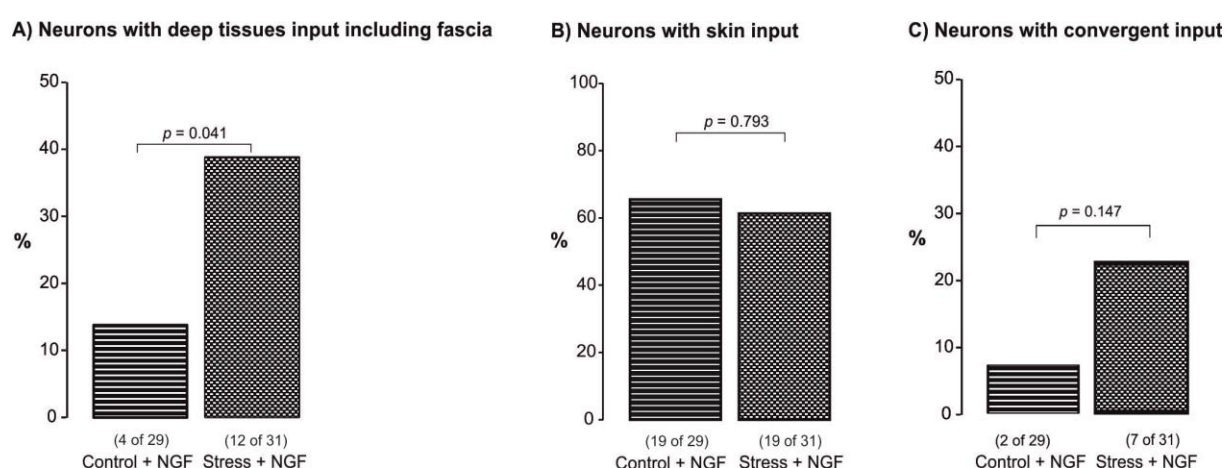


Figure 20: Proportion of neurons having deep, skin, or convergent input.

A) Neurons with input from deep tissues (including fascia) inside and outside the low back (see also Fig. 21). **B)** Neurons having input only from the skin. **C)** Neurons having convergent input from deep tissues and the skin. Data from the present study (Stress+NGF: restraint stress followed by a single NGF injection; control+NGF: handled but not stressed followed by NGF injection). p -values: Fisher's exact test.

Image modified from (Singaravelu et al., 2021b).

The most important difference between the stressed and the control animals was the appearance of new receptive fields (RFs) in deep tissues outside the low back. These receptive fields appeared mainly in the hip and the entire hind limb (gray areas in Fig. 21 A). The total number of neurons with RFs in the low back close to the site of NGF injection (open outlines in Fig. 21 A) increased about two-fold (control + NGF: 2 of 29, 7%; stress + NGF: 4 of 31, 13%; $p = 0.671$; Fig. 21 B). The proportion of neurons with RFs located outside the low back increased about four-fold (control + NGF: 2 of 29, 7%; stress + NGF: 8 of 31, 26%; $p = 0.081$; Fig. 21 B). The data from this study indicate that a single NGF-induced mild nociceptive input caused a manifest sensitization of DHNs when preceded by stress. This manifestation was not observed after the nociceptive NGF input alone. A table with the summary of p values calculated using Fisher's exact test could be found in Appendix 2. This section in parts has been taken from (Singaravelu et al., 2021b).

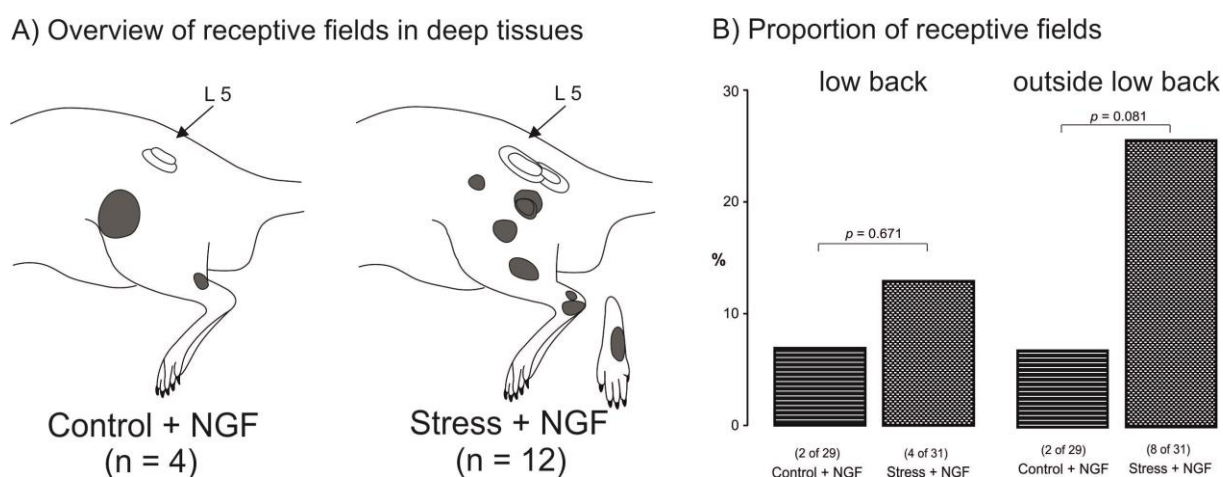


Figure 21: Location of the receptive fields (RFs) in deep tissues.

A) Open outlines show the receptive fields located in deep tissues of the low back (e.g. muscle or thoracolumbar fascia) close to vertebral level L5. RFs in deep tissues outside the low back are marked in grey. **B)** The proportion of RFs inside and outside low back. Data from the present study (Stress+NGF: restraint stress followed by a single NGF injection; control+NGF: handled but not stressed followed by NGF injection). p -values: Fisher's exact test.

Image modified from (Singaravelu et al., 2021b).

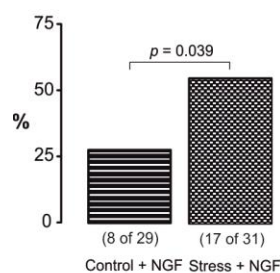
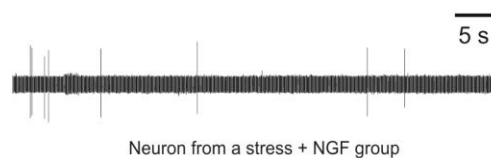
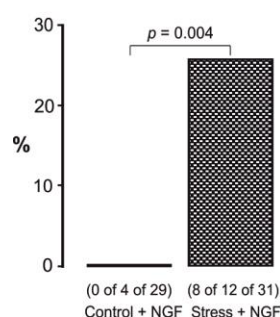
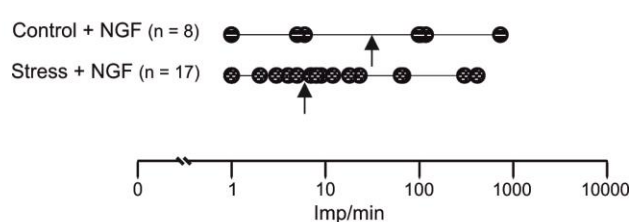
3.1.4 Resting activity of the dorsal horn neurons

The animals of the NGF groups preceded by stress showed a significant increase in the proportion of neurons with resting activity compared to the NGF alone group (control + NGF: 8 of 29, 28%; stress + NGF: 17 of 31, 55%; $p = 0.039$; Fig. 22 A; Table 1). An analysis of the resting activity stratified by the location of RFs showed us that the manifest sensitization of stress, when combined with a mild nociceptive input,

was pronounced on neurons with deep tissue input (control + NGF: 0 of 4 of 29, 0%; stress + NGF: 8 of 12 of 31, 26%; $p = 0.004$; Fig. 22 B and Table 1). This increase was not present in the neurons with skin input. These data suggests an additive effect of stress followed by NGF on the resting activity of neurons with deep tissue inputs.

In Fig. 22 C, an example of a neuron having resting activity from the stress + NGF group is shown. The mean discharge frequency was highly variable and the firing pattern was irregular both within and across the recorded neurons. Therefore, we did not see a significant difference between the stress + NGF and the NGF alone groups. The difference was not observed neither when including all-active and silent-neurons and their interquartile ranges were (control + NGF: 0[1 – 0]; stress + NGF: 1[9 – 0] impulse/min; $p = 0.065$) nor only active neurons (control + NGF: 53[114 – 2]; stress + NGF: 8[44 – 3] impulse/min; $p = 0.559$; Fig. 22 D).

Additional information on the resting activity (impulses/minute) of the recorded neurons is presented in Appendix 1 A: stress + NGF; Appendix 1 B: control + NGF. This section in parts has been taken from (Singaravelu et al., 2021b).

A) Proportion of neurons with resting activity**C) Example of a neuron having resting activity****B) Neurons with deep input having resting activity****D) Discharge frequency of active neurons only****Figure 22: Resting activity of dorsal horn neurons.**

A) The proportion of neurons having a discharge activity ≥ 1 imp/min, **B)** Neurons with deep tissue input and having resting activity, **C)** Original registration from a neuron having resting activity, 8 imp/min. **D)** Discharge frequency of active neurons only. Arrowheads indicate the median discharge frequency of the active neurons. *p*-values: Fisher's exact test.

Image modified from (Singaravelu et al., 2021b).

3.2 Study 2: behavioral and immunohistological findings

3.2.1 Body weight

The body weight was measured on the days before the start of behavioral experiments (see Fig. 9, gray line; refer to section 2.2.4). We observed no differences in body weight between stressed and control animals (see appendix 3). The results show that the well-being of the animals was not impaired.

3.2.2 Pressure pain threshold measured in the left low back after stress

The baseline measurement at postnatal day 21 (PD 21) for the PPT of the left low back multifidus muscle revealed no significant difference between the control and stress groups ($P = 0.3186$). Two days after the stress paradigm (PD 34), the PPT was significantly lower ($P < 0.0001$; $d = 2.4$) compared to the control group, suggesting that the stress paradigm induced muscle hyperalgesia but remained unchanged compared to its baseline. This sensitization was still significant ($P = 0.012$; $d = 1.2$) in adulthood (PD 85) (Fig. 23. A.a).

For PPT of the right multifidus muscle please refer to appendix 4.

This section in parts has been taken from (Singaravelu et al., 2021a) and master thesis (Goitom, 2021).

3.2.3 Paw withdrawal threshold of the left hind paw after stress

In addition to PPT, the PWT assessed the skin sensitivity on the plantar surface of the distal hind limb. The baseline measurement was not performed for the PWT (refer to sec. 2.4.2) due to our experimental design. Four days after the stress paradigm (PD 36), the PWT of the left hind paw was significantly lowered ($P = 0.0007$; $d = 2.0$) in the repeated restraint stress group, suggesting that the stress paradigm induced mechanical hyperalgesia but this sensitization was attenuated in the adulthood phase (PD 85) ($P = 0.051$; $d = 0.9$). These data suggest that the stress paradigm induced a short-term sensitization to the distal skin input (Fig. 23. B.a).

For PWT of the right hind paw please refer to appendix 5.

This section in parts has been taken from (Singaravelu et al., 2021a) and master thesis (Goitom, 2021).

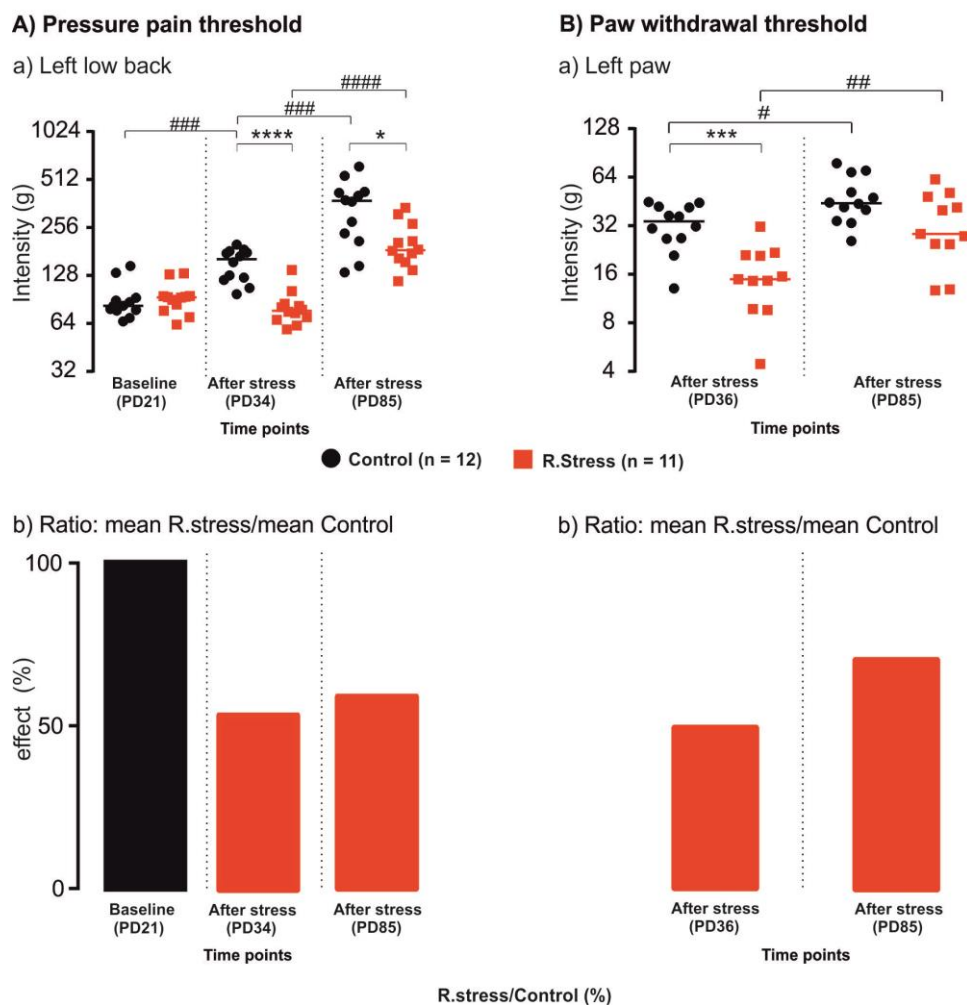


Figure 23: Pressure pain threshold and paw withdrawal threshold before and after stress.

Repeated restraint stress in early adolescence induces long-lasting muscle hyperalgesia. **A.a)** Individual data points expressed in log scale, force (in 'g' on the left y-axis) required to elicit a pain-related reaction (withdrawal behavior, escape movements, vocalization) using a blunt probe with an area of 3.46 sq.mm when applied to the left multifidus muscle of the low back. Horizontal lines indicate the median for each group. **A.b)** Ratio (in '%'), change of pressure pain threshold is shown as effect (mean of R.stress/mean of control)*100. **B.a)** Individual data points expressed in log scale, force (in 'g' on the left y-axis) required to elicit a pain-related reaction (paw licking, paw withdrawal) using a rigid cylindrical tip with an area of 0.8 sq.mm when applied on the plantar surface of the left hind paw. Horizontal lines indicate the median for each group. **B.b)** Ratio (in '%'), change of paw withdrawal threshold is shown as effect (mean of R.stress/mean of control)*100. PD, postnatal days (see Fig. 9). *P*-values: *U*-test of Mann and Whitney; *P*<0.05 is represented with (*/#), *P*<0.006 (**/##), *P*<0.0001 (***/###), and *P*<0.0001 (****/####), '*' represents the difference between the groups and '#' represents the difference within group referring to an increase with age.

Image modified from (Singaravelu et al., 2021a) and master thesis (Goitom, 2021)

3.2.4 Pressure pain threshold measured in the left low back after saline/NGF injections

Intramuscular injections of saline/NGF were administered to each animal as a second intervention to induce spinal sensitization. The animals were divided into four groups (see Sec: 2.2.1). In Fig. 24. A, a paired plot of the PPT between pre (PD 85) and post 1st injection (PD 86) of either saline or NGF is shown for individual animals. The group that received NGF injection showed a decrease in PPT with medium effect (CNN: $d = 0.7$) while the groups that received saline showed a small effect. In Fig. 24. B, the ratio for each group was calculated $(\text{post/pre}) \times 100$ and is expressed as effect (%).

In Fig. 24. C, a paired plot of the PPT between pre (PD 90) and post 2nd injection (PD 91) of either saline or NGF is shown for individual animals. The groups that received NGF injections showed a decrease in PPT with a medium (CSN: $d = 0.7$) and large effect (RSN: $d = 0.9$) while the group that received repeated NGF injections showed only a small effect (CNN: $d = 0.3$), opposite to the expected effect. In Fig. 24. D, the ratio for each group was calculated $(\text{post/pre}) \times 100$ and is expressed as effect (%) and the bars indicate the median. All the groups that received NGF showed a change in the PPT towards lesser stimulus intensities implying a drop in the PPT after NGF administration.

For PPT of the right multifidus muscle please refer to appendix 6.

This section in parts has been taken from (Singaravelu et al., 2021a) and master thesis (Goitom, 2021).

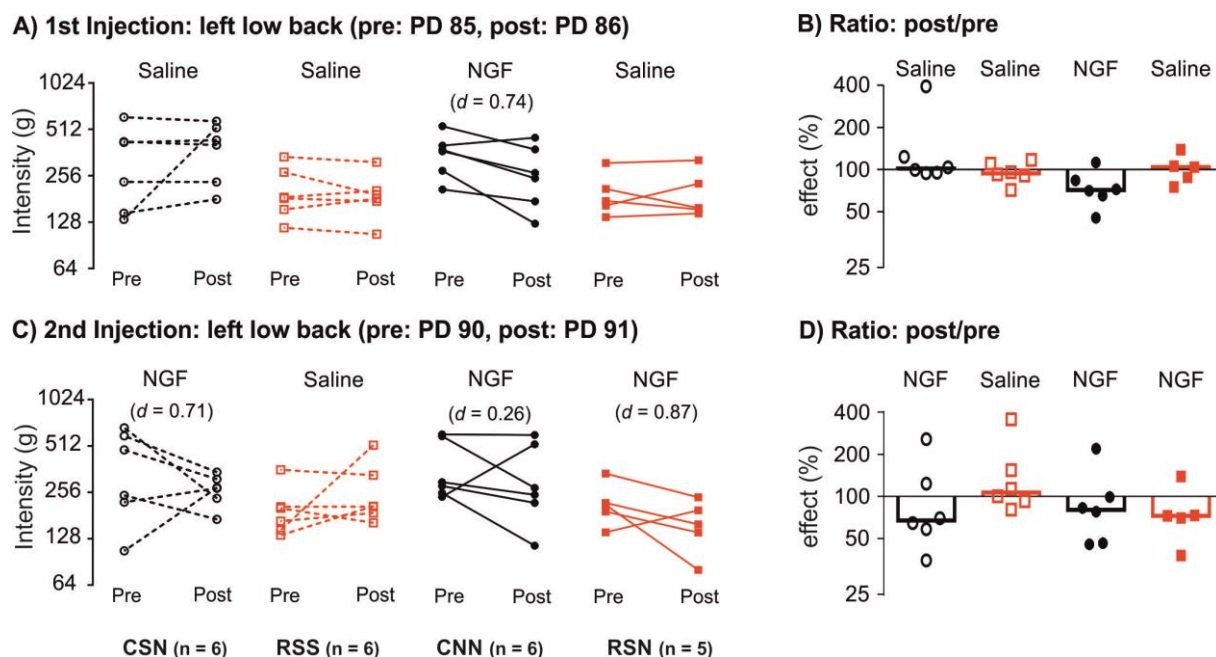


Figure 24: Pressure pain threshold before and after saline/NGF injections.

Intramuscular NGF injection leads to an increased pain-related behavior when preceded by repeated restraint stress. **A)** First injection, pair-wise comparison of individual data points pre and post injection expressed in log scale, force (in 'g' on the left y-axis) required to elicit a pain-related reaction (withdrawal behavior, escape movements, vocalization) using a blunt probe with an area of 3.46 sq.mm when applied to the left multifidus muscle of the low back. **B)** Individual data points in ratio (in '%'), change of pressure of pain threshold shown as effect post/pre. Bars indicate the median for each group. **C)** Second injection, pair-wise comparison of individual data points pre and post injection expressed in log scale, force (in 'g' on the left y-axis). **D)** Individual data points in ratio (in '%'), change of pressure pain threshold shown as effect post/pre and bars indicate the median for each group. Effect size is shown in Cohen *d*. NGF, nerve growth factor. CSN: control+saline+NGF; RSS: repeated restraint stress+saline+saline; CNN: control+NGF+NGF; and RSN: repeated restraint stress+saline+NGF. PD: postnatal day. Black circles: control animals, red squares: stressed animals.

Image modified from (Singaravelu et al., 2021a) and master thesis (Goitom, 2021).

3.2.5 Paw withdrawal threshold of the hind paws after saline/NGF injections

No effects were observed in the PWT on both the hind paws after the injections of saline/NGF (see appendix 7). This implies that NGF-induced mechanical hyperalgesia in contrast to the stress-induced hyperalgesia is local to the site of injection.

3.2.6 Iba-1 and GFAP staining intensities

In total, 60 sections of the spinal L2 segment (3 sections/animal; 5 animals/group) were stained for Iba-1 and GFAP, both well-known markers for microglia and astrocytes. We did not find significant differences in Iba-1 and GFAP staining intensity between the groups on the ipsilateral side (Fig. 25. A & B; Table 2).

For staining intensities on the contralateral side please refer to appendix 8.

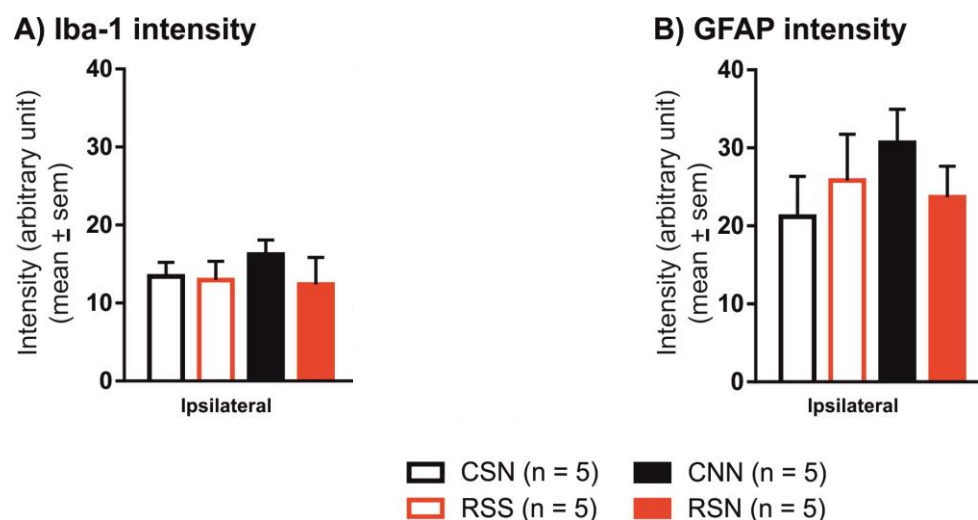


Figure 25: Quantitative analysis of Iba-1 stained microglia and GFAP stained astrocytes.

Single or repetitive intramuscular NGF injections does not change the staining intensity compared to saline injections. **A)** Intensity of Iba-1 stained microglia cells shown in arbitrary unit. Data expressed as mean ± SEM. Intensity and background was measured for each ROI. The background was subtracted and the mean staining intensity was calculated. **B)** Intensity of GFAP stained astrocyte cells shown in arbitrary unit. Data expressed as mean ± SEM. Intensity and background was measured for each ROI. The background was subtracted and the mean staining intensity was calculated. Iba-1, ionized calcium binding adapter molecule 1; GFAP, glial fibrillary acidic protein; ROI, region of interest; NGF, nerve growth factor. CSN: control+saline+NGF; RSS: repeated restraint stress+saline+saline; CNN: control+NGF+NGF; and RSN: repeated restraint stress+saline+NGF.

Table 2: Comparison of microglia and astrocytes staining intensity.

	A) Iba-1 intensity	B) GFAP intensity
Group comparisons	Ipsilateral	Ipsilateral
<u>CNN</u> vs. <u>CSN</u>		
<i>p</i> Value	$p = 0.883$	$p = 0.281$
Cohen <i>d</i> (effect size)	0.7	0.7
<u>RSN</u> vs. <u>RSS</u>		
<i>p</i> Value	$p = 0.998$	$p = 0.973$
Cohen <i>d</i> (effect size)	0.0	0.6
<u>RSN</u> vs. <u>CSN</u>		
<i>p</i> Value	$p = 0.993$	$p = 0.956$
Cohen <i>d</i> (effect size)	0.2	0.7
<u>RSS</u> vs. <u>CSN</u>		
<i>p</i> Value	$p = 0.999$	$p = 0.790$
Cohen <i>d</i> (effect size)	0.1	0.3
<u>RSN</u> vs. <u>CNN</u>		
<i>p</i> Value	$p = 0.754$	$p = 0.528$
Cohen <i>d</i> (effect size)	0.6	0.7

The table shows the statistics for **A)** Iba-1 staining intensity and **B)** GFAP staining intensity, on the ipsilateral side of saline/NGF injections. The staining intensity was analyzed for each ROI and the statistics were performed using the mean \pm SEM. $P < 0.05$ (two-way ANOVA followed by Tukey *post hoc* analysis) was considered significant and effect size was calculated using Cohen's *d*. The group comparisons shown here are based on two factors: 1) repeated restraint stress (R) and control (C), 2) NGF (N) and saline (S) injections. Iba-1, ionized calcium binding adapter molecule 1; GFAP, glial fibrillary acidic protein; NGF, nerve growth factor. CSN: control+saline+NGF; RSS: repeated restraint stress+saline+saline; CNN: control+NGF+NGF; and RSN: repeated restraint stress+saline+NGF.

For staining intensities on the contralateral side please refer to appendix 9.

A sub-analysis on the staining intensity within the dorsal horn (superficial and deep) was performed for both Iba-1 and GFAP. We did not find any significant differences between the groups both on the ipsilateral and contralateral sides of the saline/NGF injections (see appendix 10).

3.2.7 Iba-1 stained number of microglial cells

The number of Iba-1 stained cells were counted in each ROI and no differences were observed between the groups (Fig. 26). Rather we found a medium effect on the number of cells between CNN vs. CSN ($P = 0.942$; $d = 0.7$), RSN vs. RSS ($P = 0.654$; $d = 0.6$), and RSN vs. CSN ($P = 0.707$; $d = 0.7$), groups to the ipsilateral side of saline/NGF injections (Table 3).

For number of cells on the contralateral side please refer to appendix 11.

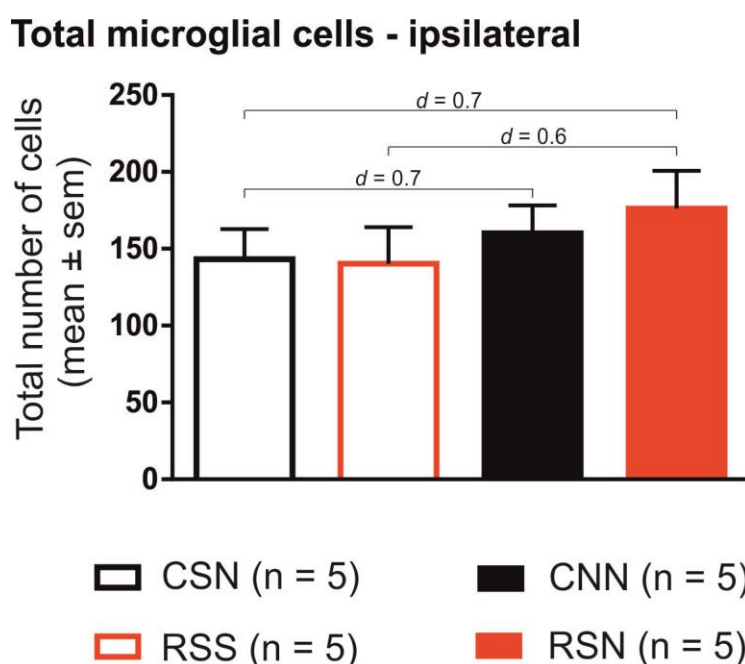


Figure 26: Quantitative analysis of Iba-1 stained microglia cells.

Single or repetitive intramuscular NGF injections does not change the number of microglia cells compared to saline injections. Data expressed as mean \pm SEM and effect size was calculated using Cohen d . Iba-1 stained microglia cells were counted in each ROI and the mean was calculated.

Table 3: Comparison of number of microglial cells.

Groups	<i>p</i> Value	Cohen <i>d</i> (effect size)
<u>CNN</u> vs. <u>CSN</u>		
Total number of microglia cells	$p = 0.952$	0.4
Ipsilateral	$p = 0.942$	0.7
<u>RSN</u> vs. <u>CSN</u>		
Total number of microglia cells	$p = 0.853$	0.5
Ipsilateral	$p = 0.707$	0.7
<u>RSN</u> vs. <u>RSS</u>		
Total number of microglia cells	$p = 0.548$	0.8
Ipsilateral	$p = 0.654$	0.6
<u>CSN</u> vs. <u>RSS</u>		
Total number of microglia cells	$p = 0.943$	0.3
Ipsilateral	$p = 0.999$	0.0
<u>CNN</u> vs. <u>RSN</u>		
Total number of microglia cells	$p = 0.992$	0.2
Ipsilateral	$p = 0.951$	0.3

The table shows the statistics for number of microglia cells, on the ipsilateral side of saline/NGF injections. The number of cells were analyzed for each ROI and the statistics were performed using the mean \pm SEM. $P < 0.05$ (two-way ANOVA followed by Tukey *post hoc* analysis) was considered significant and effect size was calculated using Cohen *d*. The group comparisons shown here are based on two factors: 1) repeated restraint stress (R) and control (C), 2) NGF (N) and saline (S) injections. Iba-1, ionized calcium binding adapter molecule 1; NGF, nerve growth factor. CSN: control+saline+NGF; RSS: repeated restraint stress+saline+saline; CNN: control+NGF+NGF; and RSN: repeated restraint stress+saline+NGF.

For comparison of the number of cells on the contralateral side please refer to appendix 12.

3.2.8 Structural plasticity of Iba-1 stained microglial cells

Microglia are known to exist in a number of states, transitioning from resting (surveillance) to phagocytic (amoeboid) with two intermediate (hyper-ramified and reactive) states.

The number of cells in resting state was significantly lowered in animals that experienced stress in adolescence (R) followed by NGF injection in adulthood compared to the animals that received two NGF injections in adulthood (RSN vs. CNN; $P = 0.024$; $d = 2.1$) (Fig. 27. A). We also observed a non-significant but large effect between RSN vs. RSS ($P = 0.202$; $d = 0.9$) (Table 4). In hyper-ramified state, no significant differences were observed between the groups but a moderate effect between RSN vs. CSN ($P = 0.816$; $d = 0.6$) (Fig. 27. B; Table 4). The majority of the Iba-1 stained microglia were in the reactive state in all four groups and no significant differences or effect sizes were observed between the groups (Fig. 27. C; Table 4). The intramuscular NGF injection led to a significant increase in the number of cells in the phagocytic state in animals that experienced stress compared to the group that received saline injections alone (RSN vs. RSS; $P = 0.013$; $d = 3.7$). Another significant difference was observed between the groups (RSN vs. CNN; $P = 0.031$; $d = 5$) (Fig. 27 D). A large effect was also seen between RSN vs. CSN but was not significant ($P = 0.202$; $d = 1.2$) (Fig. 27. D; Table 4). These findings especially the phagocytic state microglia, suggest that repeated restraint stress in early adolescence primes the spinal DHNs for a longer period and are easily susceptible to manifest sensitization when presented with a second hit (NGF) in the adulthood phase.

For comparison of the number of cells in different states on the contralateral side please refer to appendix 13.

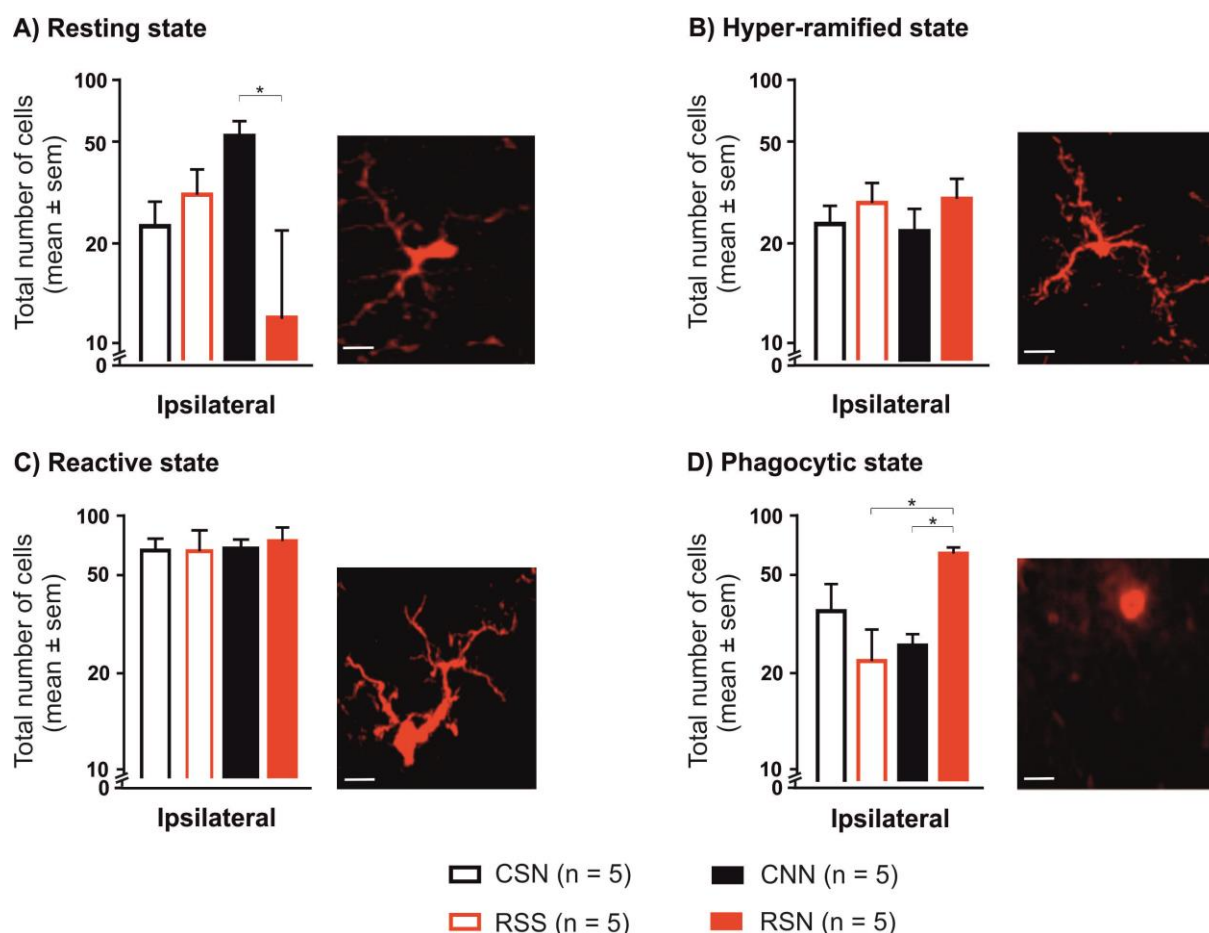


Figure 27: Microglia and its states.

Intramuscular NGF injection leads to decreased number of microglia cells in resting state and increased number of cells in phagocytic state when preceded by repeated restraint stress in early adolescence. **A)** Number of Iba-1 stained microglia cells in resting state. Inset shows a representative image of cells in resting state. **B)** Number of Iba-1 stained microglia cells in hyper-ramified state. Inset shows a representative image of a cell in hyper-ramified state. **C)** Number of Iba-1 stained microglia cells in reactive state. Inset shows a representative image of a cell in reactive state. **D)** Number of Iba-1 stained microglia cells in phagocytic state. Inset shows a representative image of a cell in phagocytic state. Number of cells were counted in each ROI and their states were classified (refer sec. 2.7.8), and the mean was calculated. Scale bars: 20 μ m. Data expressed as mean \pm SEM; $P < 0.05$: two-way ANOVA followed by Tukey *post hoc* analysis and significance is indicated by * compared to RSN and RSS or CNN. Iba-1, ionized calcium binding adapter molecule 1; NGF, nerve growth factor. CSN: control+saline+NGF; RSS: repeated restraint stress+saline+saline; CNN: control+NGF+NGF; and RSN: repeated restraint stress+saline+NGF.

Table 4: Comparison of microglia cell numbers in different states.

Groups	<i>p</i> Value	Cohen <i>d</i> (effect size)
	ipsilateral	ipsilateral
CNN vs. CSN		
Number of cells in resting state	$p = 0.286$	1.8
Number of cells in hyper-ramified state	$p = 0.994$	0.1
Number of cells in reactive state	$p = 0.997$	0
Number of cells in phagocytic state	$p = 0.687$	0.7
RSN vs. CSN		
Number of cells in resting state	$p = 0.461$	0.4
Number of cells in hyper-ramified state	$p = 0.816$	0.6
Number of cells in reactive state	$p = 0.983$	0.3
Number of cells in phagocytic state	$p = 0.202$	1.2
RSN vs. RSS		
Number of cells in resting state	$p = 0.202$	0.9
Number of cells in hyper-ramified state	$p = 0.998$	0.1
Number of cells in reactive state	$p = 0.768$	0.2
Number of cells in phagocytic state	$p = 0.013$	3.7
RSS vs. CSN		
Number of cells in resting state	$p = 0.928$	0.5
Number of cells in hyper-ramified state	$p = 0.883$	0.5
Number of cells in reactive state	$p = 0.925$	0
Number of cells in phagocytic state	$p = 0.422$	0.8
RSN vs. CNN		
Number of cells in resting state	$p = 0.024$	2.1
Number of cells in hyper-ramified state	$p = 0.684$	0.6
Number of cells in reactive state	$p = 0.997$	0.2
Number of cells in phagocytic state	$p = 0.031$	5

The table shows the statistics for number of microglia cells in different states on the ipsilateral side. The number of cells were counted for each ROI and the statistics were performed using the mean. $P < 0.05$ (two-way ANOVA followed by Tukey *post hoc* analysis) was considered significant and effect size was calculated using Cohen *d*. The group comparisons shown here are based on the factors: 1) repeated restraint stress (R) and control (C), 2) NGF (N) and saline (S) injections, and 3) both (RS) and (CN). Ip. ipsilateral; Con. contralateral; ROI, region of interest; SDH, superficial dorsal horn; DDH, deep dorsal horn; Iba-1, ionized calcium binding adapter molecule 1; NGF, nerve growth factor. CSN: control+saline+NGF; RSS: repeated restraint stress+saline+saline; CNN: control+NGF+NGF; and RSN: repeated restraint stress+saline+NGF.

For comparison of the number of cells in different states on the contralateral side please refer to appendix 14.

3.2.9 Proportion and distribution of microglial cells in dorsal horn

The proportion of Iba-1 stained microglial cells in different states (resting to phagocytic) was calculated on site of saline/NGF injections. In the CSN group, the proportion of microglial cells in resting state was 18%, hyper-ramified: 17%, reactive: 37% and phagocytic: 28%. The RSS group had 23% resting state, 21% hyper-ramified, 38% reactive and 18% phagocytic. The CNN group showed 35% resting state, 15% hyper-ramified, 34% reactive and 16% phagocytic state. In the RSN group, the resting state microglia was 11%, hyper-ramified: 17%, reactive: 36% and phagocytic: 36% (Fig. 28. A). The proportion of the phagocytic state microglia was comparatively higher in the group that experienced stress in adolescence followed by NGF injection in adulthood and was significantly different to the groups as observed in Fig. 27. D.

A sub-analysis on the location of these cells within the dorsal horn (superficial and deep) was performed. In the superficial (SDH) and deep dorsal horn (DDH), we did not observe significant differences in the proportion of cells in resting state between the groups that received two and single NGF injection (CNN vs. CSN), but a large effect both in the SDH (29% vs. 13%; $P = 0.100$; $d = 1.3$; Fig. 28. B; Table 5) and DDH (41% vs. 22%; $P = 0.150$; $d = 1.3$; Fig. 28. B; Table 5). This large effect was also observed between the groups (RSN vs. RSS) in the SDH (5% vs. 17%; $P = 0.526$; $d = 1.0$; Fig. 28. B; Table 5). The comparison between the groups (RSN vs. CSN) did not show any difference or effect size. The groups (RSN vs. CNN), showed a significantly lowered proportion of cells in resting state (5% vs. 29%; $P = 0.024$; $d = 1.8$) but not in the deep dorsal horn (DDH) (18% vs. 41%; $P = 0.071$; $d = 1.4$) (Fig. 28. B). For the proportion of cells in the hyper-ramified state, no differences were observed but a large effect only between RSN vs. CNN (15% vs. 12%; $P = 0.360$; $d = 0.9$) in the SDH (Fig. 28. B). Similar to the hyper-ramified state, neither a difference for the proportion of cells in the reactive state nor a large effect was observed between groups (Fig. 28. B; Table 5), both in the SDH and DDH. In phagocytic state, we did not observe differences between the groups (CNN vs. CSN) but a large effect in the DDH (10% vs. 20%; $P = 0.518$; $d = 1.2$; Fig. 28. B; Table 5). The proportion was significantly different between RSN vs. RSS but only in the SDH (42% vs. 19%; $P = 0.007$; $d = 3.4$) and large effect in the DDH (28% vs. 17%; $P = 0.196$; $d = 1$) (Fig. 28. B; Table 5). No significant differences were observed between RSN vs. CSN but a large effect both in the SDH and DDH (SDH: 42% vs. 35%; $P = 0.150$; $d = 1.1$) and

(DDH: 28% vs. 20%; $P = 0.389$; $d = 0.9$) (Fig. 28. B; Table 5). The significance existed both in the SDH and DDH between the groups RSN vs. CNN (SDH: 42% vs. 21%; $P = 0.007$; $d = 3.1$) and (DDH: 28% vs. 10%; $P = 0.042$; $d = 2.3$; Fig. 28. B). The findings from this sub-analysis suggest that SDH has a higher proportion of Iba-1 stained phagocytic microglia compared to the DDH. The proportion of the states of microglial cells in individual ROI's on the ipsilateral side further shows that the phagocytic state cells are higher in proportion in ROI's 1 and 2 compared to ROI's 3 and 4 (Fig. 28. C). The adversity in adolescence plays an important role in this long-term priming process especially in the SDH, which is the first synaptic relay directly, related to the transmission and modulation of pain.

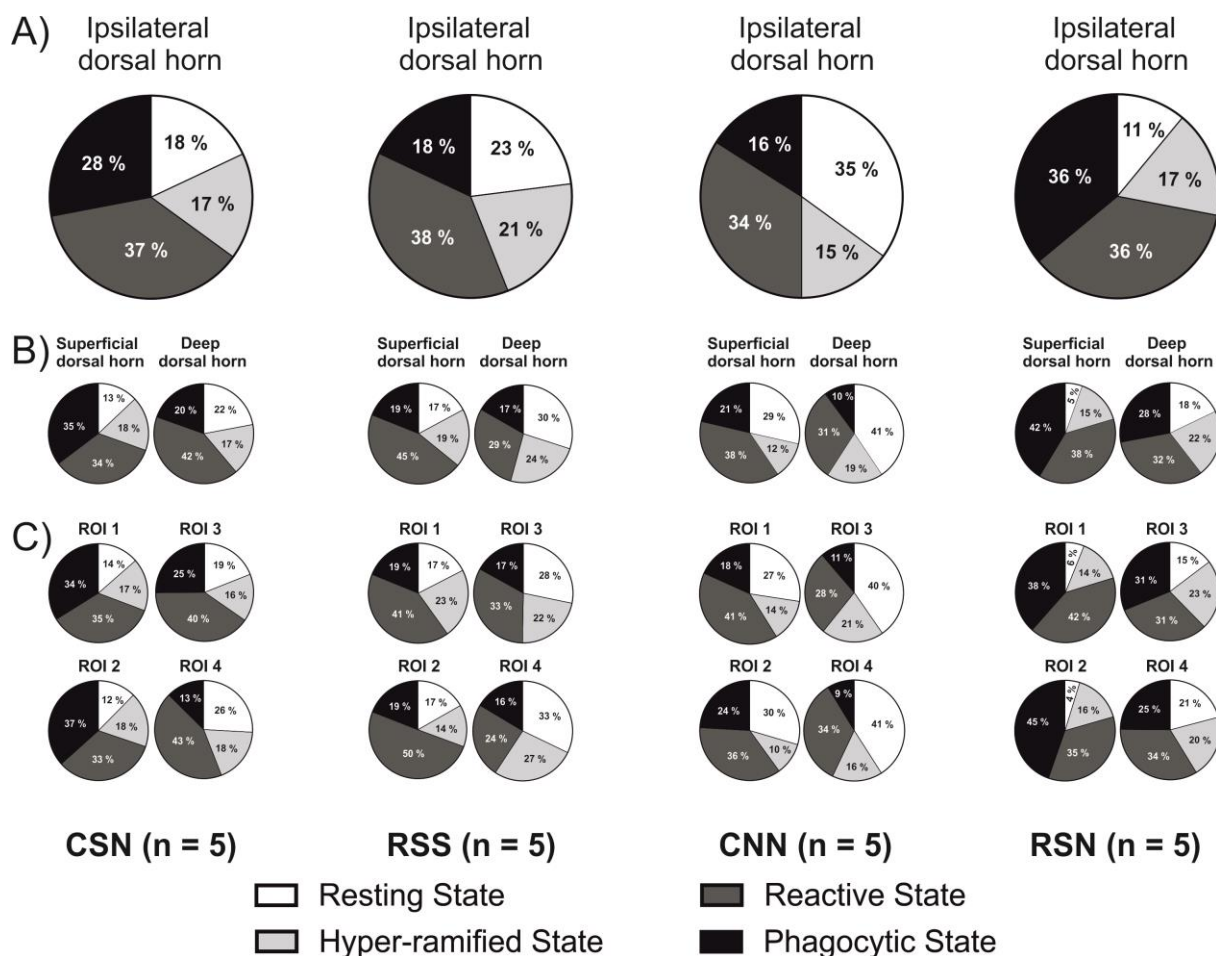


Figure 28: Proportion of Iba-1 stained microglia cell states (ipsilateral).

Repeated restraint stress in adolescence and intramuscular NGF in adulthood leads to increased phagocytic state microglia cells in the superficial dorsal horn. **A)** Pie charts showing the proportion of Iba-1 stained microglia cells in different states in each treatment group on the ipsilateral (ROI's 1+2+3+4) dorsal horn. **B)** Pie charts showing the proportion of Iba-1 stained microglia cells in different states in each treatment group on the superficial (ROI's 1+2) and deep (ROI's 3+4) dorsal horn. **C)** Pie charts showing the proportion of Iba-1 stained microglia cells in different states in each treatment group on the superficial (ROI's 1 & 2) and deep (ROI's 3 & 4) dorsal horn. ROI, region of interest; NGF, nerve growth factor. CSN: control+saline+NGF; RSS: repeated restraint stress+saline+saline; CNN: control+NGF+NGF; and RSN: repeated restraint stress+saline+NGF. White: resting state; Light grey: hyper-ramified state; Dark grey: reactive state; and Black: phagocytic state.

Table 5: Comparison of microglia cell numbers in different states.

Groups	<i>p</i> Value		Cohen <i>d</i> (effect size)	
	Ipsilateral		Ipsilateral	
	SDH	DDH	SDH	DDH
<u>CNN vs. CSN</u>				
Number of cells in resting state	<i>p</i> = 0.100	<i>p</i> = 0.150	1.3	1.3
Number of cells in hyper-ramified state	<i>p</i> = 0.705	<i>p</i> = 0.978	0.6	0.2
Number of cells in reactive state	<i>p</i> = 0.957	<i>p</i> = 0.914	0.3	0.5
Number of cells in phagocytic state	<i>p</i> = 0.460	<i>p</i> = 0.518	0.8	1.2
<u>RSN vs. CSN</u>				
Number of cells in resting state	<i>p</i> = 0.840	<i>p</i> = 0.809	0.6	0.2
Number of cells in hyper-ramified state	<i>p</i> = 0.921	<i>p</i> = 0.735	0.4	0.6
Number of cells in reactive state	<i>p</i> = 0.731	<i>p</i> = 0.970	0.7	0.2
Number of cells in phagocytic state	<i>p</i> = 0.150	<i>p</i> = 0.389	1.1	0.9
<u>RSN vs. RSS</u>				
Number of cells in resting state	<i>p</i> = 0.526	<i>p</i> = 0.381	1.0	0.7
Number of cells in hyper-ramified state	<i>p</i> = 0.967	<i>p</i> = 0.999	0.4	0.0
Number of cells in reactive state	<i>p</i> = 0.810	<i>p</i> = 0.970	0.2	0.3
Number of cells in phagocytic state	<i>p</i> = 0.007	<i>p</i> = 0.196	3.4	1.0
<u>RSS vs. CSN</u>				
Number of cells in resting state	<i>p</i> = 0.940	<i>p</i> = 0.571	0.4	0.5
Number of cells in hyper-ramified state	<i>p</i> = 0.998	<i>p</i> = 0.680	0.0	0.6
Number of cells in reactive state	<i>p</i> = 0.998	<i>p</i> = 0.815	0.3	0.5
Number of cells in phagocytic state	<i>p</i> = 0.381	<i>p</i> = 0.960	0.9	0.2
<u>RSN vs. CNN</u>				
Number of cells in resting state	<i>p</i> = 0.024	<i>p</i> = 0.071	1.8	1.4
Number of cells in hyper-ramified state	<i>p</i> = 0.360	<i>p</i> = 0.917	0.9	0.4
Number of cells in reactive state	<i>p</i> = 0.948	<i>p</i> = 0.996	0.5	0.1
Number of cells in phagocytic state	<i>p</i> = 0.007	<i>p</i> = 0.042	3.1	2.3

The table shows the statistics for number of microglia cells in different states on the superficial and deep dorsal horn on the ipsilateral side alone. The number of cells were counted for each ROI and the statistics were performed using the mean. $P < 0.05$ (two-way ANOVA followed by Tukey *post hoc* analysis) was considered significant and effect size was calculated using Cohen *d*. The group comparisons shown here are based on the factors: 1) repeated restraint stress (R) and control (C), 2) NGF (N) and saline (S) injections, and 3) both (RS) and (CN). Ip. ipsilateral; Con. contralateral; ROI, region of interest; SDH, superficial dorsal horn; DDH, deep dorsal horn; Iba-1, ionized calcium binding adapter molecule 1; NGF, nerve growth factor. CSN: control+saline+NGF; RSS: repeated restraint stress+saline+saline; CNN: control+NGF+NGF; and RSN: repeated restraint stress+saline+NGF.

3.2.10 Analysis of morphological changes in microglial cells

The analysis of morphological changes of the Iba-1 stained microglial cells was carried out for all the four states. The changes were evaluated using four parameters namely: immunoreactive area, perimeter length, feret's diameter and circularity, which are indicators of microglial activation (refer section 2.2.7).

In the resting state morphology, the immunoreactive area was significantly different between the groups CNN vs. CSN ($P = 0.040$; Fig. 29. A) and RSS vs. CSN ($P = 0.022$; Fig. 29. A). The perimeter length was significantly different between the groups CNN vs. CSN ($P = 0.015$; Fig. 29. B) and RSN vs. CSN ($P = 0.023$; Fig. 29. B). For feret's diameter we found significant difference between the group CNN vs. CSN ($P = 0.039$; Fig. 29. C). No significant differences were found between the groups for circularity (Fig. 29. D).

For comparison of the morphological changes on the contralateral side please refer to appendix 15.

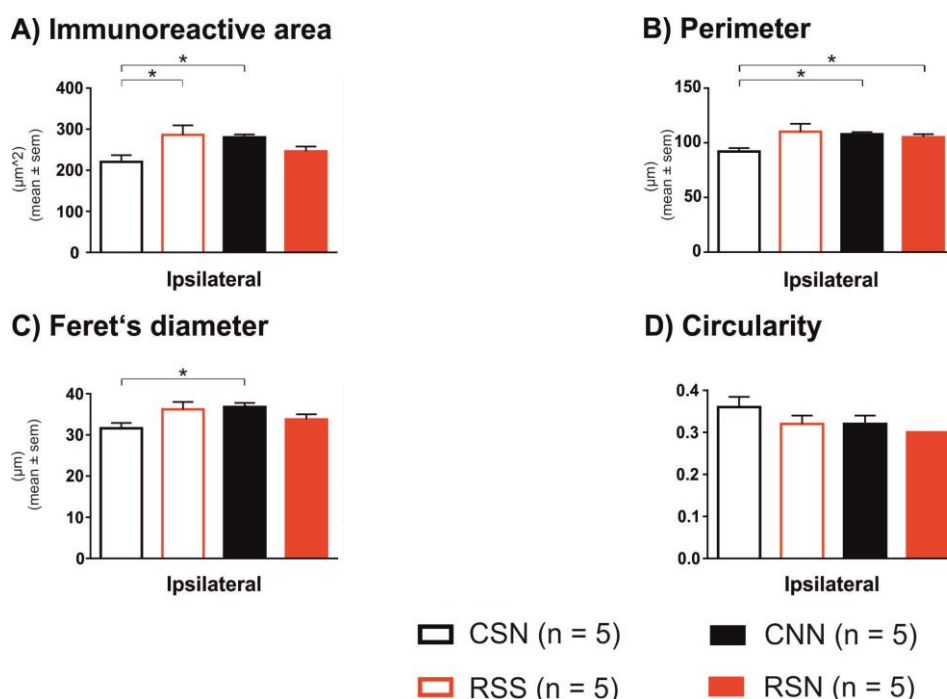


Figure 29: Morphological analysis of resting state microglial cells.

A) Immunoreactive area. **B)** Perimeter length. **C)** Feret's diameter. **D)** Circularity. NGF, nerve growth factor. The values for all the four parameters were calculated for individual cells for each ROI and the statistics were performed using the mean. $P < 0.05$ (A: two-way ANOVA followed by Tukey *post hoc* analysis; B and C: Mann-Whitney *U* test) was considered significant CSN: control+saline+NGF; RSS: repeated restraint stress+saline+saline; CNN: control+NGF+NGF; and RSN: repeated restraint stress+saline+NGF.

For the hyper-ramified state morphology, the feret's diameter was significantly difference between the group RSN vs. CNN ($P = 0.023$; Fig. 30. C) on the ipsilateral side.

For comparison of the morphological changes on the contralateral side please refer to appendix 16.

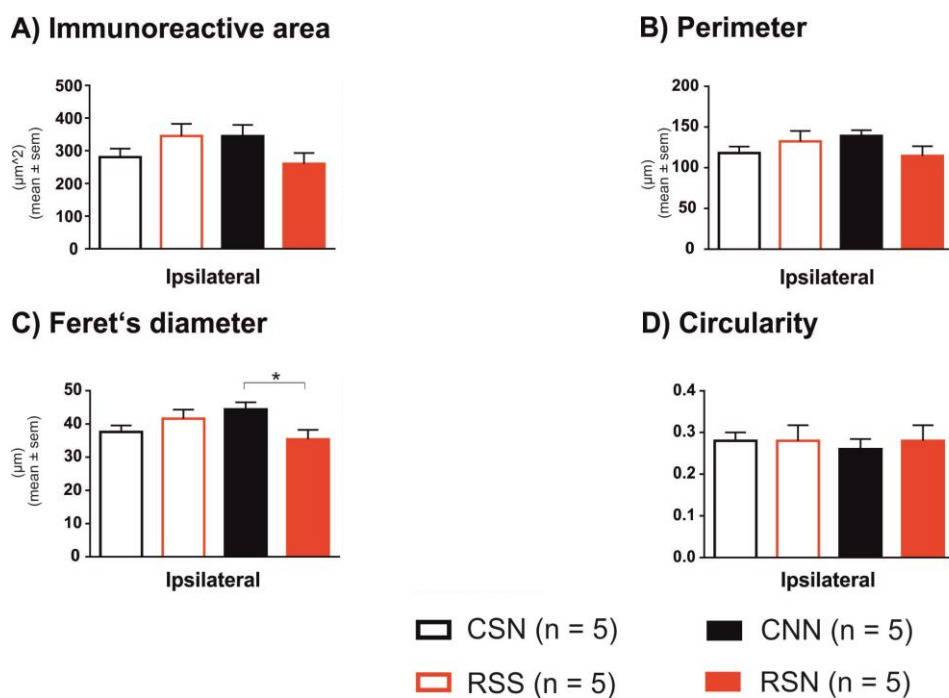


Figure 30: Morphological analysis of hyper-ramified state microglial cells.

A) Immunoreactive area. **B)** Perimeter length. **C)** Feret's diameter. **D)** Circularity. NGF, nerve growth factor. The values for all the four parameters were calculated for individual cells for each ROI and the statistics were performed using the mean. $P < 0.05$ (Mann-Whitney U test) was considered significant CSN: control+saline+NGF; RSS: repeated restraint stress+saline+saline; CNN: control+NGF+NGF; and RSN: repeated restraint stress+saline+NGF.

In the reactive state morphology, the immunoreactive area was significantly different between the groups CNN vs. CSN ($P = 0.038$; Fig. 31. A); RSN vs. CNN ($P = 0.0153$; Fig. 31. A) on the ipsilateral side of saline/NGF injections. The perimeter length was significantly different between the groups CNN vs. RSS ($P = 0.012$; Fig. 31. B); RSN vs. CNN ($P = 0.056$; Fig. 31. B) on the ipsilateral side. For feret's diameter we found significant difference between the groups CNN vs. RSS ($P = 0.007$); CNN vs. CSN ($P = 0.023$); and CNN vs. RSN ($P = 0.015$) (Fig. 31. C) on the ipsilateral side. A significant difference was observed between the group CNN vs. RSS on the ipsilateral side for circularity ($P = 0.007$; Fig. 31. D).

The morphological analysis of microglia in reactive state revealed that the cells in the CNN group responded to the NGF treatment greater than other groups while this effect was not observed in the behavioral test (see Fig. 24). The observed differences between the groups CSN and CNN, is a limited proof of the hypothesis latent vs. manifest sensitization.

For comparison of the morphological changes on the contralateral side please refer to appendix 17.

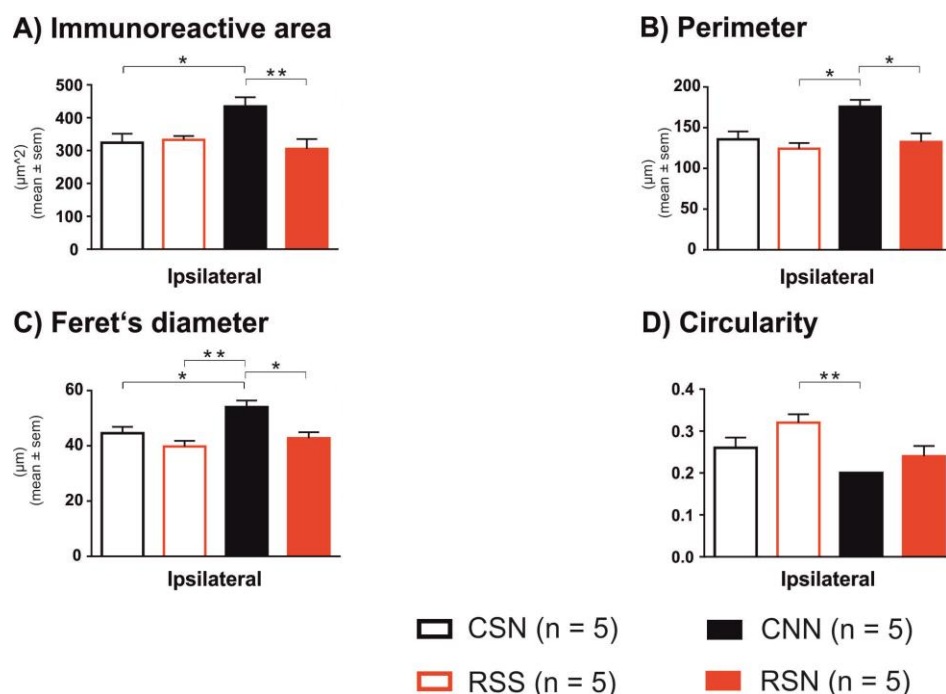


Figure 31: Morphological analysis of reactive state microglial cells.

A) Immunoreactive area. **B)** Perimeter length. **C)** Feret's diameter. **D)** Circularity. NGF, nerve growth factor. The values for all the four parameters were calculated for individual cells for each ROI and the statistics were performed using the mean. $P < 0.05$ (A and B: two-way ANOVA followed by Tukey *post hoc* analysis; C and D: Mann-Whitney *U* test) was considered significant CSN: control+saline+NGF; RSS: repeated restraint stress+saline+saline; CNN: control+NGF+NGF; and RSN: repeated restraint stress+saline+NGF.

For the phagocytic state morphology, no significant differences was observed between the groups (Fig. 32. A - D).

For comparison of the morphological changes on the contralateral side please refer to appendix 18.

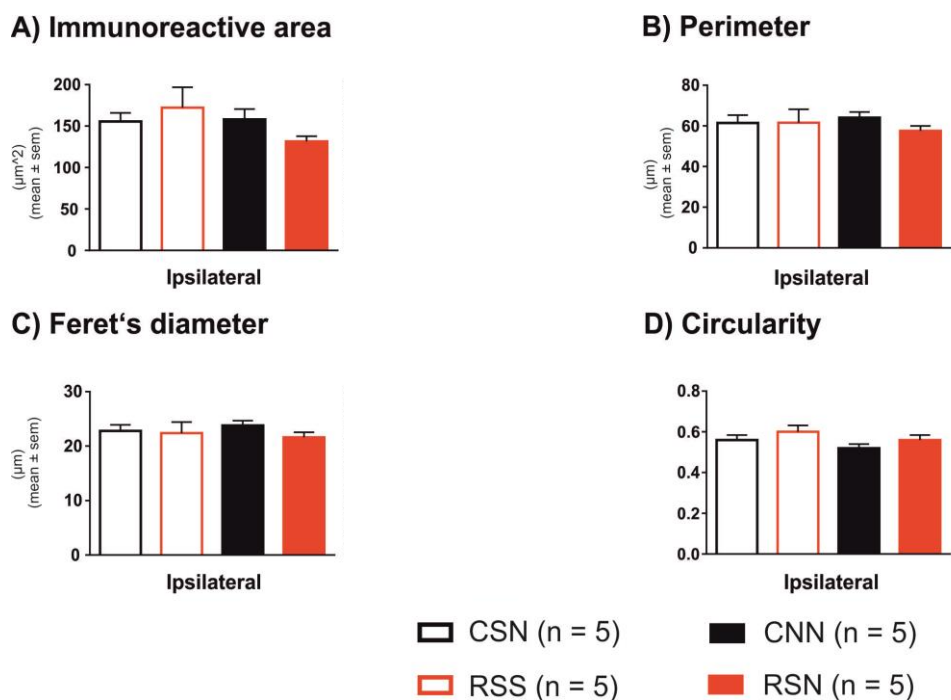


Figure 32: Morphological analysis of phagocytic state microglial cells.

A) Immunoreactive area. **B)** Perimeter length. **C)** Feret's diameter. **D)** Circularity. NGF, nerve growth factor. The values for all the four parameters were calculated for individual cells for each ROI and the statistics were performed using the mean. $P < 0.05$ (A and C: two-way ANOVA followed by Tukey *post hoc* analysis; B and D: Mann-Whitney *U* test) was considered significant CSN: control+saline+NGF; RSS: repeated restraint stress+saline+saline; CNN: control+NGF+NGF; and RSN: repeated restraint stress+saline+NGF.

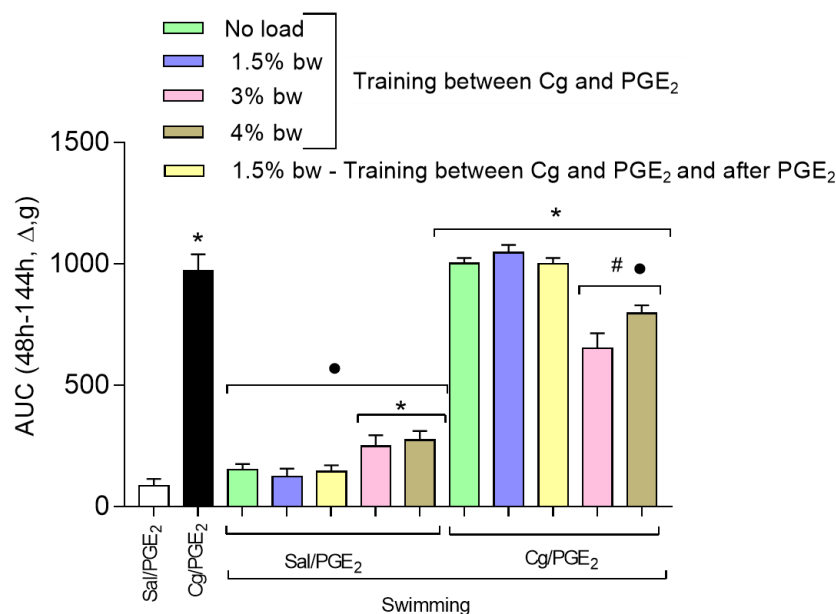
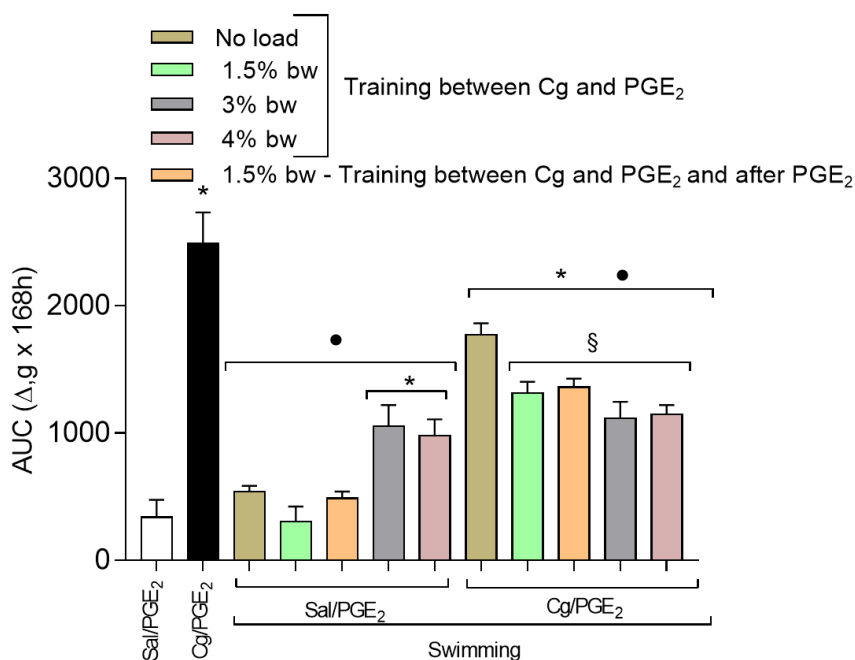
3.3 Study 3: swimming training attenuates chronic muscle pain

The combination of Cg/PGE₂ induces mechanical hyperalgesia compared to the Sal/PGE₂ group ($P < 0.05$; Fig. 33. A & B).

In the control (Sal/PGE₂) group, swimming training without and with load (1.5%) that was added to body weight has no effect compared to its sedentary group, while heavier loads i.e. 3.0% and 4.0% worsened pain-like behavior compared to the sedentary group (Sal/PGE₂). This shows a biphasic effect (Fig. 33. A).

In state of chronic pain (Cg/PGE₂), swimming training without and with loads (1.5%, 3.0%, 4.0%) that were added to body weight helped in alleviating hyperalgesia compared to the sedentary group (Cg/PGE₂) ($P < 0.05$; Fig. 33 B). Additionally, training with loads in chronic pain state has a significant effect in reducing hyperalgesia compared to the no load group (Fig. 33. B).

Swimming training with loads attached to the body helps in reducing chronic hyperalgesia while it worsens and induces hyperalgesia in state of acute pain. Also see appendix 20.

A) acute**B) chronic****Figure 33: Swimming training reduced chronic muscle hyperalgesia.**

On the 'y-axis', area under the curve (AUC) is plotted against the treatment groups in the 'x-axis'. The AUC analysis of the acute (A) and chronic (B) period indicates the effect of swimming physical training with the loads of 1.5%, 3 % and 4% of the body weight (bw) on the mechanical muscle hyperalgesia. The symbols "*" indicate differences to sedentary saline group. The symbols "•" indicate differences to sedentary carrageenan group. The symbols "#" indicate that 3 and 4% differs from 1.5%. The symbols "\$" indicate differences to No load group. Cg: carrageenan; PGE₂: prostaglandin E₂; Sal: saline. Area under the Curve was used to evaluate the chronic period of muscle hyperalgesia and the statistical analysis was performed by One Way ANOVA with Tukey post hoc test. *P* value set at 0.05.

4 DISCUSSION

The present studies have shown that

Study 1

- In male SD rats, stress in adulthood did not show behavioral signs of hyperalgesia which was indicated by no change in the PPT of the low back muscles compared to the controls.
- Stress followed by a mild-nociceptive input (NGF) into the MF muscle increased the proportion of DHNs responding to mechanical stimulation of deep soft tissues of the low back and the hind limb. An increase in the proportion of DHNs having resting activity was also observed especially in neurons with deep input. These outcomes indicate hyperexcitability/hypersensitivity of DHNs which are signs of manifest sensitization.

Study 2

- In male Wistar rats, stress in adolescence induced mechanical hyperalgesia in the local deep tissues and remote skin. This was indicated by lowered PPT of the low back muscles (local) and lowered PWT of the distal hind limb (remote).
- The PPT results showed that the local deep hyperalgesia was more pronounced and longer-lasting while the results of PWT showed that the hyperalgesia in the remote skin was short-lived.
- In adulthood, an additional mild-nociceptive input (NGF) into the MF muscle exacerbated hyperalgesia local to the site of injection and not remote especially in animals that experienced stress in adolescence.
- The NGF injection also lead to an increase in the number of phagocytic state microglial cells in the DHNs of the stressed animals.
- The increase in the number of phagocytic state cells was more pronounced on the ipsilateral side of injection. The proportion of these cells were higher in the superficial dorsal horn compared to the deep dorsal horn.

The behavioral data from both studies demonstrate that the timing of the stressor plays an important role in the induction and maintenance of hyperalgesia.

Though the stressed animals from study 1 did not show behavioral signs of hyperalgesia, the electrophysiological recordings after a subsequent NGF input showed increased hyper-excitability of the DHNs to deep tissue inputs. This was not observed in the previously published stress (Hoheisel et al., 2015) or single NGF alone (Hoheisel et al., 2013) treated animals. The electrophysiological study on male Sprague-Dawley rats suggests that restraint stress or a single NGF injection induced a state of latent sensitization and the combination of both induced manifest sensitization (Singaravelu et al., 2021b).

The animals from study 2 showed that stress in adolescence significantly increased the sensitivity to the pain-related thresholds. The local deep muscle (PPT) hyperalgesia is long-lasting and the remote skin (PWT) is short-lasting. An additional NGF injection in the exacerbated hyperalgesia in the previously stressed animals and is local to the site of injection. These animals also showed an increase in phagocytic and a decrease in resting-state spinal microglial cells.

Taken together, the PPT data immediately after stress from both studies suggest that stress in adolescence ($d = 2.4$) induces long-term significant changes to pain-like behavior compared to stress in adulthood ($d = 0.8$). We think adolescent stress has a stronger impact compared to stress in adulthood and the observed changes in microglial morphology in study 2 could be one of the first steps in pain manifestation.

4.1 Repeated stress alters pain sensitivity

The data from the current studies show in animals that experienced stress are more sensitive to pain-like behavior compared to the controls and stress in early adolescence induces stronger and long-lasting muscle hyperalgesia than stress in adulthood. This is shown by the PPT measurement of the low back multifidus muscle which elicited a stronger response in the early adolescence stressed animals (Fig. 23. A.a) but not in the adulthood stress group (Fig. 16). This difference could be explained due to the timing of the stressor. Pre-clinical studies have shown that the prevalence of prior stressful experience is linked to a high incidence of chronic pain (Greenwood-Van Meerveld and Johnson, 2017; La Porta and Tappe-Theodor, 2020; Le Coz et al., 2017; Ma et al., 2019). Particularly repeated stress is known to induce maladaptive neuroplasticity along peripheral and central pain transmission pathways facilitating the sensitization of nociceptive neurons and transiting from acute to

chronic state (Bardin et al., 2009; Imbe and Kimura, 2020; Korczeniewska et al., 2017; Ma et al., 2019). Le Coz and colleagues (2017) found that social stress led to a modulation of cold responsiveness, but not mechanical stimulation and other studies have shown chronic restraint stress to induce thermal hyperalgesia (Senba et al., 2008), mechanical and cold allodynia, and also enhances inflammatory pain (Bardin et al., 2009).

The major and new finding from study 2 is that restraint stress-induced strong mechanical hyperalgesia to both local deep tissues (PPT) and remote skin (PWT). This is relevant because clinical studies in patients with chronic low back pain along with a history of psychological trauma such as childhood maltreatment have shown altered pressure pain threshold of the low back (Tesarz et al., 2016). The findings reported that childhood maltreatment is associated with reduced PPT in adult subjects with non-specific chronic low back pain (nsCLBP), irrespective of the type of childhood maltreatment. Additionally, they also show that the enhanced deep pain sensitivity can be found in patients with a history of emotional abuse and emotional neglect (Tesarz et al., 2016). Another study with nsCLBP patients with and without trauma exposure (TE) showed that nsCLBP-TE patients presented a lower pain threshold in both the pain-free area and the pain-affected area, while the patients without TE presented lower pain thresholds only in the pain-affected area but not in the pain-free area (Tesarz et al., 2015). Thus the PPT and PWT findings from the adolescent stress animals are in-line with the human findings highlighting the association of chronic LBP and widespread pain in patients with TE and childhood maltreatment (Graven-Nielsen and Arendt-Nielsen, 2010; McBeth et al., 2007; Tesarz et al., 2015).

Apart from behavioral signs of hyperalgesia, chronic stress affects cognitive function. We did not look for changes in cognitive behavior but studies on rodents have shown that stressed animals exhibit signs of anxiety-like behavior (Hoheisel et al., 2015), depression-related behavior in mice (Sousa et al., 2018), cognitive deficits like impaired memory recognition, impaired fear memory (Sun et al., 2020). Hoheisel and colleagues (2015) showed that the stressed animals spent significantly less time in the central zone in the open-field test indicating increased anxiety-like behavior in those animals. Sun and colleagues (2020) showed that stress in juvenile rats led to

cognitive and synaptic dysfunction. In a water maze test, the stressed animals showed increased escape latency (time taken to escape on the platform) to find the target zone. This shows that repeated restraint stress exposure weakened the learning ability and impaired recognition memory, which was detected using the novel object recognition test. Humans suffering from chronic back pain showed brain-behavior pathways (prefrontal-striatal-limbic circuits) for maladaptive learning and lack motivation, which could explain why chronic pain patients can be resistant to change (Nees et al., 2020). The related pathways will be further discussed in chapter 4.4.

Collectively, the current findings are indicative of stress in adolescence induces muscle hyperalgesia to deep and cutaneous inputs, while stress in adulthood does not show this effect. This suggests the importance of timing of the stressor in modulating pain manifestation and might further contribute to longer-lasting changes in pain sensitivity.

4.2 Manifestation of altered pain sensitivity due to stress

No pre-clinical studies have followed up on the potential long-term consequences of adolescent stress on chronic low back pain and widespread pain in adulthood. The behavioral findings showed persistent effects of adolescent stress on the PPT of the low back (Fig. 23. A.a), while the PWT got stabilized, a trend towards lowered threshold was still observed (Fig. 23. B.a) in the adulthood phase.

These findings expand on the previous outcomes of early life stress (ELS) such as maternal separation (MS) showing increased mechanical sensitivity, although results vary. In animals that experienced MS, injection of formalin or CFA in the paw during the adulthood phase increased sensitivity to mechanical, thermal, and chemical stimuli (Vilela et al., 2017). Another study on MS showed resilience against neuropathic pain after CCI in adulthood. These animals showed an increased threshold to mechanical and thermal stimuli compared to the control animals (Genty et al., 2018). In another model of ELS, where the litters were submitted to restricted bedding material (neonatal limited bedding), the rats developed mild muscle hyperalgesia but got aggravated when exposed to painless sound stress in adulthood (Alvarez et al., 2013). Apart from the variability in findings which is most likely due to

the differences in experimental design, stress model, and strain differences that have been reported (Grundt et al., 2009; Hestehave et al., 2019), another factor to consider is the effects of age on pain sensitivity. Both pre-clinical and clinical studies suggest age-related anatomical, physiological, and compensatory mechanisms for the sensory changes that are typically known to occur while aging (Gonzalez-Roldan et al., 2020; Yezierski, 2012).

Thus, the manifestation of pain sensitivity after stress in earlier life depends on various factors e.g. stressor type. The current findings from study 2 showed that the sensitization to deep inputs (local) got manifested on top of the age-related increase in PPT as the animals grew, but not to skin (remote). This could be due to the stressor type. Tesarz and colleagues (2016), showed that in humans with ELS such as sexual abuse is associated with enhanced touch sensitivity and neglect with enhanced temporal summation of pain. It would be interesting to verify the current behavioral findings with a different stressor such as social isolation in adolescent rats which would be equivalent to stressors such as neglect.

NGF induced manifest sensitization

Results from study 2 showed that NGF injection in adulthood led to a drop in PPT of the low back muscles (local) but not to the skin (remote). But the drop in PPT after NGF injection in animals preceded by stress was not significant. Stress in adolescence alone was likely strong enough to induce long-lasting deep muscle hyperalgesia. This sensitization may well be manifest and NGF as a second stimulus only further exacerbated the deep muscle hyperalgesia. Similar to our previous findings, we observed that an initial NGF injection increased sensitivity to PPT in control animals (see Fig. 24) and this hypersensitivity returned to baseline on day two in Wistar rats (see appendix 6). The second NGF injections in the control animals did not lead to further sensitivity (see Fig. 24), an opposite effect as observed in our previous studies on Sprague-Dawley (SD) rats (Hoheisel et al., 2013; Zhang et al., 2017). While this effect could be due to strain differences, a recent study on adult SD rats using our NGF based myofascial LBP model, showed that only on day 12 (7 days after the 2nd NGF injection), female rats developed bilateral trunk mechanical hyperalgesia and bilateral hind paw mechanical allodynia (Reed et al., 2020). In male

SD rats, two NGF injections led only to ipsilateral cutaneous and deep trunk mechanical hypersensitivity and this was absent in the contralateral side (Reed et al., 2021). Signs of allodynia was not observed on male rats unlike female rats but the development of deep muscle hyperalgesia was already observed on day 7 (2 days after the 2nd NGF injection) and lasted until day 14, implying the occurrence of sex differences (Reed et al., 2021; Reed et al., 2020). In all cases, NGF injection led to an increase in sensitivity in the PPT in both stressed and control animals with stressed animals maintaining a significantly lowered threshold when compared to the controls. In a mouse model of NGF-induced myofascial LBP combined with stress, results suggested that exposure to chronic unpredictable stress only slightly worsened the pain-like behavior while vertical chronic restraint stress primed and highly aggravated pain in combination with NGF (La Porta and Tappe-Theodor, 2020). This was shown by back hypersensitivity to pressure and light touch, hypersensitivity towards mechanical and cold at the hind paws, and agreed with the other LBP models (Park et al., 2018; Shi et al., 2018; Strong et al., 2013).

In study 2, a single NGF injection-induced latent sensitization but when preceded by adolescence stress, it turns into manifest sensitization as observed in the PPT. An exacerbated effect of repeated NGF was not observed in the study with Wistar rats, unlike in SD rats which could be due to strain differences (Hestehave et al., 2019). In male Wistar rats, repeated restraint stress in adolescence may lead to a ceiling effect due to which a significant drop in deep muscle hyperalgesia was not observed after NGF injection in adulthood.

4.3 Persistent effects of stress in combination with NGF

Electrophysiological recordings of dorsal horn neurons

The present electrophysiological study on male SD rats showed that stress in combination with NGF led to a significant increase in the proportion of neurons responding to deep tissue mechanical stimuli, a significant increase in the proportion of neurons showing resting activity along with deep tissue input compared to the NGF alone treated group. No changes were observed in the proportion of neurons having skin and convergent input between the groups. The combination also showed

increased receptive fields to deep tissue input both in the low back and outside the low back compared to NGF alone.

Recent studies from our group have shown that the responsiveness of the dorsal horn neurons to fascia and muscle input increased after two NGF injections, which was not observed after single NGF injections (Hoheisel et al., 2013; Hoheisel et al., 2007; Zhang et al., 2017). De Azambuja and colleagues (2018) showed that physical exercise attenuated this NGF-induced sensitization of DHNs. They showed that a short-term swimming exercise after the first NGF injection decreased the hyper-excitability of the DHNs to low back input and lowered the resting activity of sensitized neurons after the administration of additional NGF injection. These results led to the concept of latent sensitization caused by the first NGF injection, which in turn primes the DHNs that can be further sensitized by a second NGF injection in the same site five days apart. In the current study, the responsiveness of the DHNs to the deep tissue input significantly increased in the animals that experienced stress in adulthood only after a subsequent NGF injection just before the recording of the DHNs, while stress alone in adulthood induced only nonsignificant changes in the DHN responsiveness (Hoheisel et al., 2015). The findings from this study suggest that restraint stress in adulthood induced a state of latent sensitization by priming the DHNs and these primed neurons had an enhanced susceptibility to developing a manifest sensitization by a subsequent mild-nociceptive input.

This manifest sensitization was input specific (i.e.) the latent sensitization was challenged with mild nociceptive input from deep soft tissues of the low back and distal hind limb and that only the DHNs with deep tissue input were upregulated. This non-significant upregulation comprised of convergent neurons but the overall cutaneous response remained unchanged not only in the current study but also in the former studies that used NGF to induce manifest sensitization (Hoheisel and Mense, 2015; Hoheisel et al., 2013; Hoheisel et al., 2015; Sessler et al., 2021; Zhang et al., 2017). The cutaneous afferents are known to have highly effective synaptic connections on DHNs and might have a ceiling effect for additional mild-nociceptive induced sensitization (Hoheisel et al., 2015).

The appearance of new RFs in the distal hind limb outside the low back indicates that the responsiveness of DHNs was enhanced also for deep tissue input, which was not activated by the NGF injection alone just before the electrophysiological recording of the spinal neurons. These results help us to support the conclusion that the manifest sensitization occurred at the DHNs and not in the periphery. This pattern is suggestive of pain referral from deep tissues, which is referred to other deep tissues but not to the skin (Eitner et al., 2017; Hoheisel et al., 1994; Hoheisel et al., 1993), similar to the ‘pseudoradicular’ pain in the proximal leg of patients with LBP (Freynhagen et al., 2008).

This section in parts has been taken from (Singaravelu et al., 2021b).

Immunohistological findings of dorsal horn neurons

In the present studies with male Wistar rats, the effect of early adolescence stress in combination with NGF injection on the sensitization of DHNs was evaluated by staining the lumbar (L2) spinal cord section for glial cells. The results showed that the combination of stress + NGF led to decreased number of microglial cells in the resting state and an increased number of cells in the phagocytic state compared to stress alone or a combination of two NGF (see Fig. 27). No changes in staining intensity were observed between the groups for microglia (Iba-1) and astrocytes (GFAP).

Stress and NGF on microglial morphology

In pre-clinical studies, the effect of stress on Iba-1 activity and morphological changes of microglial cells has been studied widely on various brain regions (Hinwood et al., 2012; Kopp et al., 2013; Paolicelli et al., 2011; Park et al., 2011; Schiavone et al., 2009; Sugama et al., 2007; Tynan et al., 2010) while only a few studies have investigated effects in the spinal cord (La Porta and Tappe-Theodor, 2020; Sessler et al., 2021; Zhang et al., 2017). However, to our knowledge, no studies have shown quantitative analysis of structural changes in microglia morphology especially the phagocytic state in the lumbar spinal cord (see Fig. 27. D). The analysis of the microglial structural morphology revealed that under all

experimental conditions many of the Iba-1 stained cells were in a reactive state (see Fig. 28; 34 to 38%) implying that all the animals responded to the treatment they received. Given the dynamic nature of microglia, the stimuli presented in our treatment groups promote the transition from resting to reactive (activated) state. We found a similar proportion (36%) of phagocytic state microglia only in the NGF group that was preceded by stress. This functional plasticity of microglia is known to be dependent on the type, duration, and intensity of the triggering stimuli (Schwartz et al., 2006).

This may imply increased migration of microglia to undertake their phagocytic state and whether the state of change is neuroprotective or neurotoxic phenotype remains elusive. Evidence suggests that the reactive microglial phenotypes have been categorized into polarization states based on the classifications used for macrophage activation states such as M1 and M2. The M1 phenotype is the classically activated and pro-inflammatory state while the M2 is the alternatively activated anti-inflammatory state, reflecting the dual natures of neurotoxicity and neuroprotection (Burke et al., 2016). Since our behavioral findings show increased sensitivity to PPT of the low back, we think the activated microglia in our results are in the M1 state, which represents the pro-inflammatory state. Former studies revealed region-specific microglia heterogeneity differences on a microscale in different brain regions (Tay et al., 2019; Tynan et al., 2010). Although in our current findings, we show that the proportion of Iba-1 stained phagocytic state microglial cells were predominantly present in the superficial DH compared to the deep DH (see Fig. 28. B. and C.), we did not evaluate other lumbar segments in the spinal cord. La Porta and colleague (2020), showed the distribution of a colorant that mimicked the distribution of injected NGF into the MF muscle at vertebral level L5. The presence of the colorant was stronger and deeper in the MF muscle at L5 compared to upper vertebral lumbar segments. This leads to an interesting question, suggesting there may be lumbar-specific differences of microglia activation in the spinal cord.

Nevertheless, the current findings provide partial evidence on the interaction of stress and NGF on microglial function, and additional assessment of microglial heterogeneity parameters are needed to characterize the microglial phenotype. Considering that LBP is the most common form of pain experienced in humans, our

findings present a novel animal model to investigate neurobiological mechanisms underlying the long-term effects of adolescent stress on pain modulation in adults. The potential mechanisms that are involved is discussed in chapter 4.4.

Stress and NGF on astrocytes activity

In the present study with male Wistar rats, no changes on staining intensity were observed between the groups for astrocytes (GFAP) but we found within group difference between the superficial and deep dorsal horn (see appendix 6).

Most of the pre-clinical studies have shown that hypertrophy of astrocytes and increase in staining intensity is the evidence of astrocyte activation (Gao and Ji, 2010; La Porta and Tappe-Theodor, 2020; Pekny and Nilsson, 2005; Zhang et al., 2017). In our study, the higher GFAP staining intensity in the SDH than the DDH could simply be explained by the anatomical location of glial cells (Ruiz-Sauri et al., 2019). This finding could as well be relevant to the increased concentration of phagocytic state microglia in the SDH compared to the DDH, though the signs of astrocytes activation was not prominent as microglia. In animal models of inflammatory and neuropathic pain, upregulation of GFAP was observed (La Porta and Tappe-Theodor, 2020; Owolabi and Saab, 2006; Sweitzer et al., 2001).

In the present study, the tissues were extracted one day after the second injection, which might be a short duration to observe activation of astrocytes. The activation of astrocytes goes through different phases and occur in different time windows and the morphological changes occurs in hours or days after the injury (Gao and Ji, 2010). Zhang and colleagues (2017) showed that the induction of spinal neuronal sensitization in the myofascial LBP model depends on microglia activation and its maintenance is regulated by astrocyte activation. The current findings shows drop in the PPT and activation of microglia, which are signs of neuronal sensitization and support the findings of Zhang and colleagues (2017). To evaluate the activation of astrocytes, the animals need to be euthanized at a later time point from the current studies (~ five days after the 2nd injection). This might help us to estimate the maintenance of the manifest sensitization after NGF injection in the animals preceded by adolescence stress and could show the activation of astrocytes.

4.4 Potential mechanisms for the stress and NGF induced sensitization

One of the major findings from the electrophysiological experiment was the appearance of new RFs, which is an important sign of central sensitization. New RFs might emerge based on increased synaptic strength of the ineffective synapses of the DHNs that are known normally only to induce sub-threshold postsynaptic potentials and not action potentials (Drdla and Sandkuhler, 2008; Hoheisel et al., 2019; Ikeda et al., 2003; Koerber et al., 2006; Wall, 1977). Studies have shown that DHNs have a subliminal fringe around their receptive fields and that central sensitization can recruit this fringe into RFs from which the neurons respond with action potentials (Pubols, 1990; Woolf and King, 1989). There are also the so-called silent synapses in the CNS that express only NMDA receptors. These receptors are known to respond to glutamate that is released only after preceding depolarization by another input and unsilencing of such synapses to the neurons in lamina I has been found in an inflammatory pain model (Torsney, 2011). Hoheisel and colleagues (2019) recently demonstrated that the hypersensitivity of the DHNs to a peripheral input was due to both unmasking of silent synapses and increased synaptic strength by intracellular recordings in a model of muscle pain.

Repeated psychophysical stress has shown to sensitize DHNs in deep laminae rather than the superficial laminae, in a rodent model of temporomandibular pain (Okamoto et al., 2012). It is known that the primary afferents from muscles project to both the superficial and deep DHNs (Craig and Mense, 1983; McMahon and Wall, 1985), and Taguchi and colleagues (2008) showed that the input from the low back muscles is more prominent in the deep laminae. In our experiments, the search for DHNs responding to electrical and mechanical stimuli included both the superficial and deep laminae and most of recorded neurons were found in the deep lamina V, (i.e.), in a region where low back input may be modulated by stress. This type of modulation might be intraspinal via microglia or astrocytes activation, both of which might be activated by stress (Bardin et al., 2009; Calcia et al., 2016; Chen et al., 2018; La Porta and Tappe-Theodor, 2020; Okada-Ogawa et al., 2009; Owolabi and Saab, 2006). Transient activation of microglia (Alexander et al., 2009), increased gene expression of proinflammatory cytokines (Rivat et al., 2010) are essential for triggering stress-induced hypersensitivity, while increased spinal glutamatergic

signaling via glucocorticoids is essential for its chronicity (Alexander et al., 2009; Li et al., 2014). Pre-clinical studies have shown that ELS or peripheral tissue or nerve damage can activate spinal microglia and astrocytes via neurotransmitters or other signaling substances like (ATP, fractalkine), which are released from the central terminals of active primary afferents. This release leads to activation of different MAPK pathways along with the release of cytokines, inflammatory mediators and many other active substances such as IL-1 β , MCP-1, TNF- α , PGE₂, which are known to be involved in the modulation of the spinal excitatory and inhibitory synaptic transmissions. This leads to neuronal activation and the nociceptive information travels via the ascending tracts of the spinal cord to the supraspinal centers (Clark and Malcangio, 2012; Genty et al., 2018).

In a study by Gruber-Schoffnerger and colleagues (2013), activation of spinal glial cells participated in the LTP induction at C-fiber synapses in the spinal cord lamina I in vitro-microglia was activated within 30 minutes after high frequency stimulation and astrocytes were activated by HFS with a delayed and prolonged time course and found the role of glial cells in inducing LTP by HFS. Since our hypothesis is based on NGF and the involvement of activated microglial cells and signaling, studies have shown that microglia can also be activated by an important feedback loop mechanism through the release of fractalkine (CX3CL1) from the primary terminals and DHNs which bind to the CX3CR1 receptors on microglial cells (Clark and Malcangio, 2014; Owolabi and Saab, 2006; Xanthos and Sandkuhler, 2014). Zhang and colleagues (2017) showed in the NGF-induced myofascial LBP model that blocking microglial activation prevented spinal latent sensitization while blocking astrocyte activation reversed the effect. Blocking fractalkine signaling via neutralizing antibodies in a dose-dependent manner also prevented NGF-induced sensitization suggesting the critical role of neuron-to-microglia signaling via the CX3CL1-CX3CR1 pathway (Sessler et al., 2021).. It is known that substances such as glutamate, ATP, Ca²⁺, Prostaglandins, etc., released from glial cells and neurons facilitate glutamatergic synaptic transmission between C-fiber afferents and DHNs by binding to their respective receptors on spinal neurons or primary afferent C-fibers (Gruber-Schoffnerger et al., 2013). Studies have shown that the substances involved in the glial cell activation participate in the modulation of synaptic transmission and induction of LTP. Clark and colleagues (2015) have shown that the release of IL-1 β

from microglia modulated NMDA in the postsynaptic neurons that resulted in the release of an eicosanoid messenger, which ended in increased release of presynaptic neurotransmitters.

One of the main observations in the early adolescence stress study was the stress-induced effects on long-lasting hyperalgesia. Central sensitization of signal processing in other CNS regions such as the amygdala, which is known to be involved in the behavioral responses, might as well play a role (Suvrathan et al., 2014). Studies on neuropathic pain models have shown that, descending facilitation via a brainstem loop is known to contribute to central sensitization and enhance excitability of the DHNs (Suzuki and Dickenson, 2005; Suzuki et al., 2002; Yu and Mense, 1990). These descending pathways could be activated by stress via an excitatory pathway from the medial hypothalamus to the rostral ventral medulla oblongata (Heinricher et al., 2009; Martenson et al., 2009) and onward to the DH and this phenomenon is known as 'stress-induced hyperalgesia'. Increased descending facilitation or decreased descending inhibition could enhance the excitability of the spinal neurons (Heinricher et al., 2009). Zhang and colleagues (2017) showed that in nociceptive DHNs in the lamina V, the descending inhibition had a stronger effect on the input from deep tissues than the cutaneous inputs to the same neurons.

All of the above mentioned mechanisms might possibly explain why stress could be a predisposing factor for myofascial pain rather than cutaneous pain in humans and that both spinal and supraspinal mechanisms are likely to be involved in the synergistic action between stress and NGF.

This section in parts has been taken from (Singaravelu et al., 2021b).

4.5 Limitations

The results in this work are based on observations made from two different rat strains and strain differences in stress sensitivity and pain sensitivity have been reported (Grundt et al., 2009; Hestehave et al., 2019). This limits us from making a direct comparison between the studies. Nevertheless, the findings are interpreted based on the timing differences of the stressor to induce sensitization of the DHNs and spinal microglia. The observed differences may be also partly due to the strains.

We did not use a biomarker to assess the stress levels, but a previous study in our group found upregulation in fecal corticosterone metabolites and lowered body weight in the stressed animals (Hoheisel et al., 2015). Since one of the study in this work is based on stress in adolescence, it would be helpful to assess stress levels in the future experiments to find the duration of elevated corticosterone levels and might add additional support to the observed findings.

In study 1

- Due to experimental design it was not possible to measure the behavioral data after the NGF injection and thus could not correlate electrophysiological findings with the behavioral results.
- The experimenters were not blinded to the treatment the animals received. In order to minimize investigator bias, an electrical search stimulus was used for unbiased sampling of DHNs and the search for RFs strictly followed a standard protocol (refer to section 2.1.5).

In study 2

- A pure negative control as a treatment group was not performed and this limits the interpretation of those results and should be considered in future studies.
- Activated macrophages are known to have a phenotype (M1: pro-inflammatory) and (M2: anti-inflammatory). Since the behavioral data show exacerbation of pain after NGF injection in stressed animals, an additional counter staining with a positive marker such as CD86 which is specifically expressed in M1 state would be helpful.

In both the studies, only male rats were used and cannot draw a generalizable conclusion on the effects of stress on female pain sensitivity. But, Reed and colleagues (2020; 2021) showed that two NGF injections into the MF muscle induced mechanical hyperalgesia in both the sexes and found timing differences on the onset of hyperalgesia.

4.6 Conclusions

The present work aimed at investigating the sensitization process of dorsal horn neurons based on the timing of repeated restraint stress and in combination with a mild-nociceptive (NGF) input to induce manifest sensitization.

The specific aims of this work (see section 1.7.3) were addressed as follows: The results from the electrophysiological experiment (study 1), suggest that repeated restraint stress in adulthood in male SD rats induces a state of latent sensitization and primes for manifest sensitization by a subsequent NGF injection. This manifest sensitization of the DHNs was indicated by increased afferent inputs from the deep tissues of the low back, an expansion of deep receptive fields to the distal hind limb, and an increase in the resting activity of the neurons especially with deep tissue inputs. These neurophysiological parameters suggest a synergy between mild noxious events in low back muscles and stress. The findings from this study might reflect the neuronal background of spontaneous and evoked pain in patients with LBP.

The results from the immunohistochemistry experiment (study 2), suggest that repeated restraint stress in adolescence in male Wistar rats induced long-term deep muscle hyperalgesia. As indicated by PPT results, the local deep hyperalgesia was more pronounced and longer lasting, while the PWT of the remote skin showed that the sensitization was short lived. A subsequent NGF into the MF muscle, led to exacerbation of pain local to the site of injection but not remote skin. Particularly, the effect of NGF is more pronounced when it is preceded by stress and is facilitated by phagocytic state microglial cells. The increased sensitivity of muscle nociceptors to inflammatory mediators via activated microglia may contribute to the pathophysiology of clinical low back pain in patients with a history of adversity in childhood.

The findings in this work provide an insight on how stress primes the DHNs and an additional mild-nociceptive input leads to manifest sensitization and that activated microglia might play a significant role in this transition. The experimental model presented here would help in understanding the clinical condition of non-specific LBP.

5 SUMMARY

Non-specific low back pain (nsLBP) is considered as the global leading cause of years lived with disability affecting more than half a billion people. Adverse childhood experiences (ACEs), are one of the major risk factors for the development of both mental and physical disorders in later life. In humans, stress and ACEs are known risk factors for the chronicity of LBP and the development of chronic widespread pain. However, very little is known about the neuronal mechanisms that contribute to the development of this enhanced chronicity and sensitization in cases of nsLBP. The present studies aimed at investigating the impact of repeated restraint stress in an animal model of nerve growth factor (NGF) - induced myofascial low back pain.

To answer the importance of timing of the stressors, in two separate experimental approaches, the animals were stressed repeatedly in a narrow plastic restrainer on 12 consecutive days for 1 hour every day. In one experiment, the animals were stressed in adulthood and in the other experiment at early adolescence. Behavioral tests to assess for mechanically-induced pain-like behavior was assessed on the low back for local pain and at the distal hind paw for spreading of pain. The tests were performed before and after stress and in conjunction with saline/NGF injections.

In deeply anesthetized rats that experienced stress in adulthood, recordings were made with glass microelectrodes from the dorsal horn neurons (DHNs) in the spinal L2 segment. To induce hyper excitability, NGF was injected into the multifidus (MF) muscle at the vertebral level L5 directly before the *in-vivo* recordings started. As control, animals were handled but not repeatedly restrained and also received NGF injection before the recordings.

Restraint stress in adulthood slightly lowered the low back pressure pain threshold (PPT) (Cohen $d = 0.8$) and a subsequent NGF injection led to an increase in the proportion of DHNs with input from deep tissues (fascia and/or muscle) of the low back (14% vs. 39%; $p = 0.041$). This increased proportion was also observed for neurons with receptive fields outside the low back (7% vs. 26%; $p = 0.081$). Furthermore, the proportion of neurons with resting activity significantly increased (28% vs. 55%; $p = 0.039$) and this was especially in neurons having deep input (0%

vs. 26%; $p = 0.004$). The proportion of neurons with convergent input (input from two types of tissues) showed an increased trend (7% vs. 23%; $p = 0.147$) but no changes were observed for neurons only with skin input (65% vs. 61%, $p = 0.793$) which are the majority in the dorsal horn.

In rats that experienced restraint stress in adolescence followed by two intramuscular injections of saline or NGF or both in adulthood, animals were transcardially perfused and lumbar spinal cord sections were extracted. Immunohistochemistry was performed on spinal L2 segments and were stained for ionized calcium-binding (Iba-1), a protein specifically expressed in microglia. Morphological analysis was performed on the Iba-1 positive cells.

Adolescent restraint stress significantly lowered the local low back PPT ($d = 2.4$) and remote paw withdrawal threshold ($d = 2.0$) (PWT) immediately after the stress. While the lowered local PPT was maintained throughout adulthood ($d = 1.2$) the distal PWT ($d = 0.9$) was stabilized but showed large effect. A subsequent NGF injection in adulthood in previously stressed animals slightly lowered the PPT ($d = 0.9$) but not PWT. These animals also showed a significant increase in the proportion and number of microglial cells in the phagocytic state compared to the stress + 2 saline group (36% vs. 18%; $p = 0.013$) and control + 2 NGF injections (36% vs. 16%; $p = 0.031$) group. The proportion and number of cells in resting state in those animals was significantly lower compared to the control + 2 NGF group (11% vs. 35%; $p = 0.024$).

The electrophysiological findings suggest that stress in adulthood followed by mild-nociceptive input causes manifest sensitization of the spinal neurons. The behavioral findings from animals stressed in adolescence show long-term central sensitization and a mild-nociceptive input in adulthood exacerbates this behavior and alters the morphology of microglial cells to phagocytic state. These findings indicate that stress in adulthood induces a state of latent sensitization and is manifested when presented with a mild-nociceptive input. While, stress in adolescence induces a long-term central sensitization and an additional insult in later life worsens this effect and that activated spinal microglial cells are involved in the development of manifest sensitization (see Fig. 34).

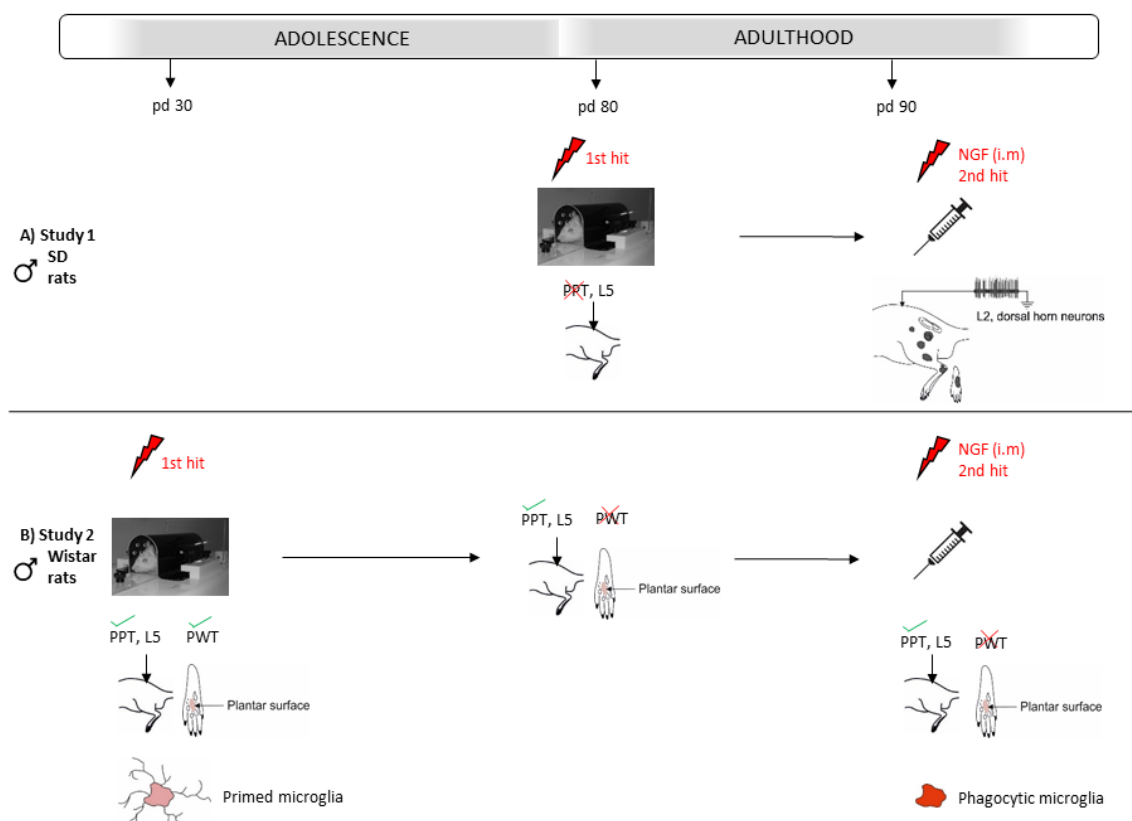


Figure 34: Summary.

A) study 1 (*in vivo* electrophysiology): repeated restraint stress in adulthood (1st hit) followed by NGF (mild-nociceptive) injection (2nd hit). **B)** study 2 (quantitative immunohistochemistry): repeated restraint stress in adolescence (1st hit) followed by NGF (mild-nociceptive) injection in adulthood (2nd hit). pd: postnatal day; PPT: pressure pain threshold; PWT: paw withdrawal threshold; i.m.: intramuscular.

6 REFERENCES

(1997). *Coping with chronic stress* (New York, NY, US: Plenum Press).

Alexander, J.K., DeVries, A.C., Kigerl, K.A., Dahlman, J.M., and Popovich, P.G. (2009). Stress exacerbates neuropathic pain via glucocorticoid and NMDA receptor activation. *Brain Behav Immun* 23, 851-860.

Alvarez, P., Green, P.G., and Levine, J.D. (2013). Stress in the adult rat exacerbates muscle pain induced by early-life stress. *Biol Psychiatry* 74, 688-695.

Andersen, S.L., Tomada, A., Vincow, E.S., Valente, E., Polcari, A., and Teicher, M.H. (2008). Preliminary evidence for sensitive periods in the effect of childhood sexual abuse on regional brain development. *J Neuropsychiatry Clin Neurosci* 20, 292-301.

Arendt-Nielsen, L., and Graven-Nielsen, T. (2003). Central sensitization in fibromyalgia and other musculoskeletal disorders. *Curr Pain Headache Rep* 7, 355-361.

Ayoub, A.E., and Salm, A.K. (2003). Increased morphological diversity of microglia in the activated hypothalamic supraoptic nucleus. *J Neurosci* 23, 7759-7766.

Baker, L.M., Williams, L.M., Korgaonkar, M.S., Cohen, R.A., Heaps, J.M., and Paul, R.H. (2013). Impact of early vs. late childhood early life stress on brain morphometrics. *Brain Imaging Behav* 7, 196-203.

Balague, F., Mannion, A.F., Pellise, F., and Cedraschi, C. (2012). Non-specific low back pain. *Lancet* 379, 482-491.

Bao, L., Zhu, Y., Elhassan, A.M., Wu, Q., Xiao, B., Zhu, J., and Lindgren, J.U. (2001). Adjuvant-induced arthritis: IL-1 beta, IL-6 and TNF-alpha are up-regulated in the spinal cord. *Neuroreport* 12, 3905-3908.

Bardin, L., Malfetes, N., Newman-Tancredi, A., and Depoortere, R. (2009). Chronic restraint stress induces mechanical and cold allodynia, and enhances inflammatory pain in rat: Relevance to human stress-associated painful pathologies. *Behav Brain Res* 205, 360-366.

Bardin, L.D., King, P., and Maher, C.G. (2017). Diagnostic triage for low back pain: a practical approach for primary care. *Med J Aust* 206, 268-273.

Baron, R., Babcock, A.A., Nemirovsky, A., Finsen, B., and Monsonego, A. (2014). Accelerated microglial pathology is associated with Abeta plaques in mouse models of Alzheimer's disease. *Aging Cell* 13, 584-595.

Bartlett, M.S. (1947). The use of transformations. *Biometrics* 3, 39-52.

- Berg, S., Kutra, D., Kroeger, T., Straehle, C.N., Kausler, B.X., Haubold, C., Schiegg, M., Ales, J., Beier, T., Rudy, M., *et al.* (2019). ilastik: interactive machine learning for (bio)image analysis. *Nat Methods* 16, 1226-1232.
- Bernstein, I.A., Malik, Q., Carville, S., and Ward, S. (2017). Low back pain and sciatica: summary of NICE guidance. *BMJ* 356, i6748.
- Brockhaus, J., Moller, T., and Kettenmann, H. (1996). Phagocytosing ameboid microglial cells studied in a mouse corpus callosum slice preparation. *Glia* 16, 81-90.
- Burke, N.N., Fan, C.Y., and Trang, T. (2016). Microglia in health and pain: impact of noxious early life events. *Exp Physiol* 101, 1003-1021.
- Burke, N.N., Geoghegan, E., Kerr, D.M., Moriarty, O., Finn, D.P., and Roche, M. (2013). Altered neuropathic pain behaviour in a rat model of depression is associated with changes in inflammatory gene expression in the amygdala. *Genes Brain Behav* 12, 705-713.
- Calcia, M.A., Bonsall, D.R., Bloomfield, P.S., Selvaraj, S., Barichello, T., and Howes, O.D. (2016). Stress and neuroinflammation: a systematic review of the effects of stress on microglia and the implications for mental illness. *Psychopharmacology (Berl)* 233, 1637-1650.
- Caspani, O., Reitz, M.C., Ceci, A., Kremer, A., and Treede, R.D. (2014). Tramadol reduces anxiety-related and depression-associated behaviors presumably induced by pain in the chronic constriction injury model of neuropathic pain in rats. *Pharmacol Biochem Behav* 124, 290-296.
- Chacur, M., Lambertz, D., Hoheisel, U., and Mense, S. (2009). Role of spinal microglia in myositis-induced central sensitisation: an immunohistochemical and behavioural study in rats. *Eur J Pain* 13, 915-923.
- Chapman, C.R., Tuckett, R.P., and Song, C.W. (2008). Pain and stress in a systems perspective: reciprocal neural, endocrine, and immune interactions. *J Pain* 9, 122-145.
- Chen, G., Zhang, Y.Q., Qadri, Y.J., Serhan, C.N., and Ji, R.R. (2018). Microglia in Pain: Detrimental and Protective Roles in Pathogenesis and Resolution of Pain. *Neuron* 100, 1292-1311.
- Chen, S.M., Liu, M.F., Cook, J., Bass, S., and Lo, S.K. (2009). Sedentary lifestyle as a risk factor for low back pain: a systematic review. *Int Arch Occup Environ Health* 82, 797-806.
- Clark, A.K., Gruber-Schoffnegger, D., Drdla-Schutting, R., Gerhold, K.J., Malcangio, M., and Sandkuhler, J. (2015). Selective activation of microglia facilitates synaptic strength. *J Neurosci* 35, 4552-4570.
- Clark, A.K., and Malcangio, M. (2012). Microglial signalling mechanisms: Cathepsin S and Fractalkine. *Exp Neurol* 234, 283-292.

- Clark, A.K., and Malcangio, M. (2014). Fractalkine/CX3CR1 signaling during neuropathic pain. *Front Cell Neurosci* 8, 121.
- Cloitre, M., Stolbach, B.C., Herman, J.L., van der Kolk, B., Pynoos, R., Wang, J., and Petkova, E. (2009). A developmental approach to complex PTSD: childhood and adult cumulative trauma as predictors of symptom complexity. *J Trauma Stress* 22, 399-408.
- Cohen, J. (1969). *Statistical power analysis for the behavioral sciences* (New York,: Academic Press).
- Colvert, E., Rutter, M., Beckett, C., Castle, J., Groothues, C., Hawkins, A., Kreppner, J., O'Connor T, G., Stevens, S., and Sonuga-Barke, E.J. (2008). Emotional difficulties in early adolescence following severe early deprivation: findings from the English and Romanian adoptees study. *Dev Psychopathol* 20, 547-567.
- Coon, D.M.J.O. (2013). *Introduction to psychology : gateways to mind and behavior* (Belmont, CA: Wadsworth Cengage Learning).
- Cowell, R.A., Cicchetti, D., Rogosch, F.A., and Toth, S.L. (2015). Childhood maltreatment and its effect on neurocognitive functioning: Timing and chronicity matter. *Dev Psychopathol* 27, 521-533.
- Craig, A.D., and Mense, S. (1983). The distribution of afferent fibers from the gastrocnemius-soleus muscle in the dorsal horn of the cat, as revealed by the transport of horseradish peroxidase. *Neurosci Lett* 41, 233-238.
- Cserep, C., Posfai, B., Lenart, N., Fekete, R., Laszlo, Z.I., Lele, Z., Orsolits, B., Molnar, G., Heindl, S., Schwarcz, A.D., *et al.* (2020). Microglia monitor and protect neuronal function through specialized somatic purinergic junctions. *Science* 367, 528-537.
- da, C.M.C.L., Maher, C.G., Hancock, M.J., McAuley, J.H., Herbert, R.D., and Costa, L.O. (2012). The prognosis of acute and persistent low-back pain: a meta-analysis. *CMAJ* 184, E613-624.
- Davis, E.J., Foster, T.D., and Thomas, W.E. (1994). Cellular forms and functions of brain microglia. *Brain Res Bull* 34, 73-78.
- de Azambuja, G., Botasso Gomes, B., Messias, L.H.D., Aquino, B.M., Jorge, C.O., Machado-Gobatto, F.B., and Oliveira-Fusaro, M.C.G. (2020). Swimming Physical Training Prevented the Onset of Acute Muscle Pain by a Mechanism Dependent of PPARgamma Receptors and CINC-1. *Neuroscience* 427, 64-74.
- Debono, D.J., Hoeksema, L.J., and Hobbs, R.D. (2013). Caring for patients with chronic pain: pearls and pitfalls. *J Am Osteopath Assoc* 113, 620-627.
- Deising, S., Weinkauff, B., Blunk, J., Obreja, O., Schmelz, M., and Rukwied, R. (2012). NGF-evoked sensitization of muscle fascia nociceptors in humans. *Pain* 153, 1673-1679.

- Demyttenaere, K., Bruffaerts, R., Lee, S., Posada-Villa, J., Kovess, V., Angermeyer, M.C., Levinson, D., de Girolamo, G., Nakane, H., Mneimneh, Z., *et al.* (2007). Mental disorders among persons with chronic back or neck pain: results from the World Mental Health Surveys. *Pain* 129, 332-342.
- Deng, J.H., Yan, W., Han, Y., Chen, C., Meng, S.Q., Sun, C.Y., Xu, L.Z., Xue, Y.X., Gao, X.J., Chen, N., *et al.* (2017). Predictable Chronic Mild Stress during Adolescence Promotes Fear Memory Extinction in Adulthood. *Sci Rep* 7, 7857.
- Deng, Y., Lu, J., Sivakumar, V., Ling, E.A., and Kaur, C. (2008). Amoeboid microglia in the periventricular white matter induce oligodendrocyte damage through expression of proinflammatory cytokines via MAP kinase signaling pathway in hypoxic neonatal rats. *Brain Pathol* 18, 387-400.
- Deyo, R.A., and Phillips, W.R. (1996). Low back pain. A primary care challenge. *Spine (Phila Pa 1976)* 21, 2826-2832.
- Diepenmaat, A.C., van der Wal, M.F., de Vet, H.C., and Hirasing, R.A. (2006). Neck/shoulder, low back, and arm pain in relation to computer use, physical activity, stress, and depression among Dutch adolescents. *Pediatrics* 117, 412-416.
- Disease, G.B.D., Injury, I., and Prevalence, C. (2016). Global, regional, and national incidence, prevalence, and years lived with disability for 310 diseases and injuries, 1990-2015: a systematic analysis for the Global Burden of Disease Study 2015. *Lancet* 388, 1545-1602.
- Djoughri, L., and Lawson, S.N. (2004). Abeta-fiber nociceptive primary afferent neurons: a review of incidence and properties in relation to other afferent A-fiber neurons in mammals. *Brain Res Brain Res Rev* 46, 131-145.
- Drdla, R., and Sandkuhler, J. (2008). Long-term potentiation at C-fibre synapses by low-level presynaptic activity in vivo. *Mol Pain* 4, 18.
- Durrenberger, P.F., Facer, P., Gray, R.A., Chessell, I.P., Naylor, A., Bountra, C., Banati, R.B., Birch, R., and Anand, P. (2004). Cyclooxygenase-2 (Cox-2) in injured human nerve and a rat model of nerve injury. *J Peripher Nerv Syst* 9, 15-25.
- Eitner, A., Hofmann, G.O., and Schaible, H.G. (2017). Mechanisms of Osteoarthritic Pain. *Studies in Humans and Experimental Models. Front Mol Neurosci* 10, 349.
- Eriksson, N.P., Persson, J.K., Svensson, M., Arvidsson, J., Molander, C., and Aldskogius, H. (1993). A quantitative analysis of the microglial cell reaction in central primary sensory projection territories following peripheral nerve injury in the adult rat. *Exp Brain Res* 96, 19-27.
- Fanning, J.R., Meyerhoff, J.J., Lee, R., and Coccaro, E.F. (2014). History of childhood maltreatment in intermittent explosive disorder and suicidal behavior. *J Psychiatr Res* 56, 10-17.
- Ferrari, L.F., Bogen, O., and Levine, J.D. (2010). Nociceptor subpopulations involved in hyperalgesic priming. *Neuroscience* 165, 896-901.

- Ferrari, S., Manni, T., Bonetti, F., Villafane, J.H., and Vanti, C. (2015). A literature review of clinical tests for lumbar instability in low back pain: validity and applicability in clinical practice. *Chiropr Man Therap* 23, 14.
- Fields, R.D., Araque, A., Johansen-Berg, H., Lim, S.S., Lynch, G., Nave, K.A., Nedergaard, M., Perez, R., Sejnowski, T., and Wake, H. (2014). Glial biology in learning and cognition. *Neuroscientist* 20, 426-431.
- Fields, R.D., and Stevens-Graham, B. (2002). New insights into neuron-glia communication. *Science* 298, 556-562.
- Folkman, S. (2013). Stress: Appraisal and Coping. In *Encyclopedia of Behavioral Medicine*, M.D. Gellman, and J.R. Turner, eds. (New York, NY: Springer New York), pp. 1913-1915.
- Frank, A. (1993). Low back pain. *BMJ* 307, 323-324.
- Freyenhagen, R., Rolke, R., Baron, R., Tolle, T.R., Rutjes, A.K., Schu, S., and Treede, R.D. (2008). Pseudoradicular and radicular low-back pain--a disease continuum rather than different entities? Answers from quantitative sensory testing. *Pain* 135, 65-74.
- Ganzel, B.L., Morris, P.A., and Wethington, E. (2010). Allostasis and the human brain: Integrating models of stress from the social and life sciences. *Psychol Rev* 117, 134-174.
- Gao, Y.J., and Ji, R.R. (2010). Targeting astrocyte signaling for chronic pain. *Neurotherapeutics* 7, 482-493.
- Garofalo, J., Robinson, R., Gatchel, R., and Wang, Z. (2007). A pain severity-hypothalamic-pituitary-adrenocortical axis interaction: The effects on pain pathways. *Journal of Applied Biobehavioral Research* 12, 35-42.
- Gatchel, R.J., Peng, Y.B., Peters, M.L., Fuchs, P.N., and Turk, D.C. (2007). The biopsychosocial approach to chronic pain: scientific advances and future directions. *Psychol Bull* 133, 581-624.
- Genty, J., Tetsi Nomigni, M., Anton, F., and Hanesch, U. (2018). Maternal separation stress leads to resilience against neuropathic pain in adulthood. *Neurobiol Stress* 8, 21-32.
- Gerhold, K.J., Drdla-Schutting, R., Honsek, S.D., Forsthuber, L., and Sandkuhler, J. (2015). Pronociceptive and Antinociceptive Effects of Buprenorphine in the Spinal Cord Dorsal Horn Cover a Dose Range of Four Orders of Magnitude. *J Neurosci* 35, 9580-9594.
- Gilbert, R., Widom, C.S., Browne, K., Fergusson, D., Webb, E., and Janson, S. (2009). Burden and consequences of child maltreatment in high-income countries. *Lancet* 373, 68-81.

- Goitom, A.D. (2021). Early life psychophysical stress primes rat dorsal horn neurons for long-term sensitization by a short-lasting nociceptive low back input involving activation of microglia.
- Gonzalez-Roldan, A.M., Terrasa, J.L., Sitges, C., van der Meulen, M., Anton, F., and Montoya, P. (2020). Age-Related Changes in Pain Perception Are Associated With Altered Functional Connectivity During Resting State. *Front Aging Neurosci* 12, 116.
- Graven-Nielsen, T., and Arendt-Nielsen, L. (2010). Assessment of mechanisms in localized and widespread musculoskeletal pain. *Nat Rev Rheumatol* 6, 599-606.
- Greenwood-Van Meerveld, B., and Johnson, A.C. (2017). Stress-Induced Chronic Visceral Pain of Gastrointestinal Origin. *Front Syst Neurosci* 11, 86.
- Gruber-Schoffnegger, D., Drdla-Schutting, R., Honigsperger, C., Wunderbaldinger, G., Gassner, M., and Sandkuhler, J. (2013). Induction of thermal hyperalgesia and synaptic long-term potentiation in the spinal cord lamina I by TNF-alpha and IL-1beta is mediated by glial cells. *J Neurosci* 33, 6540-6551.
- Grundt, A., Grundt, C., Gorbey, S., Thomas, M.A., and Lemmer, B. (2009). Strain-dependent differences of restraint stress-induced hypertension in WKY and SHR. *Physiol Behav* 97, 341-346.
- Hancock, M.J., Maher, C.G., Latimer, J., Spindler, M.F., McAuley, J.H., Laslett, M., and Bogduk, N. (2007). Systematic review of tests to identify the disc, SIJ or facet joint as the source of low back pain. *Eur Spine J* 16, 1539-1550.
- Hannibal, K.E., and Bishop, M.D. (2014). Chronic stress, cortisol dysfunction, and pain: a psychoneuroendocrine rationale for stress management in pain rehabilitation. *Phys Ther* 94, 1816-1825.
- Hayashi, K., Ozaki, N., Kawakita, K., Itoh, K., Mizumura, K., Furukawa, K., Yasui, M., Hori, K., Yi, S.Q., Yamaguchi, T., *et al.* (2011). Involvement of NGF in the rat model of persistent muscle pain associated with taut band. *J Pain* 12, 1059-1068.
- Heim, C., and Binder, E.B. (2012). Current research trends in early life stress and depression: review of human studies on sensitive periods, gene-environment interactions, and epigenetics. *Exp Neurol* 233, 102-111.
- Heim, C., Shugart, M., Craighead, W.E., and Nemeroff, C.B. (2010). Neurobiological and psychiatric consequences of child abuse and neglect. *Dev Psychobiol* 52, 671-690.
- Heinricher, M.M., Tavares, I., Leith, J.L., and Lumb, B.M. (2009). Descending control of nociception: Specificity, recruitment and plasticity. *Brain Res Rev* 60, 214-225.
- Herbert, T.B., and Cohen, S. (1993). Stress and immunity in humans: a meta-analytic review. *Psychosom Med* 55, 364-379.

- Herzog, J.I., and Schmahl, C. (2018). Adverse Childhood Experiences and the Consequences on Neurobiological, Psychosocial, and Somatic Conditions Across the Lifespan. *Front Psychiatry* 9, 420.
- Hestehave, S., Abelson, K.S., Bronnum Pedersen, T., and Munro, G. (2019). Stress sensitivity and cutaneous sensory thresholds before and after neuropathic injury in various inbred and outbred rat strains. *Behav Brain Res* 375, 112149.
- Hinwood, M., Morandini, J., Day, T.A., and Walker, F.R. (2012). Evidence that microglia mediate the neurobiological effects of chronic psychological stress on the medial prefrontal cortex. *Cereb Cortex* 22, 1442-1454.
- Hinwood, M., Tynan, R.J., Charnley, J.L., Beynon, S.B., Day, T.A., and Walker, F.R. (2013). Chronic stress induced remodeling of the prefrontal cortex: structural reorganization of microglia and the inhibitory effect of minocycline. *Cereb Cortex* 23, 1784-1797.
- Hoheisel, U., Chacur, M., Treede, R.D., and Mense, S. (2019). Action potentials and subthreshold potentials of dorsal horn neurons in a rat model of myositis: a study employing intracellular recordings in vivo. *J Neurophysiol* 122, 632-643.
- Hoheisel, U., Koch, K., and Mense, S. (1994). Functional reorganization in the rat dorsal horn during an experimental myositis. *Pain* 59, 111-118.
- Hoheisel, U., and Mense, S. (2015). Inflammation of the thoracolumbar fascia excites and sensitizes rat dorsal horn neurons. *Eur J Pain* 19, 419-428.
- Hoheisel, U., Mense, S., Simons, D.G., and Yu, X.M. (1993). Appearance of new receptive fields in rat dorsal horn neurons following noxious stimulation of skeletal muscle: a model for referral of muscle pain? *Neurosci Lett* 153, 9-12.
- Hoheisel, U., Reuter, R., de Freitas, M.F., Treede, R.D., and Mense, S. (2013). Injection of nerve growth factor into a low back muscle induces long-lasting latent hypersensitivity in rat dorsal horn neurons. *Pain* 154, 1953-1960.
- Hoheisel, U., Unger, T., and Mense, S. (2005). Excitatory and modulatory effects of inflammatory cytokines and neurotrophins on mechanosensitive group IV muscle afferents in the rat. *Pain* 114, 168-176.
- Hoheisel, U., Unger, T., and Mense, S. (2007). Sensitization of rat dorsal horn neurons by NGF-induced subthreshold potentials and low-frequency activation. A study employing intracellular recordings in vivo. *Brain Res* 1169, 34-43.
- Hoheisel, U., Vogt, M.A., Palme, R., Gass, P., and Mense, S. (2015). Immobilization stress sensitizes rat dorsal horn neurons having input from the low back. *Eur J Pain* 19, 861-870.
- Holguin, A., O'Connor, K.A., Biedenkapp, J., Campisi, J., Wieseler-Frank, J., Milligan, E.D., Hansen, M.K., Spataro, L., Maksimova, E., Bravmann, C., *et al.* (2004). HIV-1 gp120 stimulates proinflammatory cytokine-mediated pain facilitation via activation of nitric oxide synthase-I (nNOS). *Pain* 110, 517-530.

- Hoy, D., Bain, C., Williams, G., March, L., Brooks, P., Blyth, F., Woolf, A., Vos, T., and Buchbinder, R. (2012). A systematic review of the global prevalence of low back pain. *Arthritis Rheum* 64, 2028-2037.
- Hoy, D., March, L., Brooks, P., Blyth, F., Woolf, A., Bain, C., Williams, G., Smith, E., Vos, T., Barendregt, J., *et al.* (2014). The global burden of low back pain: estimates from the Global Burden of Disease 2010 study. *Ann Rheum Dis* 73, 968-974.
- Hua, N.K., and Van der Does, E. (1994). The occurrence and inter-rater reliability of myofascial trigger points in the quadratus lumborum and gluteus medius: a prospective study in non-specific low back pain patients and controls in general practice. *Pain* 58, 317-323.
- Ikeda, H., Heinke, B., Ruscheweyh, R., and Sandkuhler, J. (2003). Synaptic plasticity in spinal lamina I projection neurons that mediate hyperalgesia. *Science* 299, 1237-1240.
- Imbe, H., and Kimura, A. (2020). Significance of medial preoptic area among the subcortical and cortical areas that are related to pain regulation in the rats with stress-induced hyperalgesia. *Brain Res* 1735, 146758.
- Indahl, A. (2004). Low back pain: diagnosis, treatment, and prognosis. *Scand J Rheumatol* 33, 199-209.
- Jaffee, S.R., and Maikovich-Fong, A.K. (2011). Effects of chronic maltreatment and maltreatment timing on children's behavior and cognitive abilities. *J Child Psychol Psychiatry* 52, 184-194.
- Ji, R.R., Kohno, T., Moore, K.A., and Woolf, C.J. (2003). Central sensitization and LTP: do pain and memory share similar mechanisms? *Trends Neurosci* 26, 696-705.
- Kaplow, J.B., and Widom, C.S. (2007). Age of onset of child maltreatment predicts long-term mental health outcomes. *J Abnorm Psychol* 116, 176-187.
- Karperien, A., Ahammer, H., and Jelinek, H.F. (2013). Quantitating the subtleties of microglial morphology with fractal analysis. *Front Cell Neurosci* 7, 3.
- Kawasaki, Y., Zhang, L., Cheng, J.K., and Ji, R.R. (2008). Cytokine mechanisms of central sensitization: distinct and overlapping role of interleukin-1beta, interleukin-6, and tumor necrosis factor-alpha in regulating synaptic and neuronal activity in the superficial spinal cord. *J Neurosci* 28, 5189-5194.
- Kettenmann, H., Hanisch, U.K., Noda, M., and Verkhratsky, A. (2011). Physiology of microglia. *Physiol Rev* 91, 461-553.
- Knezevic, N.N., Candido, K.D., Vlaeyen, J.W.S., Van Zundert, J., and Cohen, S.P. (2021). Low back pain. *Lancet* 398, 78-92.
- Koerber, H.R., Mirnics, K., and Lawson, J.J. (2006). Synaptic plasticity in the adult spinal dorsal horn: the appearance of new functional connections following peripheral nerve regeneration. *Exp Neurol* 200, 468-479.

- Kopp, B.L., Wick, D., and Herman, J.P. (2013). Differential effects of homotypic vs. heterotypic chronic stress regimens on microglial activation in the prefrontal cortex. *Physiol Behav* 122, 246-252.
- Korczeniewska, O.A., Khan, J., Tao, Y., Eliav, E., and Benoliel, R. (2017). Effects of Sex and Stress on Trigeminal Neuropathic Pain-Like Behavior in Rats. *J Oral Facial Pain Headache* 31, 381-397.
- Kuner, R. (2010). Central mechanisms of pathological pain. *Nat Med* 16, 1258-1266.
- La Porta, C., and Tappe-Theodor, A. (2020). Differential impact of psychological and psychophysical stress on low back pain in mice. *Pain* 161, 1442-1458.
- Lambertz, D., Hoheisel, U., and Mense, S. (2008). Influence of a chronic myositis on rat spinal field potentials evoked by TTX-resistant unmyelinated skin and muscle afferents. *Eur J Pain* 12, 686-695.
- Le Coz, G.M., Genty, J., Anton, F., and Hanesch, U. (2017). Chronic Social Stress Time-Dependently Affects Neuropathic Pain-Related Cold Allodynia and Leads to Altered Expression of Spinal Biochemical Mediators. *Front Behav Neurosci* 11, 70.
- Ledeboer, A., Sloane, E.M., Milligan, E.D., Frank, M.G., Mahony, J.H., Maier, S.F., and Watkins, L.R. (2005). Minocycline attenuates mechanical allodynia and proinflammatory cytokine expression in rat models of pain facilitation. *Pain* 115, 71-83.
- Leeners, B., Gorres, G., Block, E., and Hengartner, M.P. (2016). Birth experiences in adult women with a history of childhood sexual abuse. *J Psychosom Res* 83, 27-32.
- Lehmann, M.L., Cooper, H.A., Maric, D., and Herkenham, M. (2016). Social defeat induces depressive-like states and microglial activation without involvement of peripheral macrophages. *J Neuroinflammation* 13, 224.
- Li, C., Yang, Y., Liu, S., Fang, H., Zhang, Y., Furmanski, O., Skinner, J., Xing, Y., Johns, R.A., Haganir, R.L., *et al.* (2014). Stress induces pain transition by potentiation of AMPA receptor phosphorylation. *J Neurosci* 34, 13737-13746.
- Lopez-Rubalcava, C., and Lucki, I. (2000). Strain differences in the behavioral effects of antidepressant drugs in the rat forced swimming test. *Neuropsychopharmacology* 22, 191-199.
- Ma, W., Li, L., and Xing, S. (2019). PGE2/EP4 receptor and TRPV1 channel are involved in repeated restraint stress-induced prolongation of sensitization pain evoked by subsequent PGE2 challenge. *Brain Res* 1721, 146335.
- Maher, C., Underwood, M., and Buchbinder, R. (2017). Non-specific low back pain. *Lancet* 389, 736-747.
- Malanga, G.A., and Cruz Colon, E.J. (2010). Myofascial low back pain: a review. *Phys Med Rehabil Clin N Am* 21, 711-724.

- Mann, M.K., Dong, X.D., Svensson, P., and Cairns, B.E. (2006). Influence of intramuscular nerve growth factor injection on the response properties of rat masseter muscle afferent fibers. *J Orofac Pain* 20, 325-336.
- Marchand, F., Perretti, M., and McMahon, S.B. (2005). Role of the immune system in chronic pain. *Nat Rev Neurosci* 6, 521-532.
- Markman, J.D., Bolash, R.B., McAlindon, T.E., Kivitz, A.J., Pombo-Suarez, M., Ohtori, S., Roemer, F.W., Li, D.J., Viktrup, L., Bramson, C., *et al.* (2020). Tanezumab for chronic low back pain: a randomized, double-blind, placebo- and active-controlled, phase 3 study of efficacy and safety. *Pain* 161, 2068-2078.
- Martenson, M.E., Cetas, J.S., and Heinricher, M.M. (2009). A possible neural basis for stress-induced hyperalgesia. *Pain* 142, 236-244.
- Mason, J.W. (1971). A re-evaluation of the concept of "non-specificity" in stress theory. *J Psychiatr Res* 8, 323-333.
- McBeth, J., Silman, A.J., Gupta, A., Chiu, Y.H., Ray, D., Morriss, R., Dickens, C., King, Y., and Macfarlane, G.J. (2007). Moderation of psychosocial risk factors through dysfunction of the hypothalamic-pituitary-adrenal stress axis in the onset of chronic widespread musculoskeletal pain: findings of a population-based prospective cohort study. *Arthritis Rheum* 56, 360-371.
- McEwen, B.S. (1998). Stress, adaptation, and disease. Allostasis and allostatic load. *Ann N Y Acad Sci* 840, 33-44.
- McEwen, B.S. (1999). Stress and hippocampal plasticity. *Annu Rev Neurosci* 22, 105-122.
- McMahon, S.B., and Wall, P.D. (1985). The distribution and central termination of single cutaneous and muscle unmyelinated fibres in rat spinal cord. *Brain Res* 359, 39-48.
- Mendelek, F., Caby, I., Pelayo, P., and Kheir, R.B. (2013). The application of a classification-tree model for predicting low back pain prevalence among hospital staff. *Arch Environ Occup Health* 68, 135-144.
- Mielke, E.L., Neukel, C., Fuchs, A., Hillmann, K., Zietlow, A.L., Bertsch, K., Reck, C., Mohler, E., and Herpertz, S.C. (2020). The Cycle of Abuse: Emotional Availability in Resilient and Non-Resilient Mothers with Early Life Maltreatment. *Psychopathology* 53, 298-305.
- Mifflin, K.A., and Kerr, B.J. (2014). The transition from acute to chronic pain: understanding how different biological systems interact. *Can J Anaesth* 61, 112-122.
- Milligan, E.D., Twining, C., Chacur, M., Biedenkapp, J., O'Connor, K., Poole, S., Tracey, K., Martin, D., Maier, S.F., and Watkins, L.R. (2003). Spinal glia and proinflammatory cytokines mediate mirror-image neuropathic pain in rats. *J Neurosci* 23, 1026-1040.

- Moraga-Amaro, R., Jerez-Baraona, J.M., Simon, F., and Stehberg, J. (2014). Role of astrocytes in memory and psychiatric disorders. *J Physiol Paris* 108, 240-251.
- Murase, S., Terazawa, E., Queme, F., Ota, H., Matsuda, T., Hirate, K., Kozaki, Y., Katanosaka, K., Taguchi, T., Urai, H., *et al.* (2010). Bradykinin and nerve growth factor play pivotal roles in muscular mechanical hyperalgesia after exercise (delayed-onset muscle soreness). *J Neurosci* 30, 3752-3761.
- Murata, Y., Olmarker, K., Takahashi, I., Takahashi, K., and Rydevik, B. (2005). Effects of selective tumor necrosis factor-alpha inhibition to pain-behavioral changes caused by nucleus pulposus-induced damage to the spinal nerve in rats. *Neurosci Lett* 382, 148-152.
- Nees, F., Ruttorf, M., Fuchs, X., Rance, M., and Beyer, N. (2020). Brain-behaviour correlates of habitual motivation in chronic back pain. *Sci Rep* 10, 11090.
- Nicholas, M., Vlaeyen, J.W.S., Rief, W., Barke, A., Aziz, Q., Benoliel, R., Cohen, M., Evers, S., Giamberardino, M.A., Goebel, A., *et al.* (2019). The IASP classification of chronic pain for ICD-11: chronic primary pain. *Pain* 160, 28-37.
- Nie, H., Madeleine, P., Arendt-Nielsen, L., and Graven-Nielsen, T. (2009). Temporal summation of pressure pain during muscle hyperalgesia evoked by nerve growth factor and eccentric contractions. *Eur J Pain* 13, 704-710.
- Nimmerjahn, A., Kirchhoff, F., and Helmchen, F. (2005). Resting microglial cells are highly dynamic surveillants of brain parenchyma in vivo. *Science* 308, 1314-1318.
- Nissl (1899). Über einige Beziehungen zwischen Nervenzellerkrankungen und gliösen Erscheinungen bei verschiedenen Psychosen. *Arch Psychiatr.*
- Obreja, O., Kluschina, O., Mayer, A., Hirth, M., Schley, M., Schmelz, M., and Rukwied, R. (2011). NGF enhances electrically induced pain, but not axon reflex sweating. *Pain* 152, 1856-1863.
- Okada-Ogawa, A., Suzuki, I., Sessle, B.J., Chiang, C.Y., Salter, M.W., Dostrovsky, J.O., Tsuboi, Y., Kondo, M., Kitagawa, J., Kobayashi, A., *et al.* (2009). Astroglia in medullary dorsal horn (trigeminal spinal subnucleus caudalis) are involved in trigeminal neuropathic pain mechanisms. *J Neurosci* 29, 11161-11171.
- Okamoto, K., Tashiro, A., Chang, Z., Thompson, R., and Bereiter, D.A. (2012). Temporomandibular joint-evoked responses by spinomedullary neurons and masseter muscle are enhanced after repeated psychophysical stress. *Eur J Neurosci* 36, 2025-2034.
- Owolabi, S.A., and Saab, C.Y. (2006). Fractalkine and minocycline alter neuronal activity in the spinal cord dorsal horn. *FEBS Lett* 580, 4306-4310.
- Paolicelli, R.C., Bolasco, G., Pagani, F., Maggi, L., Scianni, M., Panzanelli, P., Giustetto, M., Ferreira, T.A., Guiducci, E., Dumas, L., *et al.* (2011). Synaptic pruning by microglia is necessary for normal brain development. *Science* 333, 1456-1458.

- Park, J.H., Yoo, K.Y., Lee, C.H., Kim, I.H., Shin, B.N., Choi, J.H., Park, J.H., Hwang, I.K., and Won, M.H. (2011). Comparison of glucocorticoid receptor and ionized calcium-binding adapter molecule 1 immunoreactivity in the adult and aged gerbil hippocampus following repeated restraint stress. *Neurochem Res* 36, 1037-1045.
- Park, T.S.W., Khan, N., Kuo, A., Nicholson, J.R., Corradini, L., and Smith, M.T. (2020). Characterisation of a rat model of mechanical low back pain at an advanced stage using immunohistochemical methods. *Clin Exp Pharmacol Physiol*.
- Park, T.S.W., Kuo, A., and Smith, M.T. (2018). Chronic low back pain: a mini-review on pharmacological management and pathophysiological insights from clinical and pre-clinical data. *Inflammopharmacology*.
- Pechtel, P., Lyons-Ruth, K., Anderson, C.M., and Teicher, M.H. (2014). Sensitive periods of amygdala development: the role of maltreatment in preadolescence. *Neuroimage* 97, 236-244.
- Pekny, M., and Nilsson, M. (2005). Astrocyte activation and reactive gliosis. *Glia* 50, 427-434.
- Perrot, S., Cohen, M., Barke, A., Korwisi, B., Rief, W., Treede, R.D., and Pain, I.T.f.t.C.o.C. (2019). The IASP classification of chronic pain for ICD-11: chronic secondary musculoskeletal pain. *Pain* 160, 77-82.
- Petersen, M.A., and Dailey, M.E. (2004). Diverse microglial motility behaviors during clearance of dead cells in hippocampal slices. *Glia* 46, 195-206.
- Picavet, H.S., Vlaeyen, J.W., and Schouten, J.S. (2002). Pain catastrophizing and kinesiophobia: predictors of chronic low back pain. *Am J Epidemiol* 156, 1028-1034.
- Pubols, L.M. (1990). Characteristics of dorsal horn neurons expressing subliminal responses to sural nerve stimulation. *Somatosens Mot Res* 7, 137-151.
- Puli, L., Pomeshchik, Y., Olas, K., Malm, T., Koistinaho, J., and Tanila, H. (2012). Effects of human intravenous immunoglobulin on amyloid pathology and neuroinflammation in a mouse model of Alzheimer's disease. *J Neuroinflammation* 9, 105.
- Qaseem, A., Wilt, T.J., McLean, R.M., Forciea, M.A., Clinical Guidelines Committee of the American College of, P., Denberg, T.D., Barry, M.J., Boyd, C., Chow, R.D., Fitterman, N., *et al.* (2017). Noninvasive Treatments for Acute, Subacute, and Chronic Low Back Pain: A Clinical Practice Guideline From the American College of Physicians. *Ann Intern Med* 166, 514-530.
- Raabe, F.J., and Spengler, D. (2013). Epigenetic Risk Factors in PTSD and Depression. *Front Psychiatry* 4, 80.
- Raghavendra, V., Rutkowski, M.D., and DeLeo, J.A. (2002). The role of spinal neuroimmune activation in morphine tolerance/hyperalgesia in neuropathic and sham-operated rats. *J Neurosci* 22, 9980-9989.

- Raghavendra, V., Tanga, F., and DeLeo, J.A. (2003). Inhibition of microglial activation attenuates the development but not existing hypersensitivity in a rat model of neuropathy. *J Pharmacol Exp Ther* 306, 624-630.
- Raghavendra, V., Tanga, F.Y., and DeLeo, J.A. (2004). Complete Freund's adjuvant-induced peripheral inflammation evokes glial activation and proinflammatory cytokine expression in the CNS. *Eur J Neurosci* 20, 467-473.
- Raja, S.N., Carr, D.B., Cohen, M., Finnerup, N.B., Flor, H., Gibson, S., Keefe, F.J., Mogil, J.S., Ringkamp, M., Sluka, K.A., *et al.* (2020). The revised International Association for the Study of Pain definition of pain: concepts, challenges, and compromises. *Pain* 161, 1976-1982.
- Ramirez, K., Niraula, A., and Sheridan, J.F. (2016). GABAergic modulation with classical benzodiazepines prevent stress-induced neuro-immune dysregulation and behavioral alterations. *Brain Behav Immun* 51, 154-168.
- Reed, N.R., Reed, W.R., Syrett, M., Richey, M.L., Frolov, A., and Little, J.W. (2021). Somatosensory behavioral alterations in a NGF-induced persistent low back pain model. *Behav Brain Res* 418, 113617.
- Reed, W.R., Little, J.W., Lima, C.R., Sorge, R.E., Yarar-Fisher, C., Eraslan, M., Hurt, C.P., Ness, T.J., Gu, J.G., Martins, D.F., *et al.* (2020). Spinal Mobilization Prevents NGF-Induced Trunk Mechanical Hyperalgesia and Attenuates Expression of CGRP. *Front Neurosci* 14, 385.
- Reeves, A.M., Shigetomi, E., and Khakh, B.S. (2011). Bulk loading of calcium indicator dyes to study astrocyte physiology: key limitations and improvements using morphological maps. *J Neurosci* 31, 9353-9358.
- Reichling, D.B., and Levine, J.D. (2009). Critical role of nociceptor plasticity in chronic pain. *Trends Neurosci* 32, 611-618.
- Reitz, M.C., Hrnčić, D., Treede, R.D., and Caspani, O. (2016). A comparative behavioural study of mechanical hypersensitivity in 2 pain models in rats and humans. *Pain* 157, 1248-1258.
- Rice, A.S., Smith, B.H., and Blyth, F.M. (2016). Pain and the global burden of disease. *Pain* 157, 791-796.
- Rice, D., and Barone, S., Jr. (2000). Critical periods of vulnerability for the developing nervous system: evidence from humans and animal models. *Environ Health Perspect* 108 Suppl 3, 511-533.
- Riem, M.M., Alink, L.R., Out, D., Van Ijzendoorn, M.H., and Bakermans-Kranenburg, M.J. (2015). Beating the brain about abuse: Empirical and meta-analytic studies of the association between maltreatment and hippocampal volume across childhood and adolescence. *Dev Psychopathol* 27, 507-520.

- Rivat, C., Becker, C., Blugeot, A., Zeau, B., Mauborgne, A., Pohl, M., and Benoliel, J.J. (2010). Chronic stress induces transient spinal neuroinflammation, triggering sensory hypersensitivity and long-lasting anxiety-induced hyperalgesia. *Pain* 150, 358-368.
- Rolke, R., Andrews Campbell, K., Magerl, W., and Treede, R.D. (2005). Deep pain thresholds in the distal limbs of healthy human subjects. *Eur J Pain* 9, 39-48.
- Romero-Sandoval, A., Chai, N., Natile-McMenemy, N., and Deleo, J.A. (2008). A comparison of spinal Iba1 and GFAP expression in rodent models of acute and chronic pain. *Brain Res* 1219, 116-126.
- Ruiz-Sauri, A., Orduna-Valls, J.M., Blasco-Serra, A., Tornero-Tornero, C., Cedeno, D.L., Bejarano-Quisoboni, D., Valverde-Navarro, A.A., Benyamin, R., and Vallejo, R. (2019). Glia to neuron ratio in the posterior aspect of the human spinal cord at thoracic segments relevant to spinal cord stimulation. *J Anat* 235, 997-1006.
- Rukwied, B., Weinkauff, B., Main, M., Obreja, O., and Schmelz, M. (2014). Axonal hyperexcitability after combined NGF sensitization and UV-B inflammation in humans. *Eur J Pain* 18, 785-793.
- Sandrini, G., Serrao, M., Rossi, P., Romaniello, A., Cruccu, G., and Willer, J.C. (2005). The lower limb flexion reflex in humans. *Prog Neurobiol* 77, 353-395.
- Schiavone, S., Sorce, S., Dubois-Dauphin, M., Jaquet, V., Colaianna, M., Zotti, M., Cuomo, V., Trabace, L., and Krause, K.H. (2009). Involvement of NOX2 in the development of behavioral and pathologic alterations in isolated rats. *Biol Psychiatry* 66, 384-392.
- Schilder, A., Hoheisel, U., Magerl, W., Benrath, J., Klein, T., and Treede, R.D. (2014). Sensory findings after stimulation of the thoracolumbar fascia with hypertonic saline suggest its contribution to low back pain. *Pain* 155, 222-231.
- Schmidt, M.V. (2010). Molecular mechanisms of early life stress--lessons from mouse models. *Neurosci Biobehav Rev* 34, 845-852.
- Schneider, M. (2013). Adolescence as a vulnerable period to alter rodent behavior. *Cell Tissue Res* 354, 99-106.
- Schwartz, M., Butovsky, O., Bruck, W., and Hanisch, U.K. (2006). Microglial phenotype: is the commitment reversible? *Trends Neurosci* 29, 68-74.
- Selye, H. (1946). The general adaptation syndrome and the diseases of adaptation. *J Clin Endocrinol Metab* 6, 117-230.
- Selye, H. (1975). Confusion and controversy in the stress field. *J Human Stress* 1, 37-44.
- Senba, E., Imbe, H., and Okamoto, K. (2008). [Descending facilitation in chronic stress and chronic pain state]. *Nihon Shinkei Seishin Yakurigaku Zasshi* 28, 29-35.

- Sessler, K., Blechschmidt, V., Hoheisel, U., Mense, S., Schirmer, L., and Treede, R.D. (2021). Spinal cord fractalkine (CX3CL1) signaling is critical for neuronal sensitization in experimental nonspecific, myofascial low back pain. *J Neurophysiol* 125, 1598-1611.
- Shi, C., Qiu, S., Riester, S.M., Das, V., Zhu, B., Wallace, A.A., van Wijnen, A.J., Mwale, F., Iatridis, J.C., Sakai, D., *et al.* (2018). Animal models for studying the etiology and treatment of low back pain. *J Orthop Res* 36, 1305-1312.
- Sideris-Lampretsas, G., and Malcangio, M. (2021). Microglial heterogeneity in chronic pain. *Brain Behav Immun* 96, 279-289.
- Singaravelu, S.K., Goitom, A.D., Surakka, A., Moerz, H., Schilder, A., Hansson, A.C., Spanagel, R., and Treede, R.-D. (2021a). Long-term sensitization of rat spinal neurons induced by adolescent psychophysical stress is further enhanced by a mild-nociceptive lumbar input. *bioRxiv*, 2021.2004.2030.442126.
- Singaravelu, S.K., Hoheisel, U., Mense, S., and Treede, R.D. (2021b). Rat dorsal horn neurons primed by stress develop a long-lasting manifest sensitization after a short-lasting nociceptive low back input. *Pain Rep* 6, e904.
- Skyba, D.A., Lisi, T.L., and Sluka, K.A. (2005). Excitatory amino acid concentrations increase in the spinal cord dorsal horn after repeated intramuscular injection of acidic saline. *Pain* 119, 142-149.
- Sousa, F.S.S., Birman, P.T., Balaguez, R., Alves, D., Bruning, C.A., and Savegnago, L. (2018). alpha-(phenylselanyl) acetophenone abolishes acute restraint stress induced-comorbid pain, depression and anxiety-related behaviors in mice. *Neurochem Int* 120, 112-120.
- Staud, R. (2011). Evidence for shared pain mechanisms in osteoarthritis, low back pain, and fibromyalgia. *Curr Rheumatol Rep* 13, 513-520.
- Stecco, C., Stern, R., Porzionato, A., Macchi, V., Masiero, S., Stecco, A., and De Caro, R. (2011). Hyaluronan within fascia in the etiology of myofascial pain. *Surg Radiol Anat* 33, 891-896.
- Stratoulas, V., Venero, J.L., Tremblay, M.E., and Joseph, B. (2019). Microglial subtypes: diversity within the microglial community. *EMBO J* 38, e101997.
- Streit, W.J., Walter, S.A., and Pennell, N.A. (1999). Reactive microgliosis. *Prog Neurobiol* 57, 563-581.
- Strong, J.A., Xie, W., Bataille, F.J., and Zhang, J.M. (2013). Preclinical studies of low back pain. *Mol Pain* 9, 17.
- Sugama, S., Fujita, M., Hashimoto, M., and Conti, B. (2007). Stress induced morphological microglial activation in the rodent brain: involvement of interleukin-18. *Neuroscience* 146, 1388-1399.

- Sun, D.S., Zhong, G., Cao, H.X., Hu, Y., Hong, X.Y., Li, T., Li, X., Liu, Q., Wang, Q., Ke, D., *et al.* (2020). Repeated Restraint Stress Led to Cognitive Dysfunction by NMDA Receptor-Mediated Hippocampal CA3 Dendritic Spine Impairments in Juvenile Sprague-Dawley Rats. *Front Mol Neurosci* 13, 552787.
- Suvrathan, A., Bennur, S., Ghosh, S., Tomar, A., Anilkumar, S., and Chattarji, S. (2014). Stress enhances fear by forming new synapses with greater capacity for long-term potentiation in the amygdala. *Philos Trans R Soc Lond B Biol Sci* 369, 20130151.
- Suzuki, R., and Dickenson, A. (2005). Spinal and supraspinal contributions to central sensitization in peripheral neuropathy. *Neurosignals* 14, 175-181.
- Suzuki, R., Morcuende, S., Webber, M., Hunt, S.P., and Dickenson, A.H. (2002). Superficial NK1-expressing neurons control spinal excitability through activation of descending pathways. *Nat Neurosci* 5, 1319-1326.
- Svensson, P., Cairns, B.E., Wang, K., and Arendt-Nielsen, L. (2003). Injection of nerve growth factor into human masseter muscle evokes long-lasting mechanical allodynia and hyperalgesia. *Pain* 104, 241-247.
- Swanson, M.E.V., Murray, H.C., Ryan, B., Faull, R.L.M., Dragunow, M., and Curtis, M.A. (2020). Quantitative immunohistochemical analysis of myeloid cell marker expression in human cortex captures microglia heterogeneity with anatomical context. *Sci Rep* 10, 11693.
- Sweitzer, S.M., Schubert, P., and DeLeo, J.A. (2001). Propentofylline, a glial modulating agent, exhibits antiallodynic properties in a rat model of neuropathic pain. *J Pharmacol Exp Ther* 297, 1210-1217.
- Taguchi, T., Hoheisel, U., and Mense, S. (2008). Dorsal horn neurons having input from low back structures in rats. *Pain* 138, 119-129.
- Takahashi, K., Taguchi, T., Itoh, K., Okada, K., Kawakita, K., and Mizumura, K. (2005). Influence of surface anesthesia on the pressure pain threshold measured with different-sized probes. *Somatosens Mot Res* 22, 299-305.
- Tay, T.L., Carrier, M., and Tremblay, M.E. (2019). Physiology of Microglia. *Adv Exp Med Biol* 1175, 129-148.
- Teicher, M.H., and Samson, J.A. (2013). Childhood maltreatment and psychopathology: A case for ecophenotypic variants as clinically and neurobiologically distinct subtypes. *Am J Psychiatry* 170, 1114-1133.
- Tesarz, J., Eich, W., Treede, R.D., and Gerhardt, A. (2016). Altered pressure pain thresholds and increased wind-up in adult patients with chronic back pain with a history of childhood maltreatment: a quantitative sensory testing study. *Pain* 157, 1799-1809.

- Tesarz, J., Gerhardt, A., Leisner, S., Janke, S., Treede, R.D., and Eich, W. (2015). Distinct quantitative sensory testing profiles in nonspecific chronic back pain subjects with and without psychological trauma. *Pain* 156, 577-586.
- Tong, L., Gong, Y., Wang, P., Hu, W., Wang, J., Chen, Z., Zhang, W., and Huang, C. (2017). Microglia Loss Contributes to the Development of Major Depression Induced by Different Types of Chronic Stresses. *Neurochem Res* 42, 2698-2711.
- Torsney, C. (2011). Inflammatory pain unmasks heterosynaptic facilitation in lamina I neurokinin 1 receptor-expressing neurons in rat spinal cord. *J Neurosci* 31, 5158-5168.
- Treede, R.D., Rief, W., Barke, A., Aziz, Q., Bennett, M.I., Benoliel, R., Cohen, M., Evers, S., Finnerup, N.B., First, M.B., *et al.* (2019). Chronic pain as a symptom or a disease: the IASP Classification of Chronic Pain for the International Classification of Diseases (ICD-11). *Pain* 160, 19-27.
- Treede, R.D., Rief, W., Barke, A., Aziz, Q., Bennett, M.I., Benoliel, R., Cohen, M., Evers, S., Finnerup, N.B., First, M.B., *et al.* (2015). A classification of chronic pain for ICD-11. *Pain* 156, 1003-1007.
- Tremblay, M.E., Stevens, B., Sierra, A., Wake, H., Bessis, A., and Nimmerjahn, A. (2011). The role of microglia in the healthy brain. *J Neurosci* 31, 16064-16069.
- Tsuda, M., Masuda, T., Tozaki-Saitoh, H., and Inoue, K. (2013). Microglial regulation of neuropathic pain. *J Pharmacol Sci* 121, 89-94.
- Tsuda, M., Mizokoshi, A., Shigemoto-Mogami, Y., Koizumi, S., and Inoue, K. (2004). Activation of p38 mitogen-activated protein kinase in spinal hyperactive microglia contributes to pain hypersensitivity following peripheral nerve injury. *Glia* 45, 89-95.
- Tynan, R.J., Naicker, S., Hinwood, M., Nalivaiko, E., Buller, K.M., Pow, D.V., Day, T.A., and Walker, F.R. (2010). Chronic stress alters the density and morphology of microglia in a subset of stress-responsive brain regions. *Brain Behav Immun* 24, 1058-1068.
- Uveges, J.M., Parker, J.C., Smarr, K.L., McGowan, J.F., Lyon, M.G., Irvin, W.S., Meyer, A.A., Buckelew, S.P., Morgan, R.K., Delmonico, R.L., *et al.* (1990). Psychological symptoms in primary fibromyalgia syndrome: relationship to pain, life stress, and sleep disturbance. *Arthritis Rheum* 33, 1279-1283.
- van der Windt, D.A., Thomas, E., Pope, D.P., de Winter, A.F., Macfarlane, G.J., Bouter, L.M., and Silman, A.J. (2000). Occupational risk factors for shoulder pain: a systematic review. *Occup Environ Med* 57, 433-442.
- Van Uum, S.H., Sauve, B., Fraser, L.A., Morley-Forster, P., Paul, T.L., and Koren, G. (2008). Elevated content of cortisol in hair of patients with severe chronic pain: a novel biomarker for stress. *Stress* 11, 483-488.
- Vigo, D., Thornicroft, G., and Atun, R. (2016). Estimating the true global burden of mental illness. *Lancet Psychiatry* 3, 171-178.

- Vilela, F.C., Vieira, J.S., Giusti-Paiva, A., and Silva, M.L.D. (2017). Experiencing early life maternal separation increases pain sensitivity in adult offspring. *Int J Dev Neurosci* 62, 8-14.
- Vos, T., Flaxman, A.D., Naghavi, M., Lozano, R., Michaud, C., Ezzati, M., Shibuya, K., Salomon, J.A., Abdalla, S., Aboyans, V., *et al.* (2012). Years lived with disability (YLDs) for 1160 sequelae of 289 diseases and injuries 1990-2010: a systematic analysis for the Global Burden of Disease Study 2010. *Lancet* 380, 2163-2196.
- Waddell, G., Newton, M., Henderson, I., Somerville, D., and Main, C.J. (1993). A Fear-Avoidance Beliefs Questionnaire (FABQ) and the role of fear-avoidance beliefs in chronic low back pain and disability. *Pain* 52, 157-168.
- Wall, P.D. (1977). The presence of ineffective synapses and the circumstances which unmask them. *Philos Trans R Soc Lond B Biol Sci* 278, 361-372.
- Wang, H., Schiltenswolf, M., and Buchner, M. (2008). The role of TNF-alpha in patients with chronic low back pain-a prospective comparative longitudinal study. *Clin J Pain* 24, 273-278.
- Waynforth, H., and Flecknell, P. (1995). Experimental and Surgical Technique In the Rat. *Psicothema*, ISSN 0214-9915, Vol 7, Nº 2, 1995, pages 452-453.
- Weinkauf, B., Obreja, O., Schmelz, M., and Rukwied, R. (2015). Differential time course of NGF-induced hyperalgesia to heat versus mechanical and electrical stimulation in human skin. *Eur J Pain* 19, 789-796.
- Wippert, P.M., and Wiebking, C. (2018). Stress and Alterations in the Pain Matrix: A Biopsychosocial Perspective on Back Pain and Its Prevention and Treatment. *Int J Environ Res Public Health* 15.
- Wohleb, E.S., McKim, D.B., Shea, D.T., Powell, N.D., Tarr, A.J., Sheridan, J.F., and Godbout, J.P. (2014). Re-establishment of anxiety in stress-sensitized mice is caused by monocyte trafficking from the spleen to the brain. *Biol Psychiatry* 75, 970-981.
- Wolf, S.A., Boddeke, H.W., and Kettenmann, H. (2017). Microglia in Physiology and Disease. *Annu Rev Physiol* 79, 619-643.
- Woolf, C.J. (2011). Central sensitization: implications for the diagnosis and treatment of pain. *Pain* 152, S2-S15.
- Woolf, C.J., and King, A.E. (1989). Subthreshold components of the cutaneous mechanoreceptive fields of dorsal horn neurons in the rat lumbar spinal cord. *J Neurophysiol* 62, 907-916.
- Xanthos, D.N., and Sandkuhler, J. (2014). Neurogenic neuroinflammation: inflammatory CNS reactions in response to neuronal activity. *Nat Rev Neurosci* 15, 43-53.

- Yezierski, R.P. (2012). The effects of age on pain sensitivity: preclinical studies. *Pain Med* 13 Suppl 2, S27-36.
- Yu, X.M., and Mense, S. (1990). Response properties and descending control of rat dorsal horn neurons with deep receptive fields. *Neuroscience* 39, 823-831.
- Zanier, E.R., Fumagalli, S., Perego, C., Pischiutta, F., and De Simoni, M.G. (2015). Shape descriptors of the "never resting" microglia in three different acute brain injury models in mice. *Intensive Care Med Exp* 3, 39.
- Zhang, J., Hoheisel, U., Klein, T., Magerl, W., Mense, S., and Treede, R.D. (2016). High-frequency modulation of rat spinal field potentials: effects of slowly conducting muscle vs. skin afferents. *J Neurophysiol* 115, 692-700.
- Zhang, J., Mense, S., Treede, R.D., and Hoheisel, U. (2017). Prevention and reversal of latent sensitization of dorsal horn neurons by glial blockers in a model of low back pain in male rats. *J Neurophysiol* 118, 2059-2069.
- Zhang, J.J. (2016). Prevention and reversal of neuronal sensitization in the spinal cord by blocking spinal glial cell activation in an animal model of non-specific low back pain.
- Zhong, Y., Zhou, L.J., Ren, W.J., Xin, W.J., Li, Y.Y., Zhang, T., and Liu, X.G. (2010). The direction of synaptic plasticity mediated by C-fibers in spinal dorsal horn is decided by Src-family kinases in microglia: the role of tumor necrosis factor-alpha. *Brain Behav Immun* 24, 874-880.

[illegible]

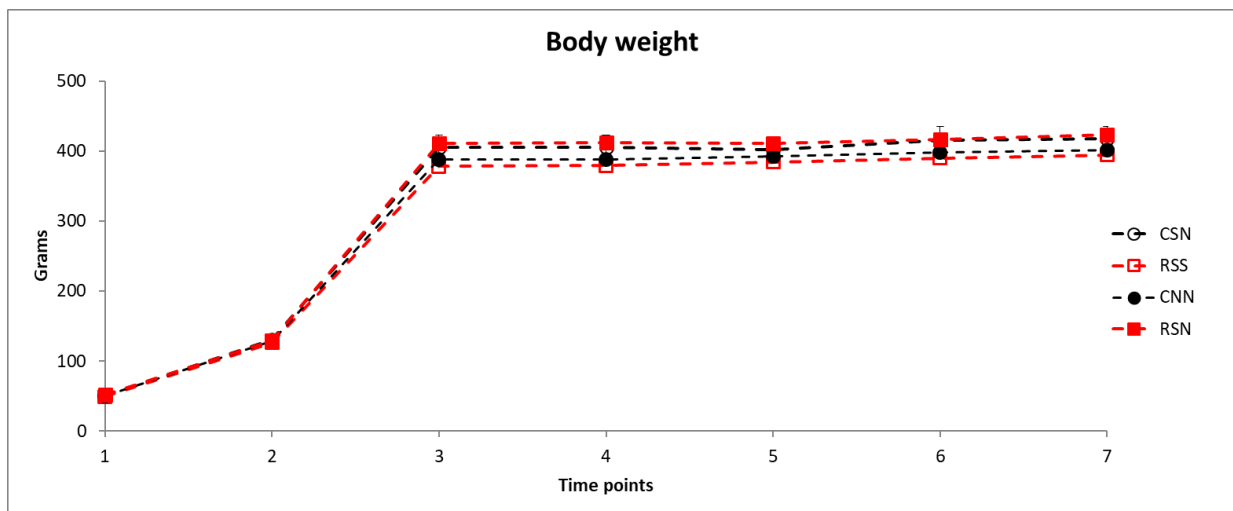
i.t.	Experiment	Neuron	MF injection	No RF	Deep input	Convergent	Skin Input	TLF	MF		Imp/ min	T (mV)	Latency (ms)			Depth (μm)	Receptor type	Conduction Velocity m/s	Distance mm		
Control + NGF	Str-Con 1	Control	1	NGF	+						0	640	1.1			1	580		31.82	35	
			2	NGF				+				0	320	1.6			1	660	LTM skin	21.88	35
			3	NGF				+				104	800	1.8			1	670	WDR skin	19.44	35
			4	NGF		+	+	+	+			0	810	2			1	800	HTM deep, HTM skin	17.50	35
	Stress-Control 2	Control	1	NGF					+			117	640	1.6			1	400	LTM skin	21.88	35
			2	NGF					+			0	470	1.8			1	420	HTM skin	19.44	35
			3	NGF	+							0	870	2.1			1	590		16.67	35
			4	NGF					+			0	460	1.7			1	710	WDR skin	20.59	35
			5	NGF	+							0	650	1.8			1	760		19.44	35
			6	NGF					+			0	610	1.4			1	650	LTM skin	25.00	35
			7	NGF	+							0	810	1.6			1	880		21.88	35
			8	NGF					+			1	610	1.4			1	730	WDR skin	25.00	35
	Str-C 6	Control	1	NGF					+			0	410	2.8			1	160	LTM skin	12.50	35
			2	NGF					+			0	320	1.8			1	300	WDR skin	19.44	35
			3	NGF	+							0	510	2.1			1	410		16.67	35
	Str-C 11	Control	1	NGF					+			0	410	2.1			1	630	WDR skin	16.67	35
			2	NGF					+			6	510	1.8			1	580	LTM skin	19.44	35
			3	NGF	+							0	710	2.2			1	650		15.91	35
			4	NGF		+	+	+	+			0	310	2.1			1	710	LTM skin, LTM deep	16.67	35
			5	NGF					+			5	300	0.8			1	710	WDR skin	43.75	35
			6	NGF		+						0	140	2.2			1	520	LTM deep	15.91	35
	S-C11	Ctl	1	NGF					+			1	300	1.8			1	700	HTM skin	19.44	35
			2	NGF					+			99	400	1.5			1	780	WDR skin	23.33	35
	Str-Con 13	Control	1	NGF					+			0	320	3.4			1	320	WDR skin	10.29	35
			2	NGF					+			730	420	2.1			1	500	HTM skin	16.67	35
			3	NGF	+							0	400	1.8			1	900		19.44	35
			4	NGF		+						0	380	1.5			1	790	HTM deep	23.33	35
			5	NGF					+			0	340	1.7			1	890	WDR skin	20.59	35
			6	NGF	+							0	370	2.1			1	250		16.67	35
																		Deep 2; Skin 6	LTM	20.3	Mean SEM SD
																	Deep 2; Skin 4	HTM	0.2		
																	Skin 9	WDR	6.1		
											Imp/ min	T (mV)	Latency (ms)			Depth (μm)					
Control + NGF			n	8	4	2	19	1	1	Mean	36.66	491.03	1.85			608.62					
			%	27.59	13.79	6.90	65.52	3.45	3.45	SEM	25.51	34.95	0.02			36.34					

Appendix 2: Summary of p values for the proportion of dorsal horn neurons having inputs from the deep tissues including fascia, skin, and convergent input.

<u>Fisher's test</u>	Data		Totals	p value		
	Ctrl + NGF	Stress + NGF		GraphPad	Social science Statistics	
Resting activity	8	17	25			
	21	14	35	0.029		One -tailed
Total	29	31	60	0.039	0.039	Two-tailed
	Ctrl + NGF	Stress + NGF				
Deep tissues	4	12	16			
	25	19	44	0.028		One -tailed
Total	29	31	60	0.041	0.041	Two-tailed
	Ctrl + NGF	Stress + NGF				
Skin input	19	19	38			
	10	12	22	0.471		One -tailed
Total	29	31	60	0.793	0.793	Two-tailed
	Ctrl + NGF	Stress + NGF				
Convergent input	2	7	9			
	27	24	51	0.089		One -tailed
Total	29	31	60	0.147	0.147	Two-tailed
	Ctrl + NGF	Stress + NGF				
Deep only	2	5	7			
	27	26	53	0.24		One -tailed
Total	29	31	60	0.425	0.425	Two-tailed
	Ctrl + NGF	Stress + NGF				
Deep tissues lowback	2	4	6			
	27	27	54	0.368		One -tailed
Total	29	31	60	0.671	0.671	Two-tailed
	Ctrl + NGF	Stress + NGF				
Deep tissues outside lowback	2	8	10			
	27	23	50	0.05		One -tailed
Total	29	31	60	0.081	0.081	Two-tailed

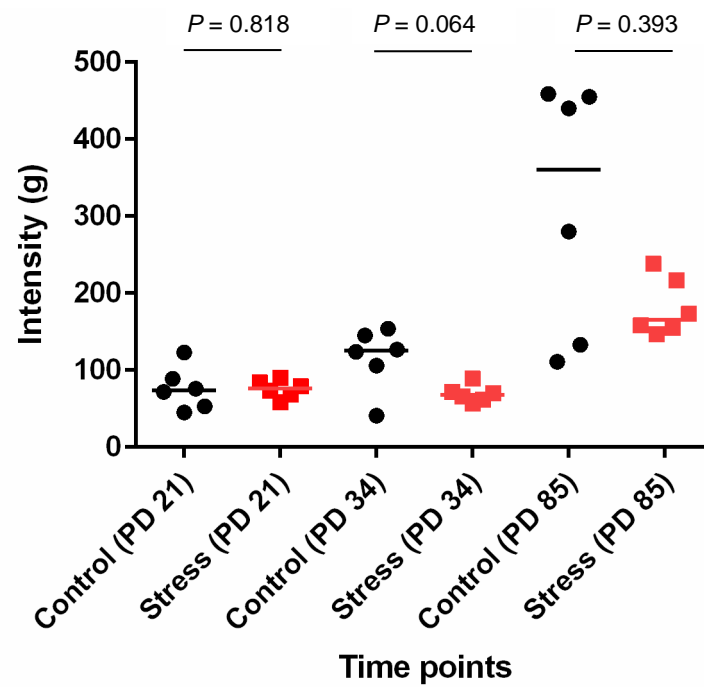
Appendix 3: Body weight shown in grams and the data is plotted with the (mean \pm SEM) values. The increase in body weight is led by increase with age. The time points mean the following (refer to Fig. 9; PD: postnatal day).

- 1: PD 21
- 2: PD 34
- 3: PD 85
- 4: PD 86
- 5: PD 87
- 6: PD 90
- 7: PD 91



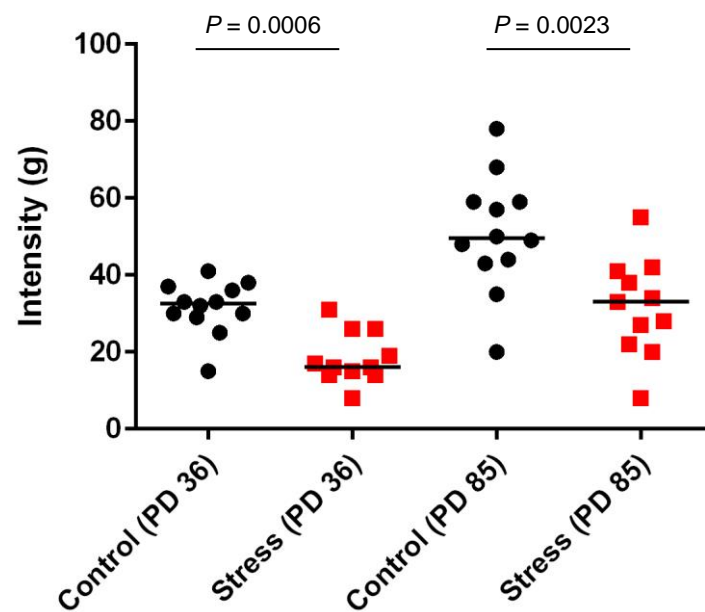
Repeated restraint stress in early adolescence did not affect the body weight of the stressed animals compared to controls ($n = 6/\text{group}$). PWT intensity expressed in (g) in the y-axis and time points in the x-axis.

Appendix 4: Pressure pain threshold of the right side low back MF muscle. Intensity shown in grams and the data is plotted with the individual values and the line indicates the median. (PD: postnatal day). Please note: the 'n' for this figure is only 6/group.



Repeated restraint stress in early adolescence did not affect the PPT of the right side low back MF muscle ($n = 6/\text{group}$). PPT intensity expressed in (g) in the y-axis and time points in the x-axis. P -values: U -test of Mann and Whitney.

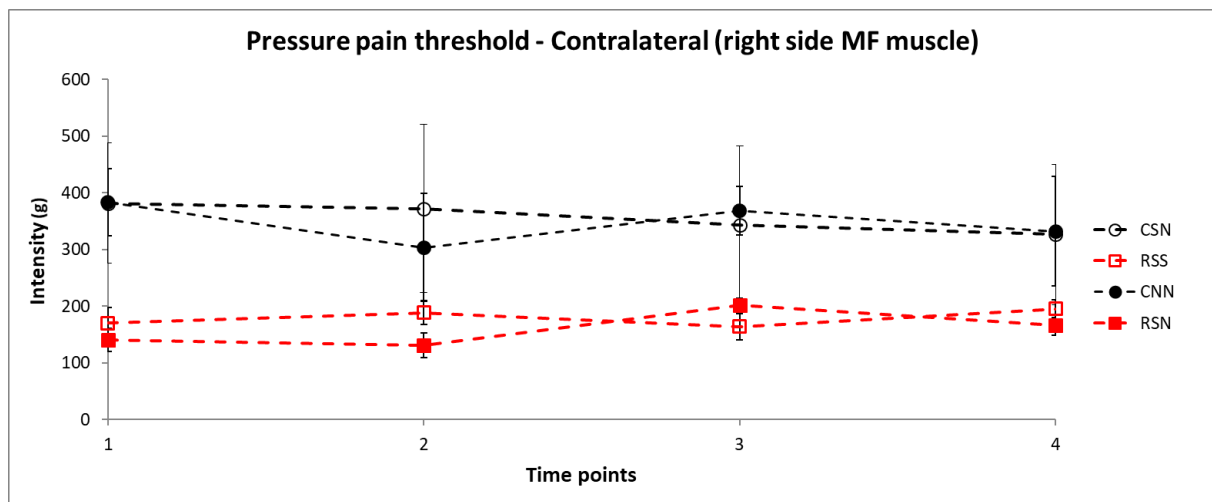
Appendix 5: Four days after the stress paradigm (PD 36), the PWT of the right hind paw was also significantly lowered ($P = 0.0006$) in the repeated restraint stress group, suggesting that the stress paradigm induced mechanical hyperalgesia and this sensitization was significant in the adulthood phase (PD 85) ($P = 0.0023$). Intensity shown in grams and the data is plotted with the individual values and the line indicates the median. The time points mean the following (refer to Fig. 9; PD: postnatal day).



Repeated restraint stress in early adolescence significantly lowered the PWT of the right hindpaw ($n = 12$ /group) and the lowered threshold was significant also in adulthood. PWT intensity expressed in (g) in the y-axis and time points in the x-axis (control: $n = 12$; stress: $n = 11$). P -values: U -test of Mann and Whitney.

Appendix 6: Pressure pain threshold of the right side low back MF muscle. Intensity shown in grams and the data is plotted with the (mean \pm SEM) values. The time points mean the following (refer to Fig. 9; PD: postnatal day). Please note: the 'n' for this figure is only 3/group.

- 1: PD 86
- 2: PD 87
- 3: PD 90
- 4: PD 91



Saline/NGF injections in adulthood did not affect the PPT of the right side low back MF muscle (n = 3/group). PPT intensity expressed in (g) in the y-axis and time points in the x-axis.

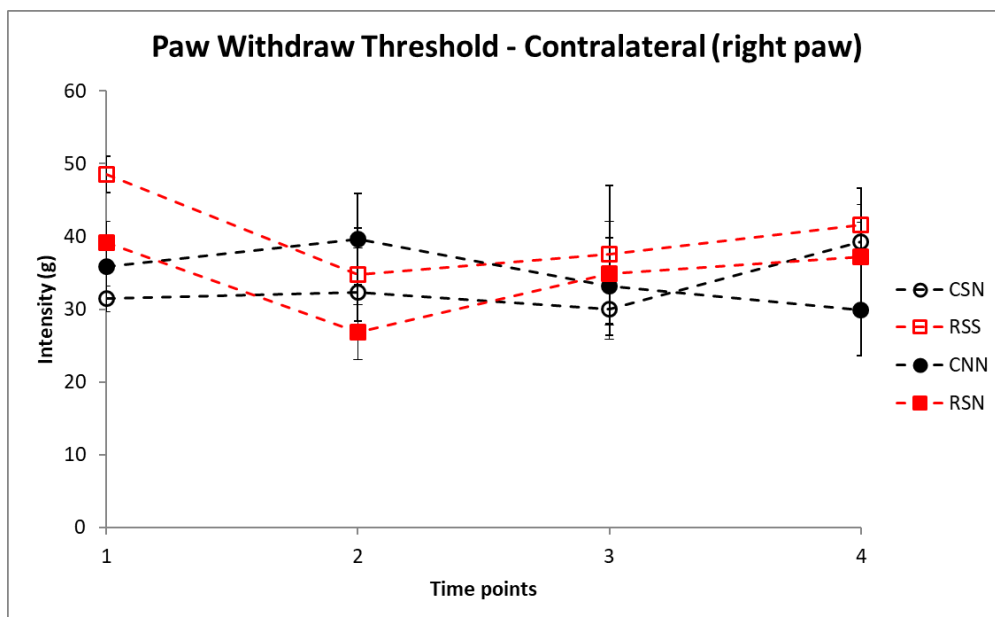
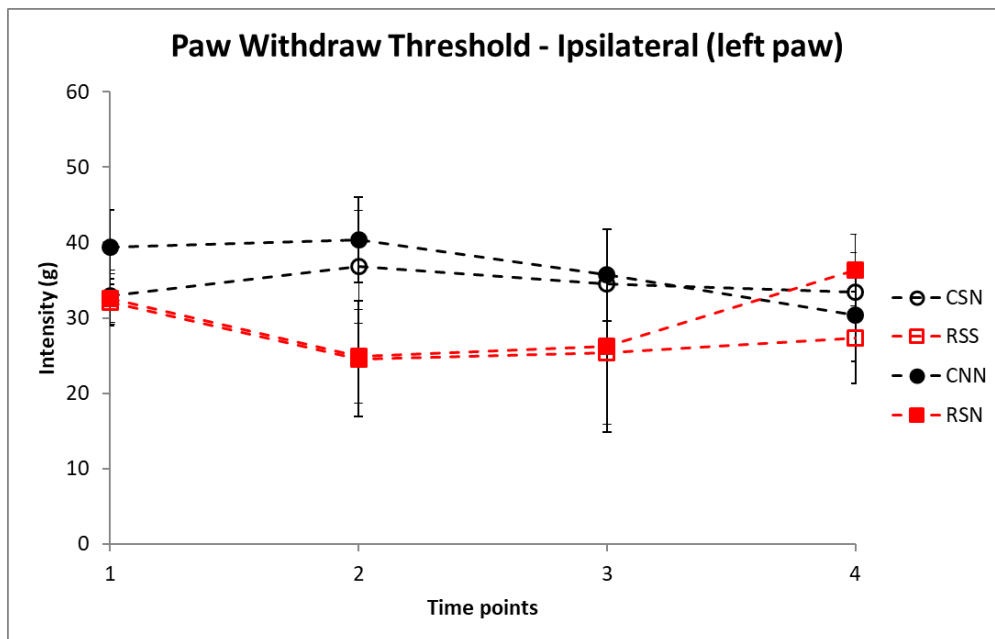
Appendix 7: Paw withdrawal threshold of both the hind paws. Intensity shown in grams and the data is plotted with the (mean \pm SEM) values. The time points mean the following (refer to Fig. 9; PD: postnatal day).

1: PD 86

2: PD 87

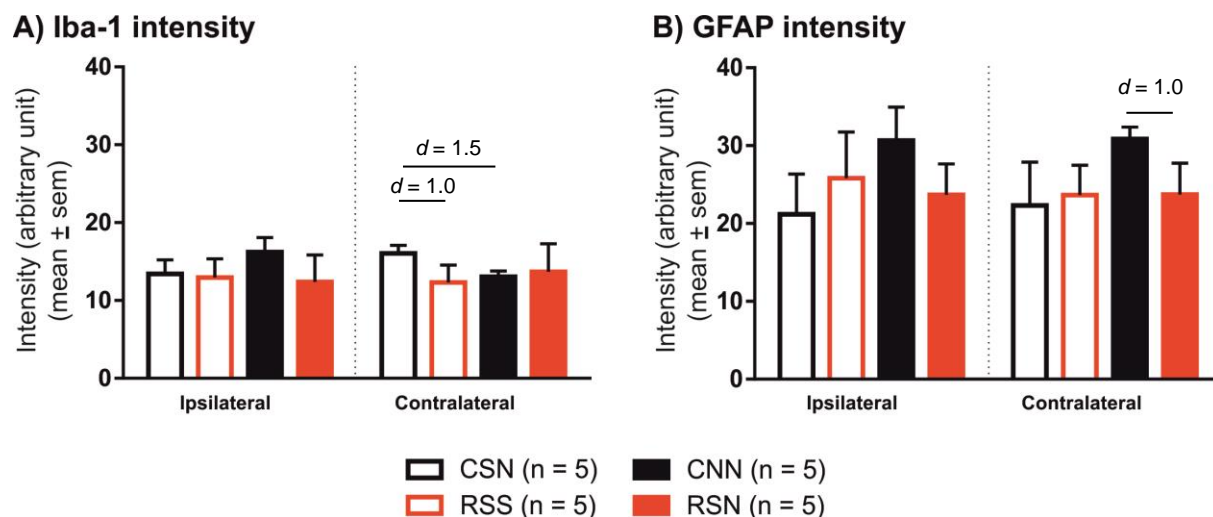
3: PD 90

4: PD 91



Saline/NGF injections in adulthood did not affect the PWT of both the hind paws ($n = 6/\text{group}$). PWT intensity expressed in (g) in the y-axis and time points in the x-axis.

Appendix 8: The staining intensity of Iba-1 and GFAP on both the ipsilateral and contralateral sides. No significant differences were observed between the groups.



Quantitative analysis of Iba-1 stained microglia and GFAP stained astrocytes.

Single or repetitive intramuscular NGF injections does not change the staining intensity compared to saline injections. **A)** Intensity of Iba-1 stained microglia cells shown in arbitrary unit. Data expressed as mean \pm SEM and effect size was calculated using Cohen's d . Intensity and background was measured for each ROI. The background was subtracted and the mean staining intensity was calculated. **B)** Intensity of GFAP stained astrocyte cells shown in arbitrary unit. Data expressed as mean \pm SEM and effect size was calculated using Cohen's d . Intensity and background was measured for each ROI. The background was subtracted and the mean staining intensity was calculated. Iba-1, ionized calcium binding adapter molecule 1; GFAP, glial fibrillary acidic protein; ROI, region of interest; NGF, nerve growth factor. CSN: control+saline+NGF; RSS: repeated restraint stress+saline+saline; CNN: control+NGF+NGF; and RSN: repeated restraint stress+saline+NGF.

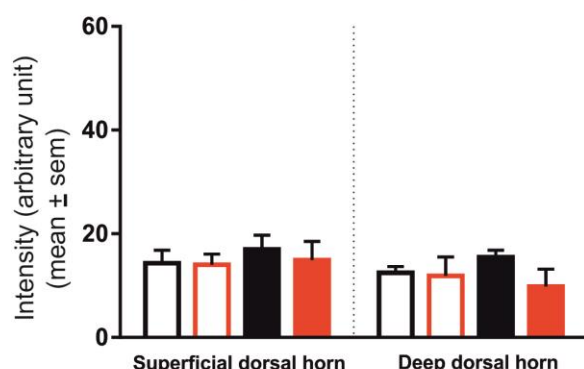
Appendix 9: Comparison table of microglia and astrocytes staining intensity.

Group comparisons	A) Iba-1 intensity		B) GFAP intensity	
	Ipsilateral	Contralateral	Ipsilateral	Contralateral
<u>CNN vs. CSN</u>				
<i>p</i> Value	<i>p</i> = 0.883	<i>p</i> = 0.810	<i>p</i> = 0.281	<i>p</i> = 0.357
Cohen <i>d</i> (effect size)	0.7	1.5	0.7	0.3
<u>RSN vs. RSS</u>				
<i>p</i> Value	<i>p</i> = 0.998	<i>p</i> = 0.977	<i>p</i> = 0.973	<i>p</i> > 0.999
Cohen <i>d</i> (effect size)	0.0	0.2	0.6	0.8
<u>RSN vs. CSN</u>				
<i>p</i> Value	<i>p</i> = 0.993	<i>p</i> = 0.894	<i>p</i> = 0.956	<i>p</i> = 0.991
Cohen <i>d</i> (effect size)	0.2	0.4	0.7	0.3
<u>RSS vs. CSN</u>				
<i>p</i> Value	<i>p</i> = 0.999	<i>p</i> = 0.694	<i>p</i> = 0.790	<i>p</i> = 0.992
Cohen <i>d</i> (effect size)	0.1	1.0	0.3	0.1
<u>RSN vs. CNN</u>				
<i>p</i> Value	<i>p</i> = 0.754	<i>p</i> = 0.997	<i>p</i> = 0.528	<i>p</i> = 0.504
Cohen <i>d</i> (effect size)	0.6	0.1	0.7	1.0

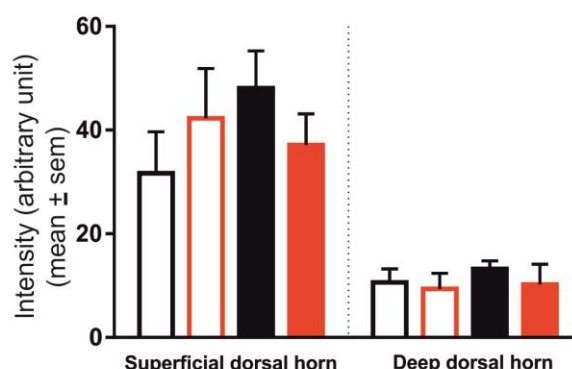
The table shows the statistics for **A)** Iba-1 staining intensity and **B)** GFAP staining intensity, both on the ipsilateral and contralateral side of saline/NGF injections. The staining intensity was analyzed for each ROI and the statistics were performed using the mean \pm SEM. $P < 0.05$ (two-way ANOVA followed by Tukey *post hoc* analysis) was considered significant and effect size was calculated using Cohen *d*. The group comparisons shown here are based on two factors: 1) repeated restraint stress (**R**) and control (**C**), 2) NGF (**N**) and saline (**S**) injections. Iba-1, ionized calcium binding adapter molecule 1; GFAP, glial fibrillary acidic protein; NGF, nerve growth factor. CSN: control+saline+NGF; RSS: repeated restraint stress+saline+saline; CNN: control+NGF+NGF; and RSN: repeated restraint stress+saline+NGF.

Appendix 10: The staining intensity of Iba-1 and GFAP in superficial and deep dorsal horn on both the ipsilateral and contralateral sides. No differences were observed between the groups.

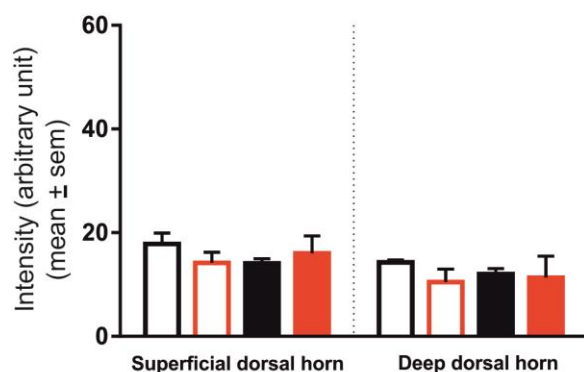
A) Iba-1 intensity: ipsilateral



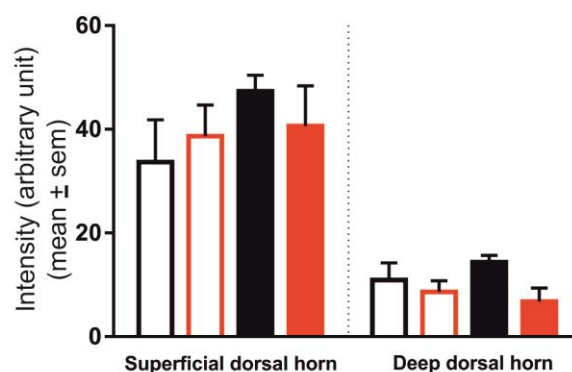
B) GFAP intensity: ipsilateral



C) Iba-1 intensity: contralateral



D) GFAP intensity: contralateral

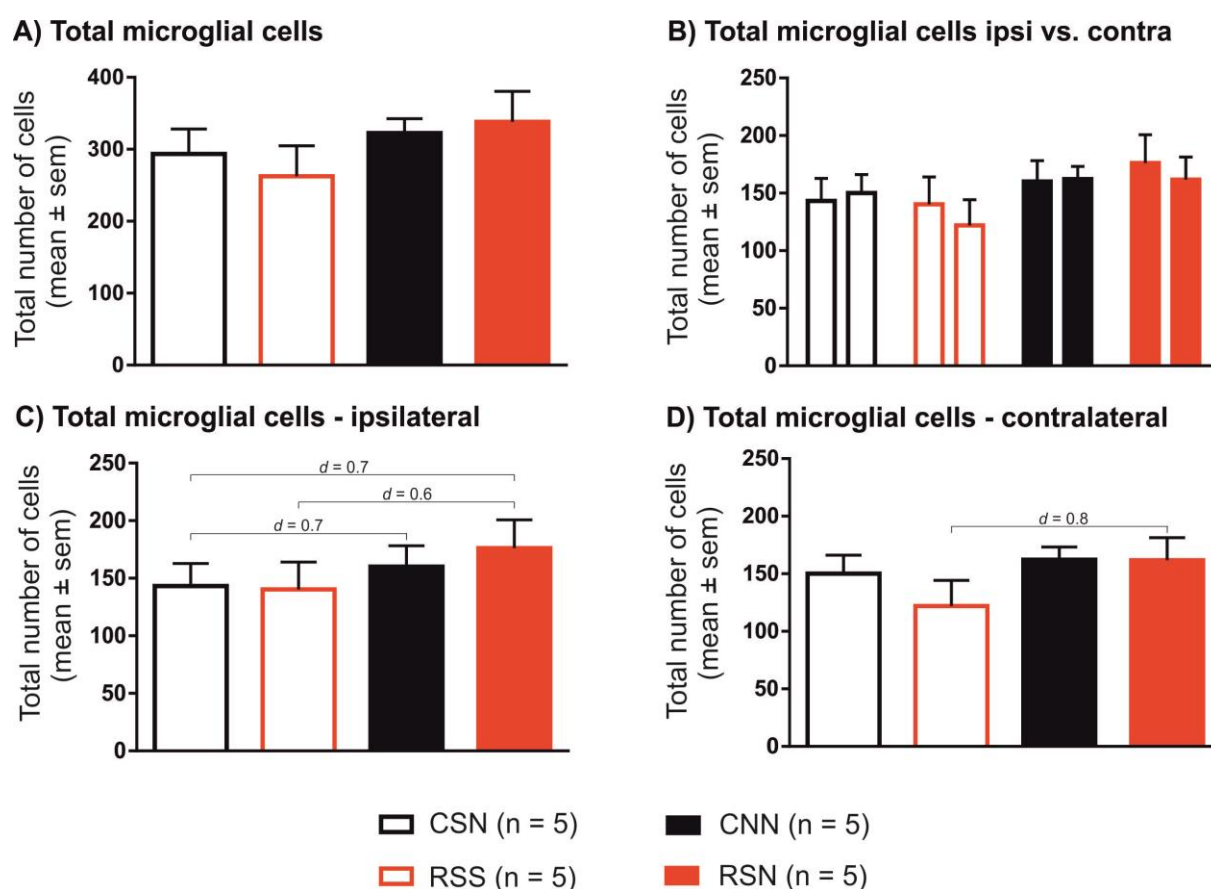


□ CSN (n = 5) ■ CNN (n = 5)
 □ RSS (n = 5) ■ RSN (n = 5)

Quantitative analysis of Iba-1 stained microglia and GFAP stained astrocytes.

Single or repetitive intramuscular NGF injections does not change the staining intensity compared to saline injections both in the superficial and deep dorsal horn. **A & C)** Intensity of Iba-1 stained microglia cells shown in arbitrary unit. Data expressed as mean \pm SEM. Intensity and background was measured for each ROI. The background was subtracted and the mean staining intensity was calculated. **B & D)** Intensity of GFAP stained astrocyte cells shown in arbitrary unit. Data expressed as mean \pm SEM. Intensity and background was measured for each ROI. The background was subtracted and the mean staining intensity was calculated. Iba-1, ionized calcium binding adapter molecule 1; GFAP, glial fibrillary acidic protein; ROI, region of interest; NGF, nerve growth factor. CSN: control+saline+NGF; RSS: repeated restraint stress+saline+saline; CNN: control+NGF+NGF; and RSN: repeated restraint stress+saline+NGF.

Appendix 11: The number of Iba-1 stained cells were counted in each ROI and no differences were observed between the groups (Fig. A). We also did not find any significant differences on neither the ipsilateral vs. contralateral sides nor the individual sides between the groups (Fig. B – D). We observed large effect in the number of microglia cells between the groups RSN vs. RSS ($P = 0.508$; $d = 0.8$) on the contralateral side (Fig. D).



Quantitative analysis of Iba-1 stained microglia cells.

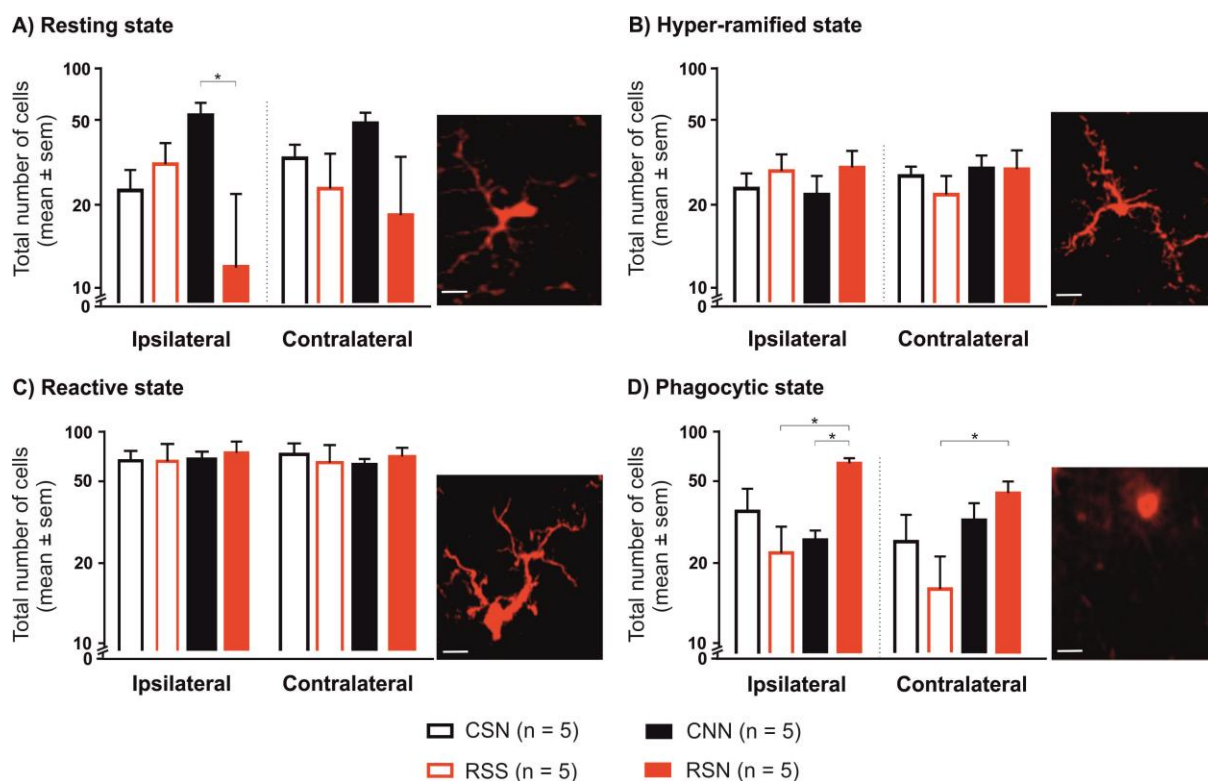
Single or repetitive intramuscular NGF injections does not change the number of microglia cells compared to saline injections. Data expressed as mean \pm SEM and effect size was calculated using Cohen's d . Iba-1 stained microglia cells were counted in each ROI and the mean was calculated. **A)** total microglial cells. **B)** total microglial cells ipsilateral vs. contralateral. **C)** total microglial cells ipsilateral. **D)** total microglial cells contralateral. Iba-1, ionized calcium binding adapter molecule 1; ROI, region of interest; NGF, nerve growth factor. CSN: control+saline+NGF; RSS: repeated restraint stress+saline+saline; CNN: control+NGF+NGF; and RSN: repeated restraint stress+saline+NGF.

Appendix 12: Comparison table for number of microglial cells.

Groups	<i>p</i> Value	Cohen <i>d</i> (effect size)
<u>CNN</u> vs. <u>CSN</u>		
Total number of microglia cells	<i>p</i> = 0.952	0.4
Ipsilateral	<i>p</i> = 0.942	0.7
Contralateral	<i>p</i> = 0.972	0.4
<u>RSN</u> vs. <u>CSN</u>		
Total number of microglia cells	<i>p</i> = 0.853	0.5
Ipsilateral	<i>p</i> = 0.707	0.7
Contralateral	<i>p</i> = 0.974	0.3
<u>RSN</u> vs. <u>RSS</u>		
Total number of microglia cells	<i>p</i> = 0.548	0.8
Ipsilateral	<i>p</i> = 0.654	0.6
Contralateral	<i>p</i> = 0.508	0.8
<u>CSN</u> vs. <u>RSS</u>		
Total number of microglia cells	<i>p</i> = 0.943	0.3
Ipsilateral	<i>p</i> = 0.999	0.0
Contralateral	<i>p</i> = 0.746	0.6
<u>CNN</u> vs. <u>RSN</u>		
Total number of microglia cells	<i>p</i> = 0.992	0.2
Ipsilateral	<i>p</i> = 0.951	0.3
Contralateral	<i>p</i> > 0.999	0.0

The table shows the statistics for number of microglia cells, and both on the ipsilateral and contralateral side of saline/NGF injections. The number of cells were analyzed for each ROI and the statistics were performed using the mean \pm SEM. $P < 0.05$ (two-way ANOVA followed by Tukey *post hoc* analysis) was considered significant and effect size was calculated using Cohen *d*. The group comparisons shown here are based on two factors: 1) repeated restraint stress (R) and control (C), 2) NGF (N) and saline (S) injections. Iba-1, ionized calcium binding adapter molecule 1; NGF, nerve growth factor. CSN: control+saline+NGF; RSS: repeated restraint stress+saline+saline; CNN: control+NGF+NGF; and RSN: repeated restraint stress+saline+NGF.

Appendix 13: On the contralateral side, we found significant difference only in the phagocytic state between (RSN vs. RSS; $P = 0.008$; $d = 2.1$) (Fig. D).



Microglia and its states.

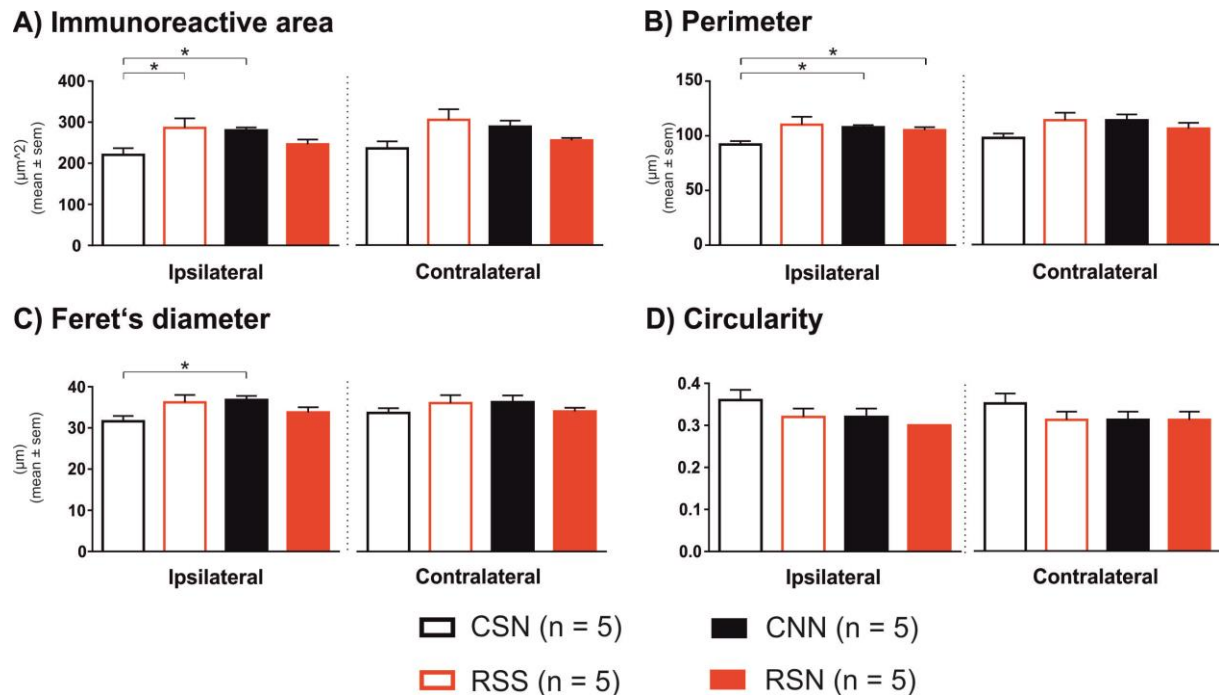
Intramuscular NGF injection leads to decreased number of microglia cells in resting state and increased number of cells in phagocytic state when preceded by repeated restraint stress in early adolescence. **A)** Number of Iba-1 stained microglia cells in resting state. Inset shows a representative image of cells in resting state. **B)** Number of Iba-1 stained microglia cells in hyper-ramified state. Inset shows a representative image of a cell in hyper-ramified state. **C)** Number of Iba-1 stained microglia cells in reactive state. Inset shows a representative image of a cell in reactive state. **D)** Number of Iba-1 stained microglia cells in phagocytic state. Inset shows a representative image of a cell in phagocytic state. Number of cells were counted in each ROI and their states were classified (refer sec. 2.7.8), and the mean was calculated. Scale bars: 20 μ m. Data expressed as mean \pm SEM; $P < 0.05$: two-way ANOVA followed by Tukey *post hoc* analysis and significance is indicated by * compared to RSN and RSS or CNN. Iba-1, ionized calcium binding adapter molecule 1; NGF, nerve growth factor. CSN: control+saline+NGF; RSS: repeated restraint stress+saline+saline; CNN: control+NGF+NGF; and RSN: repeated restraint stress+saline+NGF.

Appendix 14: Comparison table for number of microglial cells in different states.

Groups	p Value		Cohen d (effect size)	
	ipsilateral	contralateral	ipsilateral	contralateral
CNN vs. CSN				
Number of cells in resting state	$p = 0.286$	$p = 0.205$	1.8	1.2
Number of cells in hyper-ramified state	$p = 0.994$	$p = 0.982$	0.1	0.4
Number of cells in reactive state	$p = 0.997$	$p = 0.989$	0.0	0.4
Number of cells in phagocytic state	$p = 0.687$	$p = 0.791$	0.7	0.3
RSN vs. CSN				
Number of cells in resting state	$p = 0.461$	$p = 0.883$	0.4	0.4
Number of cells in hyper-ramified state	$p = 0.816$	$p = 0.987$	0.6	0.4
Number of cells in reactive state	$p = 0.983$	$p > 0.999$	0.3	0.1
Number of cells in phagocytic state	$p = 0.202$	$p = 0.183$	1.2	1.0
RSN vs. RSS				
Number of cells in resting state	$p = 0.202$	$p = 0.999$	0.9	0.0
Number of cells in hyper-ramified state	$p = 0.998$	$p = 0.635$	0.1	0.5
Number of cells in reactive state	$p = 0.768$	$p = 0.823$	0.2	0.2
Number of cells in phagocytic state	$p = 0.013$	$p = 0.008$	3.7	2.1
CSN vs. RSS				
Number of cells in resting state	$p = 0.928$	$p = 0.922$	0.5	0.4
Number of cells in hyper-ramified state	$p = 0.883$	$p = 0.813$	0.5	0.3
Number of cells in reactive state	$p = 0.925$	$p = 0.805$	0.0	0.2
Number of cells in phagocytic state	$p = 0.422$	$p = 0.312$	0.8	0.7
CNN vs. RSN				
Number of cells in resting state	$p = 0.024$	$p = 0.062$	2.1	1.2
Number of cells in hyper-ramified state	$p = 0.684$	$p > 0.999$	0.6	0.0
Number of cells in reactive state	$p = 0.997$	$p = 0.992$	0.2	0.4
Number of cells in phagocytic state	$p = 0.031$	$p = 0.606$	5.0	0.7

The table shows the statistics for number of microglia cells in different states on both the ipsilateral and contralateral side. The number of cells were counted for each ROI and the statistics were performed using the mean. $P < 0.05$ (two-way ANOVA followed by Tukey *post hoc* analysis) was considered significant and effect size was calculated using Cohen *d*. The group comparisons shown here are based on the factors: 1) repeated restraint stress (R) and control (C), 2) NGF (N) and saline (S) injections, and 3) both (RS) and (CN). Ip. ipsilateral; Con. contralateral; ROI, region of interest; SDH, superficial dorsal horn; DDH, deep dorsal horn; Iba-1, ionized calcium binding adapter molecule 1; NGF, nerve growth factor. CSN: control+saline+NGF; RSS: repeated restraint stress+saline+saline; CNN: control+NGF+NGF; and RSN: repeated restraint stress+saline+NGF.

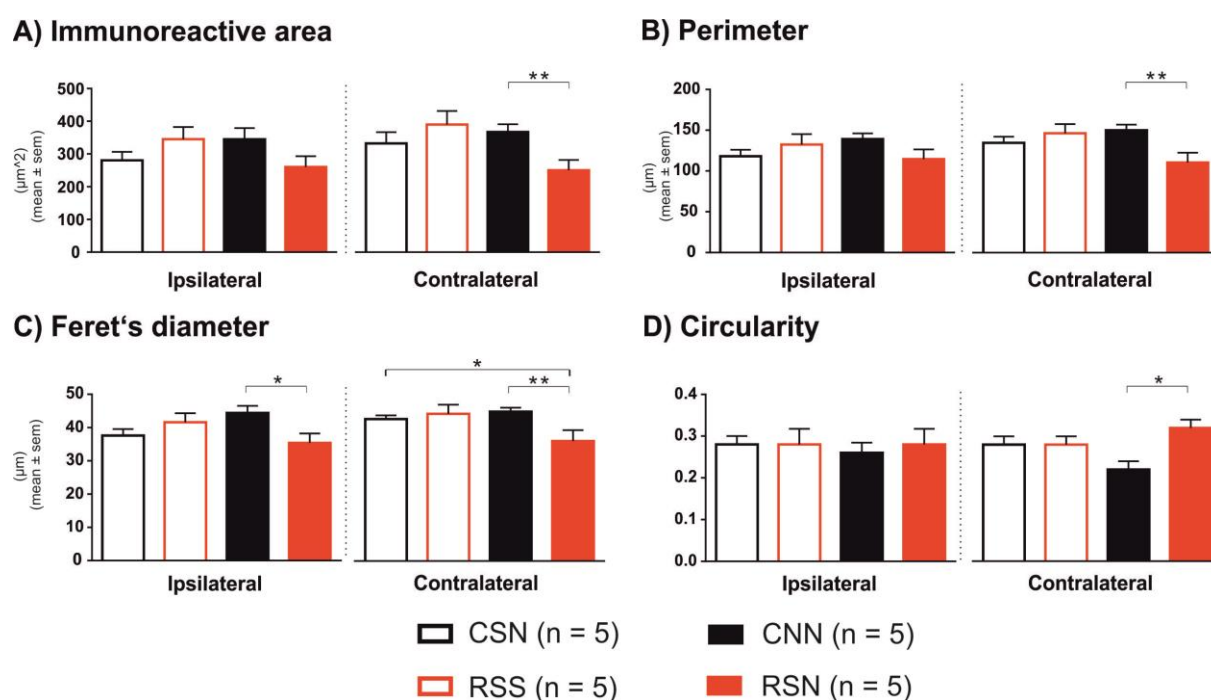
Appendix 15: The contralateral side of the saline/NGF injections also did not show any differences between the groups for all the four parameters for microglis cells in resting state.



Morphological analysis of resting state microglial cells.

A) Immunoreactive area. **B)** Perimeter length. **C)** Feret's diameter. **D)** Circularity. NGF, nerve growth factor. The values for all the four parameters were calculated for individual cells for each ROI and the statistics were performed using the mean. $P < 0.05$ (A: two-way ANOVA followed by Tukey *post hoc* analysis; B and C: Mann-Whitney *U* test) was considered significant CSN: control+saline+NGF; RSS: repeated restraint stress+saline+saline; CNN: control+NGF+NGF; and RSN: repeated restraint stress+saline+NGF.

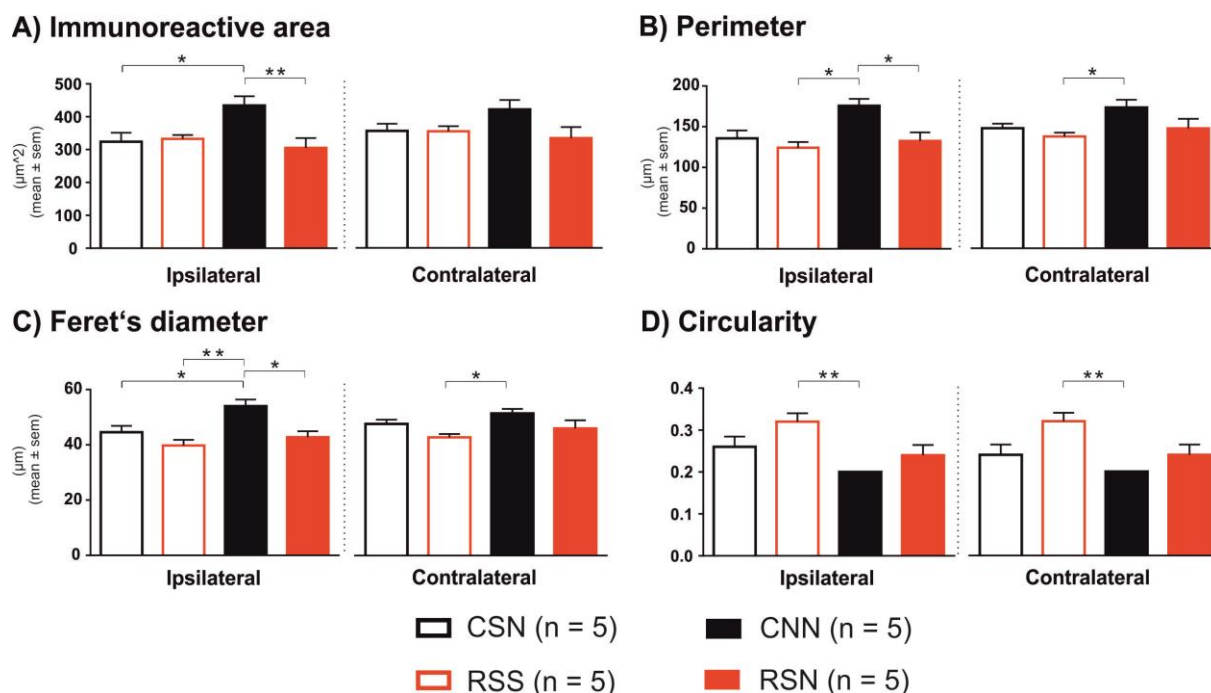
Appendix 16: For the hyper-ramified state morphology, the immunoreactive area was significantly different between the group RSN vs. CNN on the contralateral side of saline/NGF injections ($P = 0.007$; Fig. A). The perimeter length was also significantly different between the group RSN vs. CNN ($P = 0.007$; Fig. B). For feret's diameter, we found significant difference between the groups RSN vs. CSN ($P = 0.031$; Fig. C) and RSN vs. CNN ($P = 0.007$; Fig. C). A significant difference was observed between the group RSN vs. CNN for circularity ($P = 0.039$; Fig. D).



Morphological analysis of hyper-ramified state microglial cells.

A) Immunoreactive area. **B)** Perimeter length. **C)** Feret's diameter. **D)** Circularity. NGF, nerve growth factor. The values for all the four parameters were calculated for individual cells for each ROI and the statistics were performed using the mean. $P < 0.05$ (Mann-Whitney U test) was considered significant CSN: control+saline+NGF; RSS: repeated restraint stress+saline+saline; CNN: control+NGF+NGF; and RSN: repeated restraint stress+saline+NGF.

Appendix 17: In the reactive state morphology, the perimeter length was significantly different between CNN vs. RSS ($P = 0.028$) on the contralateral side (Fig. B). For feret's diameter we found significant difference between the group CNN vs. RSS ($P = 0.015$) (Fig. C) on the contralateral side. A significant difference was observed between the group CNN vs. RSS on the contralateral side ($P = 0.007$) (Fig. D) for circularity.

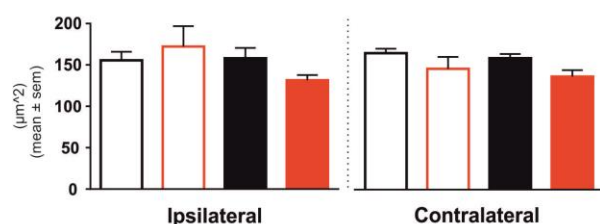


Morphological analysis of reactive state microglial cells.

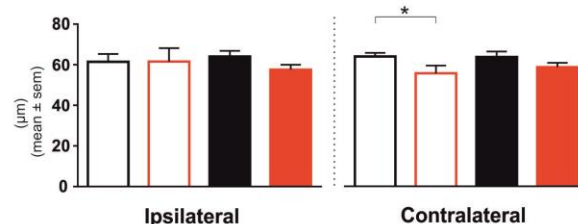
A) Immunoreactive area. **B)** Perimeter length. **C)** Feret's diameter. **D)** Circularity. NGF, nerve growth factor. The values for all the four parameters were calculated for individual cells for each ROI and the statistics were performed using the mean. $P < 0.05$ (A and B: two-way ANOVA followed by Tukey *post hoc* analysis; C and D: Mann-Whitney *U* test) was considered significant CSN: control+saline+NGF; RSS: repeated restraint stress+saline+saline; CNN: control+NGF+NGF; and RSN: repeated restraint stress+saline+NGF.

Appendix 18: For the phagocytic state morphology, the perimeter length was significantly different between the group CSN vs. RSS ($P = 0.031$) on the contralateral side (Fig. B). For feret's diameter we found significant difference between the groups CNN vs. RSS ($P = 0.033$) and CSN vs. RSS ($P = 0.033$) (Fig. C) on the contralateral side.

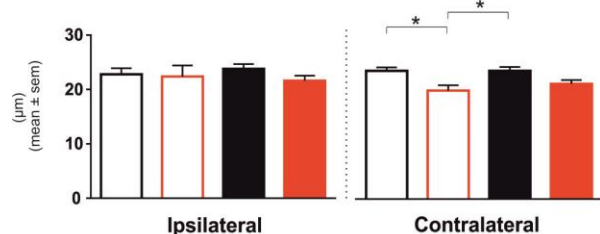
A) Immunoreactive area



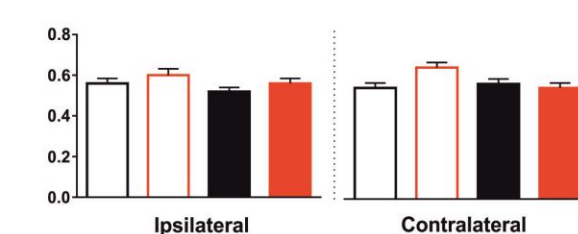
B) Perimeter



C) Feret's diameter



D) Circularity



□ CSN (n = 5) ■ CNN (n = 5)
 □ RSS (n = 5) ■ RSN (n = 5)

Morphological analysis of phagocytic state microglial cells.

A) Immunoreactive area. **B)** Perimeter length. **C)** Feret's diameter. **D)** Circularity. NGF, nerve growth factor. The values for all the four parameters were calculated for individual cells for each ROI and the statistics were performed using the mean. $P < 0.05$ (A and C: two-way ANOVA followed by Tukey *post hoc* analysis; B and D: Mann-Whitney *U* test) was considered significant CSN: control+saline+NGF; RSS: repeated restraint stress+saline+saline; CNN: control+NGF+NGF; and RSN: repeated restraint stress+saline+NGF.

Appendix 19 A: The number of resting state microglial cells in all the groups and in the individual ROI's (1 – 8) is presented in the table below.

Group 1 RS				Group 2 CN				Group 3 CN				Group 4 RSN			
Rat 1	No. Of cells	No. Of cells	Sum	Rat 2	No. Of cells	No. Of cells	Sum	Rat 1	No. Of cells	No. Of cells	Sum	Rat 2	No. Of cells	No. Of cells	Sum
ROI1	4	7	12	ROI1	3	5	8	ROI1	5	2	8	ROI1	4	0	2
ROI2	3	6	10	ROI2	0	1	1	ROI2	1	3	1	ROI2	2	1	1
Sum	7	13	22	Sum	3	6	9	Sum	6	5	9	Sum	6	1	3
ROI3	11	10	22	ROI3	2	10	12	ROI3	3	8	3	ROI3	9	5	0
ROI4	5	3	9	ROI4	4	10	14	ROI4	8	3	5	ROI4	6	6	5
Sum	16	13	30	Sum	6	20	26	Sum	11	11	8	Sum	15	11	5
ROI5	1	3	4	ROI5	0	0	0	ROI5	2	2	2	ROI5	0	6	11
ROI6	0	5	6	ROI6	4	4	4	ROI6	2	6	4	ROI6	4	4	6
Sum	1	8	10	Sum	4	0	4	Sum	4	8	6	Sum	4	10	17
ROI7	3	2	5	ROI7	6	7	6	ROI7	4	7	18	ROI7	7	5	31
ROI8	8	1	4	ROI8	6	6	6	ROI8	3	4	5	ROI8	1	2	19
Sum	11	3	23	Sum	12	0	12	Sum	7	11	12	Sum	8	9	4
Group 2 CN				Group 3 CN				Group 4 RSN				Group 4 RSN			
Rat 3	No. Of cells	No. Of cells	Sum	Rat 3	No. Of cells	No. Of cells	Sum	Rat 3	No. Of cells	No. Of cells	Sum	Rat 3	No. Of cells	No. Of cells	Sum
ROI1	4	3	5	ROI1	8	3	15	ROI1	0	1	3	ROI1	0	0	0
ROI2	0	0	6	ROI2	4	4	10	ROI2	1	6	3	ROI2	1	0	1
Sum	4	3	11	Sum	12	7	14	Sum	1	7	6	Sum	1	0	0
ROI3	1	2	4	ROI3	5	4	13	ROI3	0	1	1	ROI3	0	4	0
ROI4	4	3	2	ROI4	1	7	8	ROI4	0	0	4	ROI4	2	5	0
Sum	5	5	6	Sum	6	11	12	Sum	0	1	5	Sum	2	9	0
ROI5	4	3	2	ROI5	6	7	13	ROI5	1	7	2	ROI5	1	2	0
ROI6	5	3	16	ROI6	11	14	6	ROI6	1	4	6	ROI6	1	0	1
Sum	9	11	25	Sum	17	21	6	Sum	2	11	8	Sum	2	2	0
ROI7	3	3	9	ROI7	2	3	11	ROI7	1	1	5	ROI7	6	8	4
ROI8	5	0	6	ROI8	0	4	4	ROI8	0	0	3	ROI8	6	1	16
Sum	8	3	20	Sum	2	7	15	Sum	1	1	8	Sum	12	9	10
Group 2 CN				Group 3 CN				Group 4 RSN				Group 4 RSN			
Rat 4	No. Of cells	No. Of cells	Sum	Rat 4	No. Of cells	No. Of cells	Sum	Rat 4	No. Of cells	No. Of cells	Sum	Rat 4	No. Of cells	No. Of cells	Sum
ROI1	4	2	3	ROI1	3	7	4	ROI1	0	0	0	ROI1	1	3	0
ROI2	0	5	6	ROI2	15	7	5	ROI2	4	0	4	ROI2	0	0	2
Sum	4	7	4	Sum	18	14	9	Sum	4	0	4	Sum	1	3	0
ROI3	10	3	0	ROI3	9	7	23	ROI3	6	0	6	ROI3	0	3	0
ROI4	8	0	8	ROI4	8	6	5	ROI4	4	0	2	ROI4	3	0	2
Sum	18	3	0	Sum	17	13	12	Sum	10	0	2	Sum	3	0	4
ROI5	4	0	4	ROI5	9	5	4	ROI5	5	0	5	ROI5	3	1	2
ROI6	1	1	0	ROI6	4	3	4	ROI6	4	0	4	ROI6	0	5	6
Sum	5	1	0	Sum	13	8	8	Sum	9	0	9	Sum	3	10	13
ROI7	8	0	1	ROI7	1	5	2	ROI7	6	0	6	ROI7	0	2	1
ROI8	4	1	0	ROI8	8	4	5	ROI8	10	0	10	ROI8	1	0	4
Sum	12	1	1	Sum	9	9	7	Sum	16	0	16	Sum	1	2	8
Group 2 CN				Group 3 CN				Group 4 RSN				Group 4 RSN			
Rat 5	No. Of cells	No. Of cells	Sum	Rat 5	No. Of cells	No. Of cells	Sum	Rat 5	No. Of cells	No. Of cells	Sum	Rat 5	No. Of cells	No. Of cells	Sum
ROI1	1	2	0	ROI1	5	0	6	ROI1	0	1	0	ROI1	0	1	0
ROI2	1	3	0	ROI2	1	4	4	ROI2	0	3	3	ROI2	4	0	1
Sum	2	5	0	Sum	6	4	10	Sum	0	1	3	Sum	4	1	0
ROI3	0	2	0	ROI3	5	3	1	ROI3	3	2	4	ROI3	2	0	0
ROI4	1	2	0	ROI4	0	0	4	ROI4	4	1	3	ROI4	2	0	2
Sum	1	4	0	Sum	5	3	5	Sum	7	3	8	Sum	7	3	9
ROI5	2	6	3	ROI5	2	4	10	ROI5	0	4	0	ROI5	0	0	4
ROI6	2	1	4	ROI6	12	0	12	ROI6	1	5	0	ROI6	0	0	4
Sum	4	7	15	Sum	14	4	4	Sum	1	9	0	Sum	0	0	0
ROI7	2	2	1	ROI7	5	1	4	ROI7	0	3	0	ROI7	1	0	3
ROI8	5	2	0	ROI8	6	1	1	ROI8	1	3	3	ROI8	5	0	8
Sum	7	4	1	Sum	11	2	5	Sum	1	6	3	Sum	6	0	11
Group 2 CN				Group 3 CN				Group 4 RSN				Group 4 RSN			
Rat 6	No. Of cells	No. Of cells	Sum	Rat 6	No. Of cells	No. Of cells	Sum	Rat 6	No. Of cells	No. Of cells	Sum	Rat 6	No. Of cells	No. Of cells	Sum
ROI1	0	1	0	ROI1	1	2	3	ROI1	0	3	3	ROI1	0	0	0
ROI2	0	3	3	ROI2	2	3	5	ROI2	0	1	2	ROI2	0	0	0
Sum	0	1	3	Sum	3	5	8	Sum	0	4	5	Sum	0	0	0
ROI3	0	0	7	ROI3	9	3	6	ROI3	2	1	0	ROI3	0	0	0
ROI4	10	0	6	ROI4	6	0	2	ROI4	2	0	1	ROI4	0	0	0
Sum	10	0	13	Sum	15	3	8	Sum	4	1	1	Sum	0	0	0
ROI5	0	2	0	ROI5	1	1	1	ROI5	4	1	1	ROI5	1	0	1
ROI6	0	0	0	ROI6	0	0	7	ROI6	5	0	1	ROI6	1	0	0
Sum	0	2	0	Sum	1	1	8	Sum	6	8	2	Sum	1	0	0
ROI7	0	0	2	ROI7	1	1	8	ROI7	6	5	5	ROI7	1	0	1
ROI8	0	0	1	ROI8	8	2	2	ROI8	0	2	5	ROI8	0	0	0
Sum	0	0	3	Sum	11	6	6	Sum	6	7	10	Sum	0	0	0

Appendix 19 B: The number of hyper-ramified state microglial cells in all the groups and in the individual ROI's (1 – 8) is presented in the table below.

Group 1 RSS				Group 2 CNN				Group 3 CSN				Group 4 RSN			
Rat 1	No. Of cells	No. Of cells	Sum	Rat 2	No. Of cells	No. Of cells	Sum	Rat 1	No. Of cells	No. Of cells	Sum	Rat 2	No. Of cells	No. Of cells	Sum
ROI 1	5	1	4	ROI 1	2	0	2	ROI 1	1	3	0	ROI 1	2	1	2
ROI 2	2	6	2	ROI 2	0	0	0	ROI 2	6	2	0	ROI 2	4	3	2
ROI 3	7	7	6	ROI 3	2	0	0	ROI 3	7	5	0	ROI 3	6	4	0
ROI 4	6	2	2	ROI 4	1	3	4	ROI 4	0	1	0	ROI 4	1	4	0
Sum	11	2	15	Sum	7	2	8	Sum	2	1	1	Sum	4	6	2
ROI 5	8	0	2	ROI 5	7	5	0	ROI 5	2	2	1	ROI 5	5	7	13
ROI 6	2	0	0	ROI 6	7	4	7	ROI 6	0	2	1	ROI 6	4	4	8
ROI 7	10	0	2	ROI 7	14	0	14	ROI 7	1	2	1	ROI 7	6	5	5
ROI 8	1	0	1	ROI 8	5	1	5	ROI 8	2	5	1	ROI 8	6	5	13
Sum	0	3	1	Sum	5	1	5	Sum	4	3	2	Sum	2	3	7
ROI 1	1	3	2	ROI 1	10	0	10	ROI 1	6	8	3	ROI 1	5	5	12
ROI 2	2	1	7	ROI 2	2	2	6	ROI 2	3	3	3	ROI 2	6	0	6
ROI 3	0	1	2	ROI 3	1	6	7	ROI 3	2	3	2	ROI 3	1	10	11
ROI 4	2	2	9	ROI 4	3	8	13	ROI 4	5	6	5	ROI 4	7	0	17
ROI 5	3	5	10	ROI 5	0	3	3	ROI 5	2	1	1	ROI 5	6	5	16
ROI 6	4	3	13	ROI 6	1	5	6	ROI 6	0	1	2	ROI 6	1	0	6
ROI 7	3	5	13	ROI 7	1	5	6	ROI 7	2	3	3	ROI 7	7	5	22
ROI 8	2	1	3	ROI 8	4	1	5	ROI 8	2	2	1	ROI 8	2	6	8
Sum	6	6	12	Sum	9	2	11	Sum	8	4	5	Sum	8	2	10
ROI 1	8	7	15	ROI 1	9	3	12	ROI 1	6	4	6	ROI 1	10	8	18
ROI 2	7	6	13	ROI 2	6	2	8	ROI 2	8	6	20	ROI 2	10	4	14
ROI 3	2	3	5	ROI 3	9	3	12	ROI 3	6	3	9	ROI 3	4	3	7
ROI 4	2	3	5	ROI 4	2	2	4	ROI 4	0	3	3	ROI 4	3	4	7
ROI 5	2	1	3	ROI 5	4	1	5	ROI 5	2	1	3	ROI 5	5	2	7
ROI 6	6	3	9	ROI 6	5	2	7	ROI 6	2	4	6	ROI 6	8	2	10
ROI 7	8	7	15	ROI 7	9	3	12	ROI 7	8	6	14	ROI 7	10	8	18
ROI 8	2	3	5	ROI 8	3	2	5	ROI 8	0	3	3	ROI 8	4	3	7
Sum	3	2	5	Sum	2	3	5	Sum	0	2	2	Sum	0	6	6
ROI 1	5	13	23	ROI 1	5	5	10	ROI 1	0	5	5	ROI 1	4	9	19
ROI 2	2	1	3	ROI 2	2	2	4	ROI 2	3	3	6	ROI 2	6	2	8
ROI 3	0	1	1	ROI 3	1	6	7	ROI 3	2	3	5	ROI 3	1	10	11
ROI 4	2	2	4	ROI 4	3	8	11	ROI 4	5	6	11	ROI 4	7	0	17
ROI 5	3	5	8	ROI 5	0	3	3	ROI 5	2	1	3	ROI 5	6	5	16
ROI 6	4	3	7	ROI 6	1	5	6	ROI 6	0	1	1	ROI 6	1	0	6
ROI 7	3	5	8	ROI 7	1	5	6	ROI 7	2	3	5	ROI 7	7	5	22
ROI 8	2	1	3	ROI 8	4	1	5	ROI 8	2	2	4	ROI 8	2	6	8
Sum	6	6	12	Sum	9	2	11	Sum	8	4	5	Sum	8	2	10
ROI 1	9	2	11	ROI 1	8	2	10	ROI 1	4	0	4	ROI 1	11	4	15
ROI 2	4	0	4	ROI 2	0	3	3	ROI 2	6	0	6	ROI 2	8	2	10
ROI 3	13	2	15	ROI 3	8	5	13	ROI 3	8	0	8	ROI 3	5	7	12
ROI 4	15	1	16	ROI 4	5	6	11	ROI 4	5	1	6	ROI 4	3	4	7
ROI 5	9	4	13	ROI 5	4	2	6	ROI 5	3	0	3	ROI 5	1	0	6
ROI 6	24	1	25	ROI 6	9	8	17	ROI 6	8	0	8	ROI 6	4	12	16
ROI 7	6	0	6	ROI 7	3	3	6	ROI 7	4	0	4	ROI 7	11	4	15
ROI 8	5	0	5	ROI 8	3	3	6	ROI 8	8	0	8	ROI 8	4	3	7
Sum	11	0	11	Sum	6	7	13	Sum	4	0	4	Sum	8	2	10
ROI 1	5	0	5	ROI 1	6	7	13	ROI 1	8	0	8	ROI 1	8	2	10
ROI 2	5	0	5	ROI 2	0	3	3	ROI 2	4	0	4	ROI 2	4	0	4
ROI 3	3	0	3	ROI 3	3	3	6	ROI 3	9	0	9	ROI 3	2	1	3
ROI 4	3	0	3	ROI 4	3	3	6	ROI 4	1	0	1	ROI 4	3	6	9
ROI 5	8	0	8	ROI 5	3	6	9	ROI 5	10	0	10	ROI 5	2	3	5
ROI 6	2	0	2	ROI 6	3	6	9	ROI 6	0	0	0	ROI 6	4	6	10
ROI 7	2	0	2	ROI 7	3	6	9	ROI 7	0	0	0	ROI 7	3	6	9
ROI 8	2	0	2	ROI 8	3	6	9	ROI 8	0	0	0	ROI 8	4	6	10
Sum	8	0	8	Sum	3	6	9	Sum	10	0	10	Sum	4	6	10
ROI 1	3	3	6	ROI 1	0	0	0	ROI 1	No. Of cells	No. Of cells	Sum	ROI 1	No. Of cells	No. Of cells	Sum
ROI 2	1	1	2	ROI 2	1	0	1	ROI 2	No. Of cells	No. Of cells	Sum	ROI 2	No. Of cells	No. Of cells	Sum
ROI 3	4	4	8	ROI 3	1	0	1	ROI 3	No. Of cells	No. Of cells	Sum	ROI 3	No. Of cells	No. Of cells	Sum
ROI 4	2	2	4	ROI 4	1	0	1	ROI 4	No. Of cells	No. Of cells	Sum	ROI 4	No. Of cells	No. Of cells	Sum
ROI 5	1	1	2	ROI 5	2	1	3	ROI 5	No. Of cells	No. Of cells	Sum	ROI 5	No. Of cells	No. Of cells	Sum
ROI 6	3	3	6	ROI 6	3	5	8	ROI 6	No. Of cells	No. Of cells	Sum	ROI 6	No. Of cells	No. Of cells	Sum
ROI 7	2	2	4	ROI 7	5	2	7	ROI 7	No. Of cells	No. Of cells	Sum	ROI 7	No. Of cells	No. Of cells	Sum
ROI 8	4	4	8	ROI 8	7	7	14	ROI 8	No. Of cells	No. Of cells	Sum	ROI 8	No. Of cells	No. Of cells	Sum
Sum	6	6	12	Sum	7	7	14	Sum	No. Of cells	No. Of cells	Sum	Sum	No. Of cells	No. Of cells	Sum
ROI 1	3	3	6	ROI 1	0	5	5	ROI 1	No. Of cells	No. Of cells	Sum	ROI 1	No. Of cells	No. Of cells	Sum
ROI 2	4	4	8	ROI 2	5	2	7	ROI 2	No. Of cells	No. Of cells	Sum	ROI 2	No. Of cells	No. Of cells	Sum
ROI 3	2	2	4	ROI 3	7	7	14	ROI 3	No. Of cells	No. Of cells	Sum	ROI 3	No. Of cells	No. Of cells	Sum
ROI 4	1	1	2	ROI 4	0	5	5	ROI 4	No. Of cells	No. Of cells	Sum	ROI 4	No. Of cells	No. Of cells	Sum
ROI 5	3	3	6	ROI 5	7	7	14	ROI 5	No. Of cells	No. Of cells	Sum	ROI 5	No. Of cells	No. Of cells	Sum
ROI 6	4	4	8	ROI 6	7	7	14	ROI 6	No. Of cells	No. Of cells	Sum	ROI 6	No. Of cells	No. Of cells	Sum
ROI 7	2	2	4	ROI 7	0	5	5	ROI 7	No. Of cells	No. Of cells	Sum	ROI 7	No. Of cells	No. Of cells	Sum
ROI 8	4	4	8	ROI 8	3	3	6	ROI 8	No. Of cells	No. Of cells	Sum	ROI 8	No. Of cells	No. Of cells	Sum
Sum	5	5	10	Sum	3	3	6	Sum	No. Of cells	No. Of cells	Sum	Sum	No. Of cells	No. Of cells	Sum
ROI 1	0	4	4	ROI 1	1	2	3	ROI 1	No. Of cells	No. Of cells	Sum	ROI 1	No. Of cells	No. Of cells	Sum
ROI 2	0	1	1	ROI 2	1	3	4	ROI 2	No. Of cells	No. Of cells	Sum	ROI 2	No. Of cells	No. Of cells	Sum
ROI 3	0	5	5	ROI 3	2	5	7	ROI 3	No. Of cells	No. Of cells	Sum	ROI 3	No. Of cells	No. Of cells	Sum
ROI 4	0	1	1	ROI 4	2	5	7	ROI 4	No. Of cells	No. Of cells	Sum	ROI 4	No. Of cells	No. Of cells	Sum
ROI 5	2	0	2	ROI 5	2	1	3	ROI 5	No. Of cells	No. Of cells	Sum	ROI 5	No. Of cells	No. Of cells	Sum
ROI 6	2	1	3	ROI 6	3	5	8	ROI 6	No. Of cells	No. Of cells	Sum	ROI 6	No. Of cells	No. Of cells	Sum
ROI 7	0	4	4	ROI 7	2	1	3	ROI 7	No. Of cells	No. Of cells	Sum	ROI 7	No. Of cells	No. Of cells	Sum
ROI 8	0	1	1	ROI 8	1	2	3	ROI 8	No. Of cells	No. Of cells	Sum	ROI 8	No. Of cells	No. Of cells	Sum
Sum	0	11	11	Sum	3	5	8	Sum	No. Of cells	No. Of cells	Sum	Sum	No. Of cells	No. Of cells	Sum
ROI 1	0	4	4	ROI 1	2	1	3	ROI 1	No. Of cells	No. Of cells	Sum	ROI 1	No. Of cells	No. Of cells	Sum
ROI 2	0	1	1	ROI 2	1	3	4	ROI 2	No. Of cells	No. Of cells	Sum	ROI 2	No. Of cells	No. Of cells	Sum
ROI 3	0	5	5	ROI 3	2	5	7	ROI 3	No. Of cells	No. Of cells	Sum	ROI 3	No. Of cells	No. Of cells	Sum
ROI 4	0	1	1	ROI 4	2	5	7	ROI 4	No. Of cells	No. Of cells	Sum	ROI 4	No. Of cells	No. Of cells	Sum
ROI 5	2	0	2	ROI 5	2	1	3	ROI 5	No. Of cells	No. Of cells	Sum	ROI 5	No. Of cells	No. Of cells	Sum
ROI 6	2	1	3	ROI 6	3	5	8	ROI 6	No. Of cells	No. Of cells	Sum	ROI 6	No. Of cells	No. Of cells	Sum
ROI 7	0	4	4	ROI 7	2	1	3	ROI 7	No. Of cells	No. Of cells	Sum	ROI 7	No. Of cells	No. Of cells	Sum
ROI 8	0	1	1	ROI 8	1	2	3	ROI 8	No. Of cells	No. Of cells	Sum	ROI 8	No. Of cells	No. Of cells	Sum
Sum	0	11	11	Sum	3	5	8	Sum	No. Of cells	No. Of cells	Sum	Sum	No. Of cells	No. Of cells	Sum
ROI 1	0	4	4	ROI 1	2	1	3	ROI 1	No. Of cells	No. Of cells	Sum	ROI 1	No. Of cells	No. Of cells	Sum
ROI 2	0	1	1	ROI 2	1	3	4	ROI 2	No. Of cells	No. Of cells	Sum	ROI 2	No. Of cells	No. Of cells	Sum
ROI 3	0	5	5	ROI 3	2	5	7	ROI 3	No. Of cells	No. Of cells	Sum	ROI 3	No. Of cells	No. Of cells	Sum
ROI 4	0	1	1	ROI 4	2	5	7	ROI 4	No. Of cells	No. Of cells	Sum	ROI 4	No. Of cells	No. Of cells	Sum
ROI 5	2	0	2	ROI 5	2	1	3	ROI 5	No. Of cells	No. Of cells	Sum	ROI 5	No. Of cells	No. Of cells	Sum
ROI 6	2	1	3	ROI 6	3	5	8	ROI 6	No. Of cells	No. Of cells	Sum	ROI 6	No. Of cells	No. Of cells	Sum
ROI 7	0	4	4	ROI 7	2	1	3	ROI 7	No. Of cells	No. Of cells	Sum	ROI 7	No. Of cells	No. Of cells	Sum
ROI 8	0	1	1	ROI 8	1	2	3	ROI 8	No. Of cells	No. Of cells	Sum	ROI 8	No. Of cells	No. Of cells	Sum
Sum	0	11	11	Sum	3	5	8	Sum	No. Of cells	No. Of cells	Sum	Sum	No. Of cells	No. Of cells	Sum
ROI 1	0	4	4	ROI 1	2	1	3	ROI 1	No. Of cells	No. Of cells	Sum	ROI 1	No. Of cells	No. Of cells	Sum
ROI 2	0	1	1	ROI 2	1	3	4	ROI 2	No. Of cells	No. Of cells	Sum	ROI 2	No. Of cells	No. Of cells	Sum
ROI 3	0	5	5	ROI 3	2	5	7	ROI 3	No. Of cells	No. Of cells	Sum	ROI 3	No. Of cells	No. Of cells	Sum
ROI 4	0	1	1	ROI 4	2	5	7	ROI 4	No. Of cells	No. Of cells	Sum	ROI 4	No. Of cells	No. Of cells	Sum
ROI 5	2	0	2	ROI 5	2	1	3	ROI 5	No. Of cells	No. Of cells	Sum	ROI 5	No. Of cells</		

Appendix 19 C: The number of reactive state microglial cells in all the groups and in the individual ROI's (1 – 8) is presented in the table below.

Group 1RSS				Group 2CWN				Group 3CSN				Group 4RSN			
Rat 1	No. Of cells	No. Of cells	Sum	Rat 2	No. Of cells	No. Of cells	Sum	Rat 1	No. Of cells	No. Of cells	Sum	Rat 2	No. Of cells	No. Of cells	Sum
ROI1	1	4	5	ROI1	15	15	30	ROI1	5	6	1	ROI1	4	2	3
ROI2	5	2	7	ROI2	12	9	21	ROI2	1	4	4	ROI2	6	8	3
Sum	6	6	12	Sum	27	24	51	Sum	6	10	5	Sum	10	10	6
ROI3	0	0	0	ROI3	7	4	11	ROI3	3	3	2	ROI3	5	5	0
ROI4	1	1	2	ROI4	5	4	9	ROI4	2	2	3	ROI4	3	3	0
Sum	1	1	2	Sum	12	8	20	Sum	5	5	15	Sum	8	10	3
ROI5	0	0	0	ROI5	12	12	24	ROI5	8	4	17	ROI5	1	6	1
ROI6	0	0	0	ROI6	11	0	11	ROI6	0	1	4	ROI6	4	10	0
Sum	0	0	0	Sum	23	0	23	Sum	8	5	9	Sum	5	16	1
ROI7	2	1	3	ROI7	3	3	6	ROI7	0	3	3	ROI7	4	4	0
ROI8	0	1	1	ROI8	5	5	10	ROI8	0	4	4	ROI8	3	5	0
Sum	2	2	4	Sum	8	8	16	Sum	0	7	7	Sum	7	9	0
Rat 2				Rat 3				Rat 4				Rat 5			
ROI1	4	6	10	ROI1	0	5	5	ROI1	2	5	1	ROI1	14	21	6
ROI2	3	8	11	ROI2	0	8	8	ROI2	2	2	8	ROI2	6	7	2
Sum	7	14	21	Sum	0	13	13	Sum	4	7	9	Sum	20	28	8
ROI3	1	6	7	ROI3	1	3	4	ROI3	2	2	6	ROI3	2	8	0
ROI4	2	3	5	ROI4	0	3	3	ROI4	2	2	4	ROI4	1	1	0
Sum	3	9	12	Sum	1	6	7	Sum	4	5	10	Sum	3	8	1
ROI5	4	6	10	ROI5	0	4	4	ROI5	3	4	7	ROI5	13	14	3
ROI6	3	5	8	ROI6	2	7	9	ROI6	1	3	4	ROI6	3	4	14
Sum	7	11	18	Sum	2	11	13	Sum	4	7	11	Sum	16	18	0
ROI7	2	5	7	ROI7	0	2	2	ROI7	3	3	5	ROI7	2	6	3
ROI8	2	5	7	ROI8	2	1	3	ROI8	4	3	7	ROI8	0	10	7
Sum	4	10	14	Sum	2	3	5	Sum	7	6	13	Sum	2	16	10
Rat 3				Rat 4				Rat 5				Rat 6			
ROI1	8	2	10	ROI1	9	6	15	ROI1	4	5	9	ROI1	12	13	5
ROI2	6	0	6	ROI2	14	8	22	ROI2	8	11	19	ROI2	4	10	12
Sum	14	2	16	Sum	23	14	37	Sum	16	18	34	Sum	16	23	10
ROI3	5	0	5	ROI3	2	3	5	ROI3	6	8	14	ROI3	7	9	4
ROI4	4	1	5	ROI4	2	0	2	ROI4	3	10	11	ROI4	8	14	9
Sum	9	1	10	Sum	8	3	11	Sum	9	18	22	Sum	15	18	6
ROI5	6	0	6	ROI5	5	5	10	ROI5	11	6	17	ROI5	7	3	5
ROI6	8	2	10	ROI6	6	4	10	ROI6	4	11	20	ROI6	4	3	35
Sum	14	2	16	Sum	11	9	20	Sum	15	17	32	Sum	11	6	18
ROI7	5	0	5	ROI7	5	3	8	ROI7	4	4	14	ROI7	2	5	13
ROI8	2	0	2	ROI8	2	1	3	ROI8	4	5	13	ROI8	5	7	8
Sum	7	0	7	Sum	7	4	11	Sum	8	9	27	Sum	7	12	21
Rat 4				Rat 5				Rat 6				Rat 7			
ROI1	0	0	0	ROI1	4	2	6	ROI1	4	5	9	ROI1	3	4	7
ROI2	2	0	2	ROI2	2	3	5	ROI2	5	4	9	ROI2	4	5	9
Sum	2	0	2	Sum	6	5	11	Sum	9	9	18	Sum	7	9	0
ROI3	2	0	2	ROI3	4	5	9	ROI3	7	4	11	ROI3	4	4	0
ROI4	2	1	3	ROI4	4	6	10	ROI4	6	2	8	ROI4	2	3	2
Sum	4	1	5	Sum	8	11	19	Sum	13	6	19	Sum	6	7	2
ROI5	1	2	3	ROI5	3	3	6	ROI5	9	3	12	ROI5	6	6	5
ROI6	2	0	2	ROI6	5	3	8	ROI6	6	11	20	ROI6	8	6	19
Sum	3	2	5	Sum	8	6	14	Sum	15	14	29	Sum	14	12	0
ROI7	3	2	5	ROI7	8	4	12	ROI7	5	4	9	ROI7	3	2	3
ROI8	0	4	4	ROI8	3	5	8	ROI8	5	5	10	ROI8	2	11	1
Sum	2	4	6	Sum	9	9	18	Sum	10	9	19	Sum	5	13	4
Rat 5				Rat 6				Rat 7				Rat 8			
ROI1	28	10	38	ROI1	7	0	7	ROI1	2	2	4	ROI1	0	4	4
ROI2	29	10	39	ROI2	3	6	9	ROI2	0	3	3	ROI2	4	6	2
Sum	57	20	77	Sum	10	6	16	Sum	2	5	7	Sum	4	10	9
ROI3	21	14	35	ROI3	6	3	9	ROI3	5	2	7	ROI3	0	1	3
ROI4	6	10	16	ROI4	2	4	6	ROI4	3	5	8	ROI4	1	0	6
Sum	27	24	51	Sum	8	7	15	Sum	8	7	15	Sum	1	1	9
ROI5	16	9	25	ROI5	8	7	15	ROI5	3	3	6	ROI5	2	1	0
ROI6	25	20	45	ROI6	5	4	9	ROI6	5	1	6	ROI6	5	7	3
Sum	41	29	70	Sum	13	11	24	Sum	8	4	12	Sum	7	8	3
ROI7	14	13	27	ROI7	2	4	6	ROI7	2	4	6	ROI7	1	3	2
ROI8	13	8	21	ROI8	4	0	4	ROI8	5	6	11	ROI8	3	1	0
Sum	27	21	48	Sum	6	4	10	Sum	7	10	17	Sum	4	4	2

Appendix 19 D: The number of phagocytic state microglial cells in all the groups and in the individual ROI's (1 – 8) is presented in the table below.

Group 1 RSS				Group 2 CNN				Group 3 CSN				Group 4 RSN			
Rat 1	No. Of cells	No. Of cells	Sum	Rat 2	No. Of cells	No. Of cells	Sum	Rat 1	No. Of cells	No. Of cells	Sum	Rat 2	No. Of cells	No. Of cells	Sum
ROI 1	0	0	2	ROI 1	4	3	7	ROI 1	1	2	3	ROI 1	8	8	25
ROI 2	2	0	4	ROI 2	9	6	15	ROI 2	0	3	3	ROI 2	8	1	19
Sum	2	0	6	Sum	13	9	22	Sum	1	5	6	Sum	16	9	44
ROI 3	0	0	0	ROI 3	4	0	4	ROI 3	1	0	1	ROI 3	3	2	13
ROI 4	1	0	1	ROI 4	1	2	3	ROI 4	1	0	1	ROI 4	10	1	13
Sum	1	0	2	Sum	5	2	7	Sum	2	0	2	Sum	13	3	26
ROI 5	1	0	5	ROI 5	8	1	9	ROI 5	1	1	2	ROI 5	6	4	13
ROI 6	0	0	1	ROI 6	2	3	5	ROI 6	1	1	2	ROI 6	2	4	8
Sum	1	0	6	Sum	10	4	14	Sum	2	2	4	Sum	8	6	21
ROI 7	0	1	1	ROI 7	0	0	0	ROI 7	0	0	0	ROI 7	0	1	1
ROI 8	0	0	0	ROI 8	0	0	0	ROI 8	1	0	1	ROI 8	4	1	6
Sum	0	1	1	Sum	0	0	0	Sum	1	0	1	Sum	4	2	8
Group 2 CNN				Group 3 CSN				Group 4 RSN				Group 5			
Rat 1	No. Of cells	No. Of cells	Sum	Rat 2	No. Of cells	No. Of cells	Sum	Rat 3	No. Of cells	No. Of cells	Sum	Rat 4	No. Of cells	No. Of cells	Sum
ROI 1	1	4	5	ROI 1	1	4	5	ROI 1	3	1	4	ROI 1	8	15	23
ROI 2	2	8	10	ROI 2	2	3	5	ROI 2	6	0	6	ROI 2	9	9	18
Sum	3	12	15	Sum	3	7	10	Sum	9	1	10	Sum	17	24	41
ROI 3	6	4	10	ROI 3	2	3	5	ROI 3	3	2	5	ROI 3	2	4	6
ROI 4	2	0	2	ROI 4	2	0	2	ROI 4	0	1	1	ROI 4	2	1	3
Sum	8	4	12	Sum	4	3	7	Sum	3	3	6	Sum	4	5	9
ROI 5	0	3	3	ROI 5	1	2	3	ROI 5	1	1	2	ROI 5	4	16	20
ROI 6	3	1	4	ROI 6	7	2	9	ROI 6	1	1	2	ROI 6	3	11	14
Sum	3	4	7	Sum	8	4	12	Sum	2	2	4	Sum	7	27	31
ROI 7	0	3	3	ROI 7	0	4	4	ROI 7	4	1	5	ROI 7	1	3	4
ROI 8	0	1	1	ROI 8	2	1	3	ROI 8	3	0	3	ROI 8	0	2	2
Sum	0	4	4	Sum	2	5	7	Sum	7	1	8	Sum	1	5	6
Group 3 CSN				Group 4 RSN				Group 5				Group 6			
Rat 1	No. Of cells	No. Of cells	Sum	Rat 2	No. Of cells	No. Of cells	Sum	Rat 3	No. Of cells	No. Of cells	Sum	Rat 4	No. Of cells	No. Of cells	Sum
ROI 1	7	3	10	ROI 1	4	3	7	ROI 1	11	15	26	ROI 1	6	3	9
ROI 2	15	6	21	ROI 2	3	2	5	ROI 2	8	6	14	ROI 2	8	3	11
Sum	22	9	31	Sum	7	5	12	Sum	19	21	40	Sum	14	6	20
ROI 3	0	0	0	ROI 3	2	3	5	ROI 3	1	6	7	ROI 3	2	5	7
ROI 4	4	0	4	ROI 4	0	1	1	ROI 4	1	2	3	ROI 4	2	3	5
Sum	4	0	4	Sum	2	4	6	Sum	2	8	10	Sum	4	8	12
ROI 5	3	1	4	ROI 5	1	2	3	ROI 5	2	5	7	ROI 5	2	3	5
ROI 6	1	2	3	ROI 6	7	1	8	ROI 6	3	3	6	ROI 6	3	2	5
Sum	4	3	7	Sum	8	3	11	Sum	5	8	13	Sum	5	5	10
ROI 7	0	0	0	ROI 7	0	4	4	ROI 7	7	7	14	ROI 7	6	1	7
ROI 8	0	0	0	ROI 8	0	1	1	ROI 8	1	3	4	ROI 8	3	1	4
Sum	0	0	0	Sum	0	5	5	Sum	8	10	18	Sum	9	2	11
Group 4 RSN				Group 5				Group 6				Group 7			
Rat 1	No. Of cells	No. Of cells	Sum	Rat 2	No. Of cells	No. Of cells	Sum	Rat 3	No. Of cells	No. Of cells	Sum	Rat 4	No. Of cells	No. Of cells	Sum
ROI 1	10	2	12	ROI 1	1	5	6	ROI 1	15	4	19	ROI 1	6	3	9
ROI 2	0	1	1	ROI 2	6	4	10	ROI 2	8	11	19	ROI 2	8	3	11
Sum	10	3	13	Sum	7	9	16	Sum	23	15	38	Sum	14	6	20
ROI 3	1	1	2	ROI 3	0	3	3	ROI 3	7	5	12	ROI 3	2	5	7
ROI 4	2	2	4	ROI 4	4	1	5	ROI 4	3	3	6	ROI 4	2	3	5
Sum	3	3	6	Sum	4	4	8	Sum	10	8	18	Sum	4	8	12
ROI 5	1	0	1	ROI 5	10	7	17	ROI 5	7	8	15	ROI 5	13	7	20
ROI 6	0	8	8	ROI 6	6	10	16	ROI 6	3	5	8	ROI 6	6	4	10
Sum	1	8	9	Sum	16	17	33	Sum	10	13	23	Sum	19	11	30
ROI 7	0	0	0	ROI 7	5	3	8	ROI 7	5	7	12	ROI 7	3	4	7
ROI 8	0	2	2	ROI 8	0	0	0	ROI 8	3	2	5	ROI 8	0	1	1
Sum	0	2	2	Sum	5	3	8	Sum	8	9	17	Sum	3	5	8
Group 5				Group 6				Group 7				Group 8			
Rat 1	No. Of cells	No. Of cells	Sum	Rat 2	No. Of cells	No. Of cells	Sum	Rat 3	No. Of cells	No. Of cells	Sum	Rat 4	No. Of cells	No. Of cells	Sum
ROI 1	12	10	22	ROI 1	5	1	6	ROI 1	0	3	3	ROI 1	11	13	24
ROI 2	0	4	4	ROI 2	4	2	6	ROI 2	8	4	12	ROI 2	11	7	18
Sum	12	14	26	Sum	9	3	12	Sum	8	7	15	Sum	22	20	42
ROI 3	1	6	7	ROI 3	0	3	3	ROI 3	5	4	9	ROI 3	5	1	6
ROI 4	2	12	14	ROI 4	0	1	1	ROI 4	3	4	7	ROI 4	5	1	6
Sum	3	18	21	Sum	0	4	4	Sum	8	8	16	Sum	10	2	12
ROI 5	1	5	6	ROI 5	4	4	8	ROI 5	6	4	10	ROI 5	5	6	11
ROI 6	0	8	8	ROI 6	6	10	16	ROI 6	3	5	8	ROI 6	3	10	13
Sum	1	13	14	Sum	10	14	24	Sum	9	9	18	Sum	8	16	24
ROI 7	0	6	6	ROI 7	5	3	8	ROI 7	5	7	12	ROI 7	3	4	7
ROI 8	0	2	2	ROI 8	0	0	0	ROI 8	3	2	5	ROI 8	0	1	1
Sum	0	8	8	Sum	5	3	8	Sum	8	9	17	Sum	3	5	8
Group 6				Group 7				Group 8				Group 9			
Rat 1	No. Of cells	No. Of cells	Sum	Rat 2	No. Of cells	No. Of cells	Sum	Rat 3	No. Of cells	No. Of cells	Sum	Rat 4	No. Of cells	No. Of cells	Sum
ROI 1	1	2	3	ROI 1	5	1	6	ROI 1	0	3	3	ROI 1	11	13	24
ROI 2	3	1	4	ROI 2	4	2	6	ROI 2	8	4	12	ROI 2	11	7	18
Sum	4	3	7	Sum	9	3	12	Sum	8	7	15	Sum	22	20	42
ROI 3	9	0	9	ROI 3	0	3	3	ROI 3	5	4	9	ROI 3	5	1	6
ROI 4	0	0	0	ROI 4	0	1	1	ROI 4	1	0	1	ROI 4	5	1	6
Sum	9	0	9	Sum	0	4	4	Sum	6	4	10	Sum	10	2	12
ROI 5	3	2	5	ROI 5	4	4	8	ROI 5	6	4	10	ROI 5	5	6	11
ROI 6	8	3	11	ROI 6	6	4	10	ROI 6	3	5	8	ROI 6	3	10	13
Sum	11	5	16	Sum	10	8	18	Sum	9	9	18	Sum	8	16	24
ROI 7	0	0	0	ROI 7	4	0	4	ROI 7	5	7	12	ROI 7	3	4	7
ROI 8	10	1	11	ROI 8	2	1	3	ROI 8	3	2	5	ROI 8	0	1	1
Sum	10	1	11	Sum	6	1	7	Sum	8	9	17	Sum	3	5	8

Appendix 20: Internship work, 'Short-term swimming exercise after an inflammatory insult reduces chronic muscle pain'.

Introduction: Prior study demonstrated that regular physical exercise prevents the onset of acute muscle hyperalgesia induced by an inflammatory insult (de Azambuja et al., 2020).

Objective: The study aimed to evaluate whether short-term swimming exercise performed after an inflammatory insult prevents chronic muscle hyperalgesia.

Conclusion:

The study concludes that swimming training helps in alleviating the development chronic muscle hyperalgesia but worsens and induces hyperalgesia in state of acute pain. Therefore, the strategy of using swimming exercise to decrease the intensity of chronic muscle hyperalgesia seems to be interesting. New studies are necessary to investigate the mechanisms by which the performance of a swimming exercise after an inflammatory insult induce a reduction of the intensity of chronic muscle hyperalgesia.

Acknowledgements:

This work was a part of bachelor thesis of Guilherme Domingos Brisque, and I would like to thank the group of Prof. Maria Claudia G. Oliveira Fusaro.

8 CURRICULUM VIATE

PERSONAL DETAILS

Name and Firstname: *Singaravelu Sathish Kumar*

Date of Birth: 30.12.1988

Place of Birth: Salem, Tamil Nadu, India

Family status: Single

Father: *Murugesan Singaravelu*

Mother: *Singaravelu Gomathi Devi*

SCHOOL EDUCATION

(2000) – (2006) Holy Cross Matriculation Higher Secondary School, Salem

(04/2006) Higher Secondary Certificate Examination (HSC)

UNIVERSITY EDUCATION

Since 04/2018 Doctoral student at the University of Heidelberg, Medical Faculty Mannheim, Germany

Supervisor: Prof. Dr. med. Rolf-Detlef Treede

09/2011 – 08/2013 Master of Science in Biomedical Engineering (Biomedicine), Hochschule Furtwangen University, Germany
Grade: 1.9

03/2013 – 08/2013 Master thesis at Gambro Dialysatoren GmbH, Germany
Title: Implementation of an online photometer to measure the sieving co-efficient of protein solutions in an automated test stand filter

06/2006 – 05/2010 Bachelor of Engineering in Biomedical Engineering, Anna University, Chennai, India
Grade: First class with distinction
Bachelor thesis title: Smart care systems

LANGUAGE SKILLS

English	Fluently in speaking and writing
German	Fluently in speaking
Tamil	Mother tongue

PUBLICATIONS that arose from this doctoral thesis

Singaravelu SK, Hoheisel U, Mense S, Treede RD. Rat dorsal horn neurons primed by stress develop a long-lasting manifest sensitization after a short-lasting nociceptive low back input. *Pain Rep.* 2021. PMID: 33688602.

Preprint: **Singaravelu SK**, Goitom A D, Surakka A P, Moerz H, Schilder A, Hansson A C, Spanagel R, Treede RD. (2021). Long-term sensitization of rat spinal neurons induced by adolescent psychophysical stress is further enhanced by a mild-nociceptive lumbar input. *bioRxiv* 2021.04.30.442126; doi: <https://doi.org/10.1101/2021.04.30.442126>

POSTERS AND TALKS that arose from this doctoral thesis

Poster: **Sathish Kumar Singaravelu**, Ulrike Hortscht, Ellen Hofmann, Ulrich Hoheisel, Siegfried Mense, Rolf-Detlef Treede. *Impact of repeated immobilization stress on the NGF induced sensitization process of rat dorsal horn neurons*. Mannheim, Germany at the 1st spring school of the graduate school 'GRK 2350', 2018.

Poster: **Sathish Kumar Singaravelu**, Alexander Dawit Goitom, Akseli P Surakka, Handan Moerz, Andreas Schilder, Anita C Hansson, Ulrich Hoheisel, Rainer Spanagel, Rolf-Detlef Treede. *Microglia contributes to long-term sensitization of rat spinal neurons: a double hit model*. Alicante, Spain at the International workshop on chronic pain and itch: mechanisms and circuits, 2021.

Talk: **Sathish Kumar Singaravelu**, Alexander Dawit Goitom, Akseli P Surakka, Handan Moerz, Andreas Schilder, Anita C Hansson, Ulrich Hoheisel, Rainer Spanagel, Rolf-Detlef Treede. *Adolescent psychophysical stress and nerve growth factor: a synergistic effect on the sensitization of rat spinal cord*. Siena, Italy at the European Pain School, 2021.

Talk: **Sathish Kumar Singaravelu**, Alexander Dawit Goitom, Akseli P Surakka, Handan Moerz, Andreas Schilder, Anita C Hansson, Ulrich Hoheisel, Rainer Spanagel, Rolf-Detlef Treede. *Microglia contributes to long-term sensitization of rat spinal neurons: a double hit model*. Alicante, Spain at the International workshop on chronic pain and itch: mechanisms and circuits, 2021.

FELLOWSHIP ABROAD

Summer internship as a part of my Ph.D. graduate school program at the 'Laboratory of Pain and Inflammation Research, School of Applied Sciences, State University of Campinas'.

Co-authorship outside this doctoral thesis

Bilbao A, Falfán-Melgoza C, Leixner S, Becker R, **Singaravelu SK**, Sack M, Sartorius A, Spanagel R, Weber-Fahr W. Longitudinal Structural and Functional Brain Network Alterations in a Mouse Model of Neuropathic Pain. *Neuroscience*. 2018 PMID: 29694917.

9 ACKNOWLEDGEMENTS

First and foremost, I would like to express my gratitude to my supervisor Professor Dr. med. Rolf-Detlef Treede for choosing me to work on this topic for my doctoral thesis, for mentoring and encouraging my research and for allowing me to experience what does it require to be a scientist. I would also like to thank Professor Dr. med. Christian Schmahl, spokesperson of the GRK 2350 for giving me an opportunity to be a part of the graduate school program.

I am thankful to Professor Dr. rer. nat. Rainer Spanagel for being my co-supervisor and for referring me for this position. He has always provided suggestions and reviews for my doctoral work during our TAC meetings.

I would like to thank PD Dr. Susanna Becker for being my mentor and giving me valuable tips during our meetings.

I am very grateful to have worked with Dr. Ulrich Hoheisel. Though the work time with him on a daily basis was only for six months, it laid the basis for my research work starting with experimental design, data analysis, and interpretation of the results. The training from Prof. Treede and Dr. Hoheisel always helped me to be one-step ahead than what is expected from me.

I would also like to thank PD Dr. rer. biol. hum. Walter Magerl who was always available for any questions regarding statistics and insightful scientific and non-scientific discussions.

I am also thankful to Dr. med. Wolfgang Greffrath for being available whenever I had questions related to animal experiments, ethics and supporting me with advice.

I like to thank PD Dr. Richard Carr who was always willing to help and answer my questions related to my electrophysiological work.

Many thanks to BTA Handan Mörz, MTLA Ulrike Hortscht and TA Ellen Hofmann who are undoubtedly the backbone support of our lab. They were always available for all kind of work-related support starting from ordering substances for work to ordering food once a while for lunch. Their technical support throughout my experiments was very helpful.

I am thankful to Dipl.-Ing. Ina Schäfer for giving me introduction to the microscopes that are available in the facility and for helping to solve any issues that I faced while working with the microscope.

I would like to thank Chief Secretary Mr. Robert Läufer and Secretary Ms. Sigrid Hugues for their support.

I like to thank Dr. Sylvia Steinmann and Dr. Julia Isabell Herzog, the co-ordinators for my graduate school program and for organizing seminars, workshops and events.

This acknowledgement would not be complete without thanking my fellow colleagues and friends with whom I shared a lot during this almost 4 years journey. Carmel Kerem, Hannah Schmidt, Anna Kostenko, Vivian Blechschmidt, Akseli Surakka, Alexander Dawit Goitom and many others who were always available for both work-related and emotional support. A special thanks to Lena Skatulla for offering to proofread my thesis and reminding me of the nightmares of my English grammar lessons.

My greatest gratitude goes to my guru Mr. Acharya Vinay Vinekar who planted this idea inside me of pursuing a scientific career. This incredible journey was possible because of you.

I would like to thank my parents and my brothers for believing in me and giving me a supporting shoulder whenever I needed one. You are all the reason for what I am today.

I would like to end this section by thanking all the animals that I had used for my research work and for making my dream come true.